



UNIVERSITÄT  
**DUISBURG  
ESSEN**

*Offen im Denken*

---

# MODULATION OF SURVIVIN'S CANCER-PROMOTING FUNCTIONS WITH SUPRAMOLECULAR LIGANDS

---

**Dissertation**

zur Erlangung des Doktorgrades

Dr. rer. nat.

an der Universität Duisburg-Essen

vorgelegt von

**Cecilia Vallet**

aus Bochum

Essen, 01.04.2019

# DuEPublico

Duisburg-Essen Publications online

UNIVERSITÄT  
DUISBURG  
ESSEN

*Offen im Denken*

ub | universitäts  
bibliothek

Diese Dissertation wird via DuEPublico, dem Dokumenten- und Publikationsserver der Universität Duisburg-Essen, zur Verfügung gestellt und liegt auch als Print-Version vor.

**DOI:** 10.17185/duepublico/70227

**URN:** urn:nbn:de:hbz:465-20231025-121749-7

Alle Rechte vorbehalten.

Die der vorliegenden Arbeit zugrundeliegenden Experimente wurden am Zentrum für medizinische Biotechnologie (ZMB) in der Abteilung für Molekularbiologie II der Universität Duisburg-Essen durchgeführt.

1. Gutachter: Prof. Dr. Shirley Knauer
2. Gutachter: Prof. Dr. Perihan Nalbant
3. Gutachter: Prof. Dr. Mark Brönstrup

Vorsitzender des Prüfungsausschusses: Prof. Dr. Peter Bayer

Tag der mündlichen Prüfung: 17.06.2019

# TABLE OF CONTENTS

TABLE OF CONTENTS.....	2
ZUSAMMENFASSUNG .....	6
SUMMARY .....	7
1 INTRODUCTION.....	8
1.1 SURVIVIN'S ROLE IN CANCER .....	8
1.2 STRUCTURE AND DOMAIN ORGANIZATION OF SURVIVIN .....	9
1.3 NUCLEOCYTOPLASMIC SHUTTLING OF SURVIVIN .....	11
1.4 SURVIVIN AS A MEMBER OF THE CPC DURING MITOSIS.....	16
1.5 SURVIVIN'S ROLE IN APOPTOSIS.....	20
1.6 HOMODIMERIZATION OF SURVIVIN .....	23
1.7 SURVIVIN AS A TARGET IN CANCER THERAPY .....	24
1.8 AIM OF THIS THESIS: TARGETING SURVIVIN'S CELLULAR FUNCTIONS WITH SUPRAMOLECULAR LIGANDS .....	26
2 MATERIAL AND METHODS.....	29
2.1 MATERIAL .....	29
2.1.1 INSTRUMENTS .....	29
2.1.2 CONSUMABLES.....	31
2.1.3 CHEMICALS.....	32
2.1.4 BUFFERS, SOLUTIONS AND MEDIA .....	34
2.1.5 BACTERIAL STRAINS.....	37
2.1.6 EUKARYOTIC CELLS.....	38
2.1.7 PLASMIDS .....	38
2.1.8 SEQUENCING PRIMERS.....	40
2.1.9 ANTIBODIES .....	40
2.1.10 DNA AND PROTEIN STANDARDS.....	42
2.1.11 KITS .....	42
2.1.12 SOFTWARE .....	43
2.2 METHODS .....	44
2.2.1 MOLECULAR BIOLOGY .....	44
2.2.1.1 POLYMERASE CHAIN REACTION (PCR).....	44
2.2.1.2 AGAROSE GEL ELECTROPHORESIS.....	45
2.2.1.3 PURIFICATION OF DNA FRAGMENTS.....	45
2.2.1.4 PHOTOMETRIC DETERMINATION OF DNA CONCENTRATION.....	46
2.2.1.5 RESTRICTION DIGEST .....	46

2.2.1.6	LIGATION .....	46
2.2.1.7	DNA SEQUENCE ANALYSIS .....	47
2.2.2	MICROBIOLOGY .....	47
2.2.2.1	TRANSFORMATION OF COMPETENT E. COLI CELLS .....	47
2.2.2.2	LONG-TERM STORAGE OF TRANSFORMED E. COLI CELLS.....	47
2.2.2.3	PLASMID ISOLATION FROM E. COLI CELLS.....	47
2.2.3	BIOCHEMISTRY .....	48
2.2.3.1	DETERMINATION OF PROTEIN CONCENTRATION .....	48
2.2.3.2	SDS-POLYACRYLAMIDE GEL ELECTROPHORESIS .....	48
2.2.3.3	COOMASSIE-STAINING OF POLYACRYLAMIDE GELS.....	49
2.2.3.4	WESTERN BLOTTING.....	50
2.2.3.5	ISOTHERMAL TITRATION CALORIMETRY .....	50
2.2.3.6	NMR SPECTROSCOPY .....	51
2.2.4	CELL BIOLOGY .....	53
2.2.4.1	CULTIVATION OF EUKARYOTIC CELLS .....	53
2.2.4.2	FREEZING AND THAWING CELLS.....	53
2.2.4.3	TRANSIENT TRANSFECTION OF EUKARYOTIC CELLS.....	53
2.2.4.4	PREPARATION OF WHOLE CELL LYSATES FROM EUKARYOTIC CELLS .....	54
2.2.4.5	IMMUNOPRECIPITATION.....	54
2.2.4.6	CONFOCAL FLUORESCENCE MICROSCOPY.....	55
2.2.4.7	IMMUNOFLUORESCENCE STAINING.....	55
2.2.4.8	PROXIMITY LIGATION ASSAY .....	56
2.2.4.9	SRV100 BIOSENSOR ASSAY.....	59
2.2.4.10	FÖRSTER RESONANCE ENERGY TRANSFER (FRET) .....	60
2.2.4.11	CELL PROLIFERATION, VIABILITY AND APOPTOSIS ASSAYS .....	61
2.2.5	BIOINFORMATICS .....	63
2.2.5.1	DOCKING .....	63
3	RESULTS .....	64
3.1	TARGETING THE SURVIVIN-HISTONE H3 INTERACTION WITH SUPRAMOLECULAR GCP LIGANDS.....	64
3.1.1	DOCKING STUDIES PREDICT BINDING OF MM138 TO SURVIVIN'S HISTONE H3 BINDING SITE .....	64
3.1.2	NMR TITRATION EXPERIMENTS CONFIRM BINDING OF MM138 TO SURVIVIN'S HISTONE H3 BINDING SITE .....	67
3.1.3	MM138 INHIBITS THE INTERACTION BETWEEN SURVIVIN AND HISTONE H3 DURING MITOSIS .....	70

3.1.4	SURVIVIN DIMERIZATION IS INCREASED BY MM138 TREATMENT.....	74
3.1.5	MM138 CAUSES MITOTIC DEFECTS IN HELA CELLS.....	77
3.1.6	MM138 REDUCES PROLIFERATION OF CANCER CELLS.....	79
3.2	TARGETING THE SURVIVIN-CRM1 INTERACTION WITH SUPRAMOLECULAR GCP LIGANDS.....	82
3.2.1	DOCKING STUDIES PREDICT BINDING OF DA162 TO SURVIVIN'S NUCLEAR EXPORT SIGNAL.....	82
3.2.2	ITC EXPERIMENTS CONFIRM BINDING OF DA162 TO SURVIVIN.....	86
3.2.3	DA162 INHIBITS THE INTERACTION BETWEEN SURVIVIN AND CRM1.....	87
3.2.4	CRM1-MEDIATED NUCLEAR EXPORT OF SURVIVIN IS REDUCED BY DA162.....	89
3.2.5	DA162 HAS NO SIGNIFICANT INFLUENCE ON SURVIVIN DIMERIZATION.....	91
3.2.6	DA162 REDUCES PROLIFERATION OF CANCER CELLS.....	93
3.2.7	APOPTOSIS INCREASES AFTER DA162 TREATMENT.....	95
4	DISCUSSION.....	97
4.1	INHIBITION OF SURVIVIN-HISTONE H3 INTERACTION WITH GCP LIGAND MM138.....	98
4.1.1	MM138 BINDS TO SURVIVIN'S HISTONE H3 BINDING SITE.....	98
4.1.2	MM138 INHIBITS THE SURVIVIN-HISTONE H3 INTERACTION.....	99
4.1.3	SURVIVIN DIMERIZATION IS INCREASED BY MM138 TREATMENT.....	100
4.1.4	MM138 INTERFERES WITH SURVIVIN'S ROLE IN CELL PROLIFERATION.....	102
4.2	INHIBITION OF SURVIVIN-CRM1 INTERACTION WITH GCP LIGAND DA162.....	105
4.2.1	DA162 ADDRESSES SURVIVIN'S NES.....	105
4.2.2	SURVIVIN'S CRM1-MEDIATED NUCLEAR EXPORT IS INHIBITED BY DA162 TREATMENT.....	107
4.2.3	DA162 HAS NO SIGNIFICANT EFFECT ON SURVIVIN DIMERIZATION.....	108
4.2.4	DA162 INTERFERES WITH SURVIVIN'S MITOTIC AND ANTI-APOPTOTIC FUNCTIONS.....	108
4.3	CONCLUSION AND OUTLOOK.....	110
5	REFERENCES.....	112
6	APPENDIX.....	I
6.1	LIST OF ABBREVIATIONS.....	I
6.2	LIST OF FIGURES.....	V
6.3	LIST OF TABLES.....	VII
6.4	AMINO ACIDS.....	VIII
	DANKSAGUNG.....	IX
	PUBLICATIONS.....	XII
	TALKS.....	XIV

POSTER PRESENTATIONS.....	XIV
AWARDS .....	XIV
CURRICULUM VITAE .....	XV
EIDESSTÄTTLICHE ERKLÄRUNGEN .....	XVI

## ZUSAMMENFASSUNG

Survivin ist in den meisten Krebsarten hochreguliert und wurde mit einer Resistenz gegenüber Chemo- und Bestrahlungstherapien sowie einem schlechteren Krankheitsverlauf in Verbindung gebracht. Dem Protein wird aufgrund seiner anti-apoptotischen Eigenschaften und seiner Funktion in der Zellproliferation eine Schlüsselrolle bei der Karzinogenese zugesprochen. Da Survivin hauptsächlich während der Embryonalentwicklung exprimiert wird, jedoch kaum in ausdifferenzierten adulten Geweben, gilt es als eines der krebsspezifischsten Proteine, die bisher bekannt sind. Survivin besitzt keine enzymatische Aktivität und stellt daher ein schwierig anzugreifendes Wirkstoffziel dar. Bisherige Strategien zur Inhibition des Proteins basieren auf *Antisense*-Oligonukleotiden, siRNAs, *small molecule*-Inhibitoren, Gen- und Immuntherapien. Allerdings findet bislang keiner dieser Ansätze klinische Anwendung.

In dieser Arbeit sollten als neuer Ansatz Protein-Protein-Interaktionen zwischen Survivin und funktionell relevanten Bindungspartnern inhibiert werden. Supramolekulare Liganden auf der Basis des Guanidiniocarbonyl-Pyrrol Kations dienen hierbei als hochspezifische Anionen-Binder, um entsprechende anionische *hot spots* auf der Oberfläche des Proteins anzugreifen.

Der Ligand MM138 wurde entwickelt, um die Interaktion zwischen Survivin und Histon H3, und damit Survivins Rolle in der Zellproliferation, zu inhibieren. Die Bindung von MM138 an die Histon-H3-Bindungsstelle von Survivin konnte mittels NMR bestätigt werden. Darüber hinaus konnte durch die Etablierung verschiedener mikroskopischer und zellbasierter Assays gezeigt werden, dass der supramolekulare Ligand die Interaktion zwischen Survivin und Histon H3 im Zellinneren hemmt und so die Proliferation von Krebszellen vermindert.

Der Ligand DA162 hingegen soll die Bindung von Survivin an seinen Exportrezeptor Crm1 verhindern. Diese ist nicht nur für den Crm1-vermittelten Kernexport von Survivin in das Zytoplasma relevant, wo das Protein als Apoptose-Inhibitor fungiert, sondern auch für seine Rolle im *Chromosomal Passenger Complex* in der Mitose. Es konnte gezeigt werden, dass DA162 mit einem niedrigen mikromolaren  $K_D$  an Survivin bindet und die Interaktion zwischen Survivin und Crm1 innerhalb der Zelle hemmt. Dies führt zu einer Inhibition des Kernexports von Survivin sowie einer Verminderung der Zellproliferation und Erhöhung der Caspase-vermittelten Apoptose in Krebszellen.

Die Strategie anionische *hot spots* als Angriffspunkt für supramolekulare Guanidiniocarbonyl-Pyrrol Liganden zu nutzen scheint daher ein vielversprechender Ansatz für die Entwicklung neuer Krebstherapien zu sein.

## SUMMARY

Survivin is highly upregulated in most cancers and has been associated with a resistance against chemo- and radiotherapy and a poor clinical outcome. The protein is considered to be a key player of carcinogenesis due to its anti-apoptotic function and its role in cell proliferation. As it is mainly expressed during embryonic development but mostly absent in terminally differentiated adult tissues, it might be one of the most cancer-specific proteins identified so far. Survivin possesses no enzymatic activity, which makes it challenging to address the protein as a drug target. Various strategies so far have included antisense oligonucleotides, siRNAs, small molecule inhibitors, gene therapy and immunotherapy but none of these approaches has yet reached the clinic.

This thesis aimed to explore a novel approaches by targeting protein-protein interactions of Survivin and its functionally relevant binding partners. Supramolecular ligands based on the guanidiniocarbonyl pyrrole cation served as highly specific anion binders in order to target respective anionic hot spots on the surface of the protein.

Ligand MM138 was designed to interfere with the interaction between Survivin and Histone H3, which is essential for Survivin to fulfil its role in cell proliferation. The binding of MM138 to Survivin's Histone H3 binding site could be verified by NMR analyses. In addition, the establishment of several microscopic and cellular assays allowed it to be demonstrated that the supramolecular ligand is able to inhibit Survivin-Histone H3 interaction inside the cell and thereby reduce cancer cell proliferation.

Ligand DA162 aimed to target the interaction between Survivin and its export receptor Crm1, which is not only relevant for Survivin's Crm1-mediated nuclear export into the cytoplasm where it acts as an inhibitor of apoptosis, but also for its role within the chromosomal passenger complex during mitosis. It could be shown that DA162 binds to Survivin with a low micromolar  $K_D$  and is able to inhibit the interaction between Survivin and Crm1 inside the cell. This leads to an inhibition of Survivin's nuclear export, a decrease in cell proliferation and an increase of caspase-mediated apoptosis in cancer cells.

Targeting Survivin's anionic hot spots with supramolecular guanidiniocarbonyl pyrrole ligands therefore seems to be a promising approach for the development of new cancer therapies.

# 1 INTRODUCTION

## 1.1 SURVIVIN'S ROLE IN CANCER

Cancer is the second leading cause of death worldwide following cardiovascular diseases. In 2015, 8.8 million people died from cancer, which corresponds to nearly 17 % of all global deaths. The most common causes of cancer death are lung cancer (1,690,000 deaths), liver cancer (788,000 deaths), colorectal cancer (774,000 deaths), stomach cancer (754,000 deaths) and breast cancer (571,000 deaths) (1).

Cancer is a generic term for a group of diseases involving the transformation of normal cells into malignant tumor cells. In contrast to benign tumors, malignant tumors are able to invade adjacent tissues and form metastases in distant parts of the body (1).

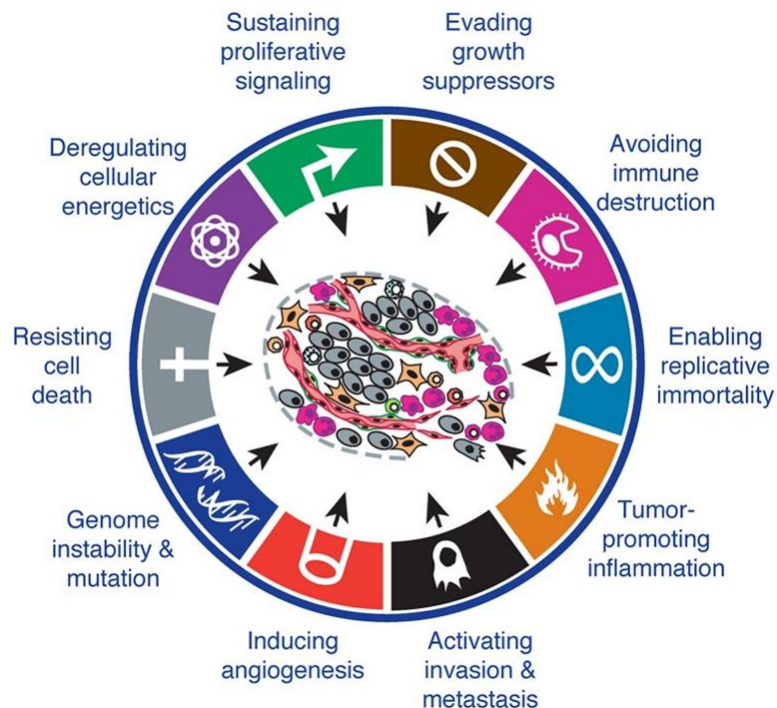


**Figure 1.1: The hallmarks of cancer.** The acquired characteristics of malignant cancer cells during carcinogenesis are the capability to metastasize, the ability to resist cell death, enable replicative immortality, induce angiogenesis, evade growth suppressors, sustain proliferative signalling, gain genome instability and mutation, show tumor-promoting inflammation, deregulate cellular energetics and avoid immune destruction (modified after (2)).

Carcinogenesis is a multi-step process, where a single cell gradually accumulates genetic mutations that provide characteristics required for malignant transformation. Those characteristics are called “hallmarks of cancer” and were described by Hanahan and Weinberg in 2000. Besides the capability to metastasize, the ability to resist cell death, enable replicative immortality, induce angiogenesis, evade growth suppressors and sustain proliferative signaling are part of those characteristics. In 2011, Hanahan and Weinberg added genome instability and mutation, tumor-promoting inflammation and the capability to deregulate cellular energetics and avoid immune destruction to the existing hallmarks (Figure 1.1).

The protein Survivin is involved in several cellular functions linked to carcinogenesis. As a member of the inhibitor of apoptosis protein (IAP) family, it exhibits anti-apoptotic functions, but is also necessary for proper chromosome segregation during mitosis and able to promote angiogenesis (3–5). Survivin was found to be upregulated in virtually all types of human cancers due to downregulation of transcriptional repressors like retinoblastoma protein and p53, gene duplications, promoter mutations, NF- $\kappa$ B-induced transcription or IGF-1-mediated mRNA stabilization (6–10). Its upregulation is associated with resistance against chemo- and radiotherapy, an increased tumor recurrence and an abbreviated patient survival (11–15). Besides its overexpression in cancer cells, Survivin is upregulated during embryonic development but mostly absent in adult tissues (11).

## 1.2 STRUCTURE AND DOMAIN ORGANIZATION OF SURVIVIN

Survivin is encoded by the *baculoviral inhibitor of apoptosis repeat containing 5 (BIRC5)* gene, located on the human chromosome 17q25. Besides wildtype (WT) Survivin, there are ten known splice variants, whose functions are still not fully understood but seem to have a diagnostic significance in cancer (16). WT Survivin consists of 142 amino acids (aa), has a molecular weight of 16.5 kDa and is composed of several different domains. The N-terminal baculovirus IAP repeat (BIR) domain (aa 15–88) is a structural motif that is present in all proteins of the IAP family and is responsible for Survivin’s anti-apoptotic functions (17). The Histone H3 binding site of Survivin (aa 51–80) is located within the BIR domain and essential for binding Histone H3 phosphorylated on threonine 3 (H3T3p) during mitosis (18, 19). The C-terminal  $\alpha$ -helix forms a three helix bundle together with inner centromere protein (INCENP) and Borealin as part of the chromosomal passenger complex (CPC) during

mitosis (20). Furthermore, Survivin possesses a nuclear export signal (NES, <sup>89</sup>VKKQFEELTL<sup>98</sup>), which interacts with the export receptor Crm1 and mediates not only Survivin's nuclear export into the cytoplasm but also the centromeric targeting of the CPC in early mitosis (21–23). Survivin's dimer interface (aa 6–10 and 89–102) partly overlaps with the NES, which is why Survivin's homodimerization and its interaction with the export receptor Crm1 are thought to be competitive processes (24). Survivin forms a homodimer in solution with both  $\alpha$ -helices arranged in an angle of  $110^\circ$  (Figure 1.2) (25).

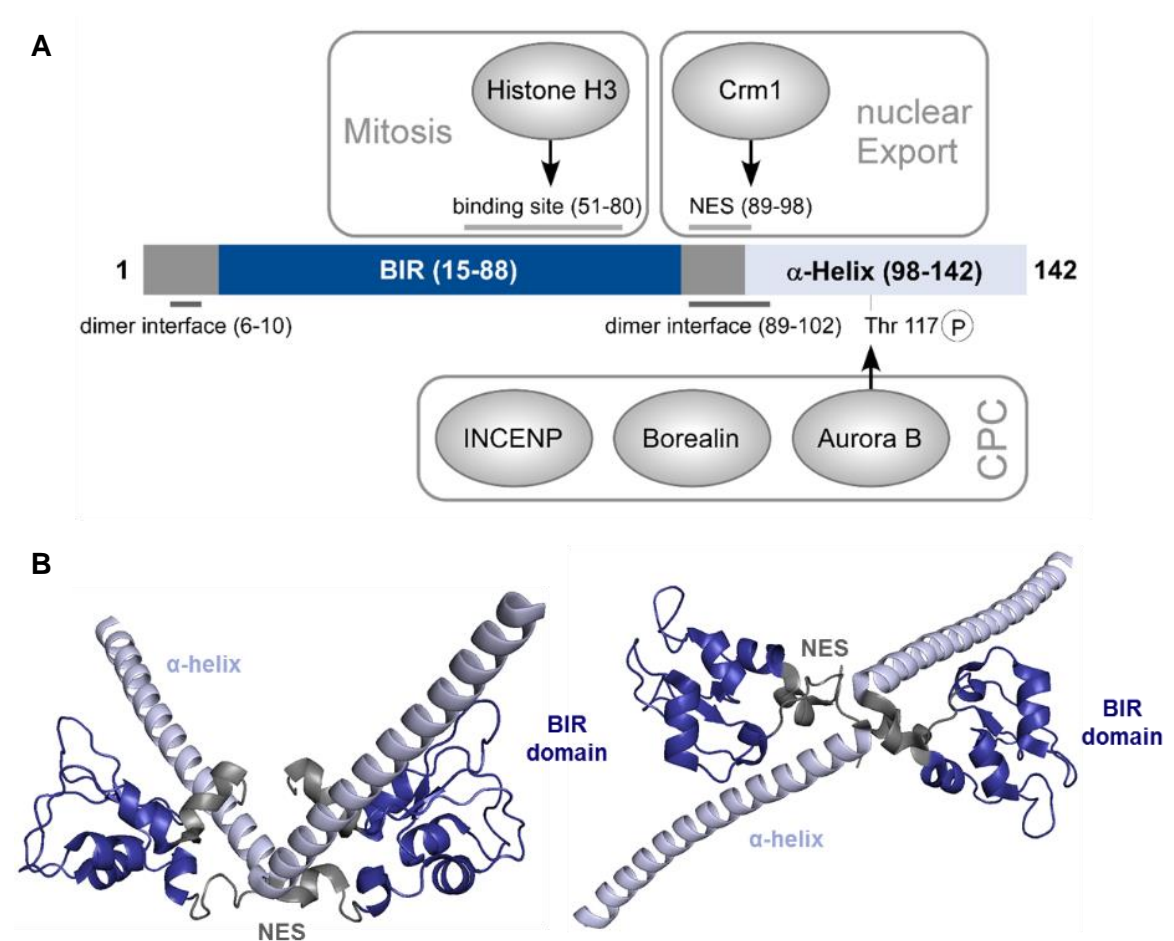


**Figure 1.2: Structure and domain organization of Survivin. A)** Survivin consists of an N-terminal BIR domain (dark blue), containing the Histone H3 binding site, and a C-terminal  $\alpha$ -helix (light blue), which interacts with the CPC during mitosis. Survivin's NES (grey) overlaps with its dimer interface. **B)** Survivin forms a homodimer in solution with an angle of  $110^\circ$  between both  $\alpha$ -helices (25). (PDB: 1E31).

### 1.3 NUCLEOCYTOPLASMIC SHUTTLING OF SURVIVIN

The shuttling of proteins and RNAs between the nucleus and the cytoplasm is a pivotal process in eukaryotic cells. While DNA replication and RNA transcription occur in the nucleus, protein synthesis takes place in the cytoplasm. This requires a selective transport of various proteins, molecules and ions between the two compartments. During interphase, the nucleus and the cytoplasm are separated by the nuclear membrane. Nuclear pore complexes (NPCs), which are embedded into the nuclear membrane, are the only gateway between the nucleus and the cytoplasm (26–29).

NPCs are large protein complexes that have a molecular weight of approximately 125 MDa and are composed of multiple copies of around 30 different nuclear pore proteins called nucleoporins (NUPs), which are arranged in an octagonal symmetry (29). There are four different classes of NUPs. Transmembrane NUPs anchor the complex to the nuclear membrane. FG NUPs form filaments in the central pore of the NPC with their phenylalanine-glycine (FG) repeats. Scaffold NUPs form the outer and inner ring of the NPC and connect the transmembrane NUPs to the FG NUPs, and peripheral NUPs form the cytoplasmic filaments and the nuclear basket (30, 31) (Figure 1.3).

The nuclear membrane of a typical mammalian cell contains on average 3000 NPCs (32–34). Small molecules, ions and proteins with a size of less than 40 kDa are, depending on their charge and conformation, able to pass freely across the nuclear envelope, while larger proteins, tRNAs and mRNAs must be actively transported through the NPC (26, 34). Up to 1000 macromolecules per second can be transported through each NPC and the transport can occur in both directions at the same time (35).

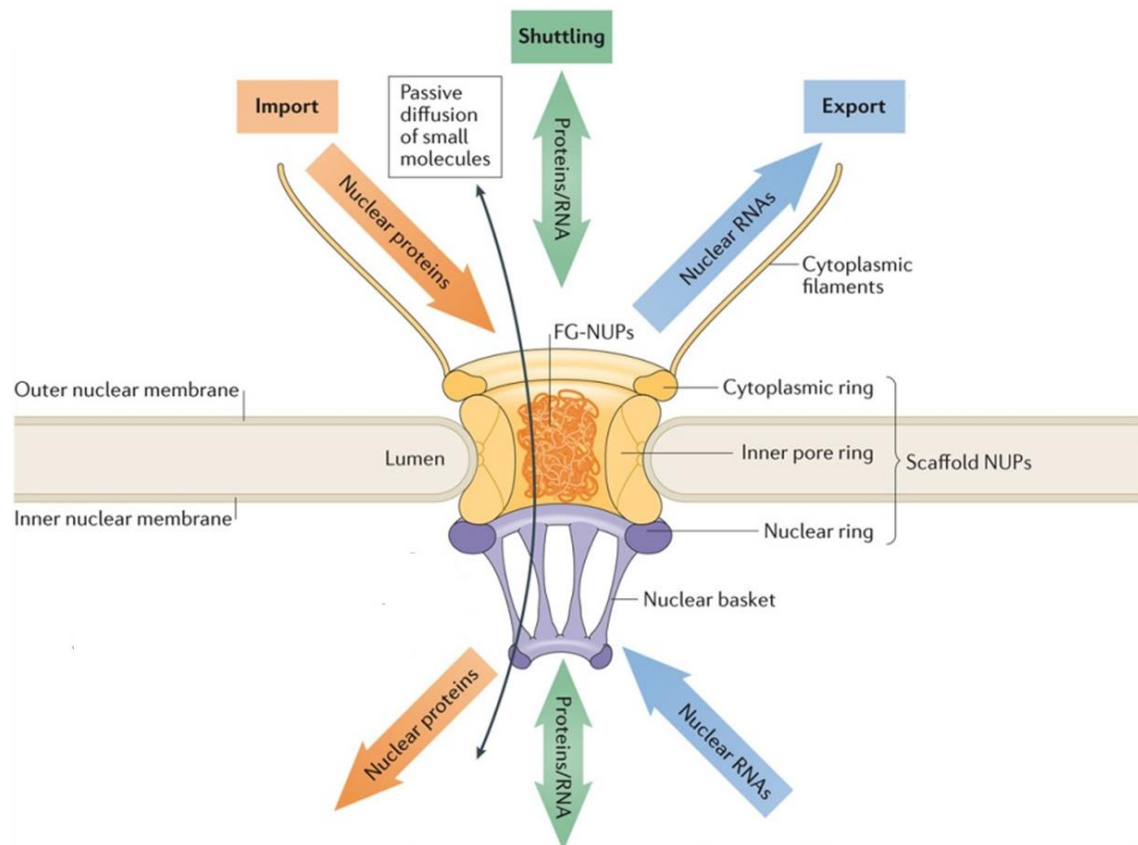


**Figure 1.3: The Nuclear Pore Complex (NPC).** The NPC is embedded into the nuclear membrane. It consists of different nucleoporins (NUPs), which form the cytoplasmic ring, the nuclear ring, the inner pore ring, the nuclear basket, the cytoplasmic filaments and the central channel. The NPC allows free diffusion of small molecules, whereas larger molecules such as proteins and RNAs are actively transported through the complex (modified after (29)).

Karyopherins are nucleocytoplasmic transport factors that can act as export receptors (exportins) or import receptors (importins). They are able to carry larger proteins and other macromolecules through the NPC and thereby across the nuclear membrane (36, 37). Their transport selectivity is ensured by the FG repeats of nucleoporines, which are specific binding sites for karyopherines. However, the exact gating mechanism of the NPC is still not fully understood (31). The current model is the “selective-phase model”, which was suggested by Ribbeck and Görlich in 2001 and has been further improved ever since (38). The model postulates that the FG repeat domains of the nucleoporines interact via hydrophobic interactions, thereby forming a hydrogel in the central pore of the channel, which is only permeable for molecules up to a certain size. Karyopherins, which bind to the FG repeats, are able to disrupt the hydrogel and transport their cargo through the NPC (38–40).

To be actively transported through the nuclear membrane, proteins have to interact with import or export receptors via specific transport signals. Nuclear localization signals (NLSs) mediate the interaction between cargo proteins and importins. They are short sequences, which are composed of basic and positively charged amino acids like lysines and arginines. NLSs are classified either as monopartite, if they consist of only one cluster of basic and positively charged amino acids, or bipartite, if two clusters are separated by a spacer sequence (39–41). Nuclear export signals (NESs) mediate the interaction with exportins and are composed of hydrophobic and leucine-rich amino acid sequences. The NES consensus sequence is “L-X<sub>2-3</sub>-L-X<sub>2-3</sub>-L-X-L”. “L” stands for a hydrophobic amino acid, which is most likely leucine but can also be phenylalanine, methionine, isoleucine or valine, while “X” is an arbitrary amino acid (42, 43).

The first step of the nuclear import of a protein is the formation of an importin-cargo complex via the NLS of the cargo protein. The loaded nuclear import receptor then moves through the NPC along the FG repeats displayed by nucleoporines in the central pore (Figure 1.3). In the nucleus, the binding of RanGTP to the importin-cargo complex promotes dissociation of the cargo, while RanGTP-bound importin is returned to the cytoplasm (44–46).

Exportins bind to cargo proteins containing a NES to form a trimeric complex with RanGTP, which increases the affinity of the export receptor to its cargo protein. Following complex formation, the cargo protein is transported through the NPC along the FG repeats. In the cytoplasm, the complex dissociates following GTP hydrolysis. Afterwards, RanGDP is reimported into the nucleus with the help of nuclear transport factor 2 (30, 44, 46) (Figure 1.4).

The Ras-related nuclear protein (Ran) belongs to the family of Ras-like GTPases. Ran can be found in the nucleus and in the cytoplasm. It exists in two conformations depending on whether it is bound to GDP or GTP. The conversion between the two conformations depends on the regulatory proteins GTPase-activating protein (GAP) and nuclear guanine exchange factor (GEF). GAP is located in the cytoplasm and triggers GTP hydrolysis, while GEF promotes the exchange of GDP for GTP in the nucleus. This leads to a 100-fold excess of RanGTP in the nucleus compared to the cytoplasm. This gradient gives the nuclear transport its directionality as the guanine nucleotide switch causes conformational changes in Ran and thereby regulates the assembly and disassembly of import and export complexes (44, 46–48).

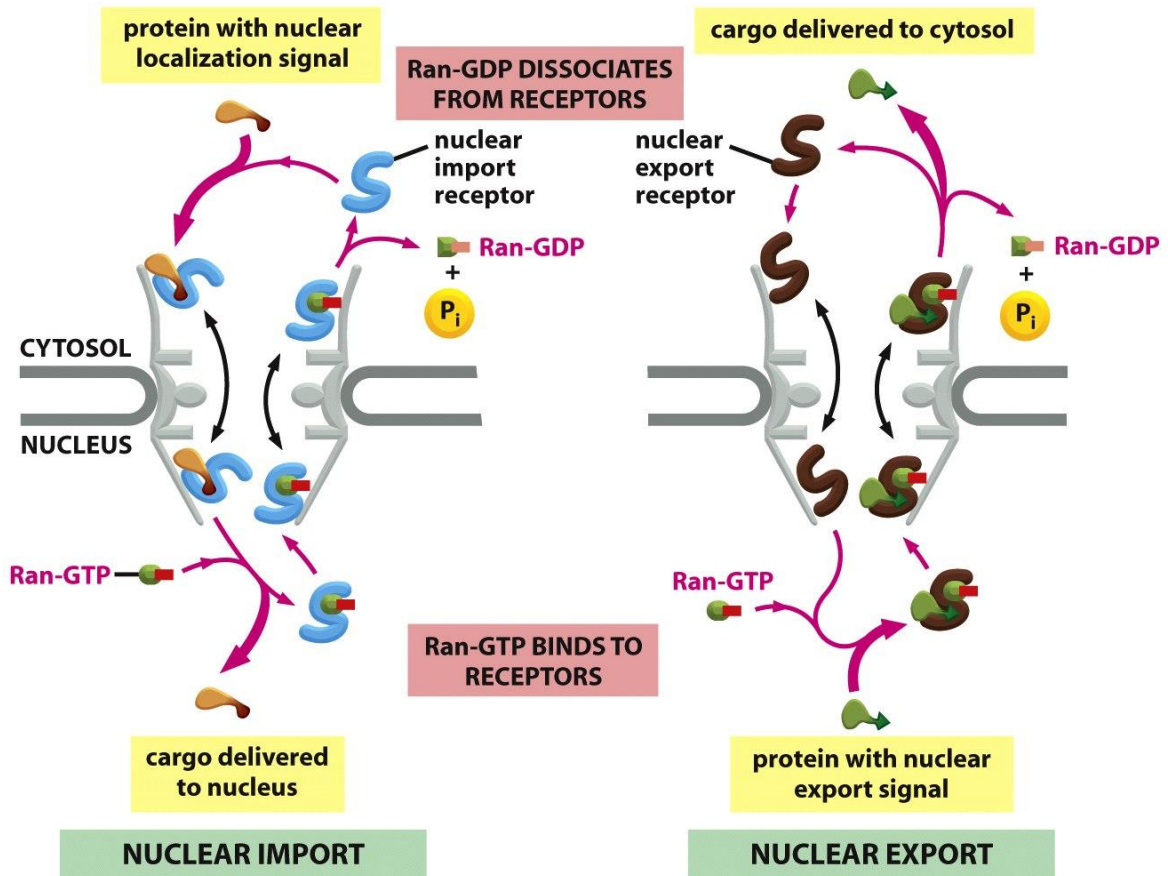


**Figure 1.4: Nuclear import and export of proteins.** Loaded transport receptors move along the FG repeats of nucleoporines in the central channel of the NPC. The gradient of RanGTP in the nucleus and RanGDP in the cytoplasm provides the directionality of nuclear transport. GAP induces GTP hydrolysis in the cytosol and GEF promotes the exchange of GDP for GTP in the nucleus. After the nuclear export of a cargo protein, RanGDP is reimported into the nucleus with the help of nuclear transport factor 2 (49).

Survivin has a dual role inside the cell. In the nucleus, it is part of the chromosomal passenger complex (CPC) during mitosis (section 1.4) and in the cytoplasm it acts as an inhibitor of apoptosis (section 1.5). This means that shuttling between the two compartments is essential in order for Survivin to fulfil its cellular functions. While Survivin seems to be able to enter the nucleus passively, its nuclear export is, despite its molecular weight of only 16.5 kDa, dependent on the nuclear export receptor chromosome region maintenance 1 (Crm1).

Crm1 is the major nuclear export receptor in eukaryotic cells. It has a molecular weight of 123.4 kDa and consists of 21 tandem HEAT repeats, each including two anti-parallel helices A and B, which form a ring-like structure. The outer surface of the receptor is composed of

A helices, which interact with the FG NUPs of the NPC, while the inner surface of the ring consists of B helices, which are able to interact with the NESs of cargo proteins and RanGTP (50, 51). The CRIME (Crm1, importin- $\beta$  etc.) domain and the acidic loop at the N-terminus of the protein are particularly important for RanGTP binding. The hydrophobic NES cleft between HEAT repeats 11 and 12 is responsible for NES binding (52–54) (Figure 1.5). Crm1 can be found in two different conformations depending on whether it is cargo-bound or cargo-free. In the cargo-free conformation the helix 21B reaches across the molecule and interacts with HEAT repeat 9, thereby preventing RanGTP binding. The acidic loop is “flipped back” and interacts with the NES cleft, which prevents cargo binding. In the cargo-bound conformation, helix 21B lies in parallel to helix 21A outside of the molecule and the acidic loop rearranges in the “seatbelt” conformation, thereby fixing RanGTP at its binding site and opening the NES cleft to allow cargo binding. The conformational change between the cargo-bound and cargo-free form of Crm1 is induced by RanBP1 binding in the cytoplasm after the cargo protein was transported through the NPC (52, 53, 55, 56).

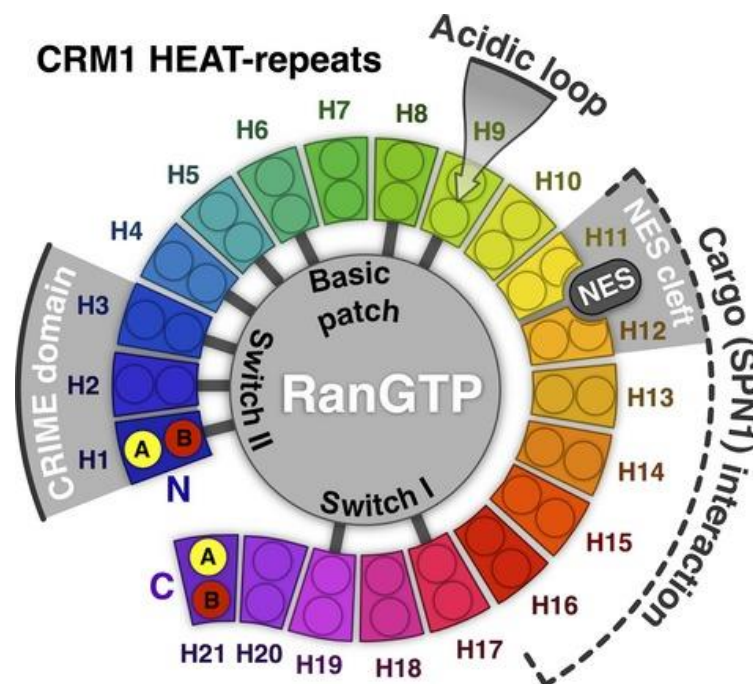


**Figure 1.5: Domain organization of Crm1.** Crm1 consists of 21 HEAT repeats, each composed of a pair of anti-parallel helices A and B, which form a ring-like structure. The CRIME domain and acidic loop are important for RanGTP binding, while the NES cleft between HEAT repeats 11 and 12 is responsible for binding NESs of cargo proteins (56).

Besides its role as major export receptor, Crm1 has additional functions during mitosis. Crm1-RanGTP localizes to the kinetochores during mitosis where it ensures stable kinetochore fibre formation and proper chromosome segregation (57, 58). The interaction with Survivin is not only necessary for Survivin's Crm1-mediated nuclear export into the cytoplasm, where it acts as an inhibitor of apoptosis, but also to fulfil its role with the CPC during mitosis, as Crm1 is crucially involved in tethering the CPC to the centromeres by interacting with Survivin's NES (21).

#### **1.4 SURVIVIN AS A MEMBER OF THE CPC DURING MITOSIS**

The cell cycle is divided into four phases: G<sub>1</sub> (gap 1), S (synthesis), G<sub>2</sub> (gap 2) and M phase (mitosis) (Figure 1.6). In G<sub>1</sub> phase the cell increases in size, prepares for DNA synthesis and ensures that all extra- and intracellular conditions are favorable before entering S phase. In S phase DNA replication takes place and the chromosomes duplicate. During G<sub>2</sub> phase the cell continues to grow and verifies that the DNA was replicated correctly before entering mitosis. M phase, during which the cell divides into two daughter cells, can be split into several stages. In prophase, the chromosomes start to condense and the mitotic spindle begins to form. The chromosomes finish condensing in prometaphase and the nuclear envelope breaks down. During metaphase the chromosomes align at the equatorial plane and their kinetochores attach to microtubules of opposite spindle poles. In anaphase, the microtubules pull the sister chromatids towards opposite poles of the cell. The mitotic spindle breaks down during telophase, two new nuclear membranes begin to form and the chromosomes begin to decondense. During cytokinesis, the contractile ring divides the cytoplasm into two daughter cells, each with a complete set of chromosomes (49).

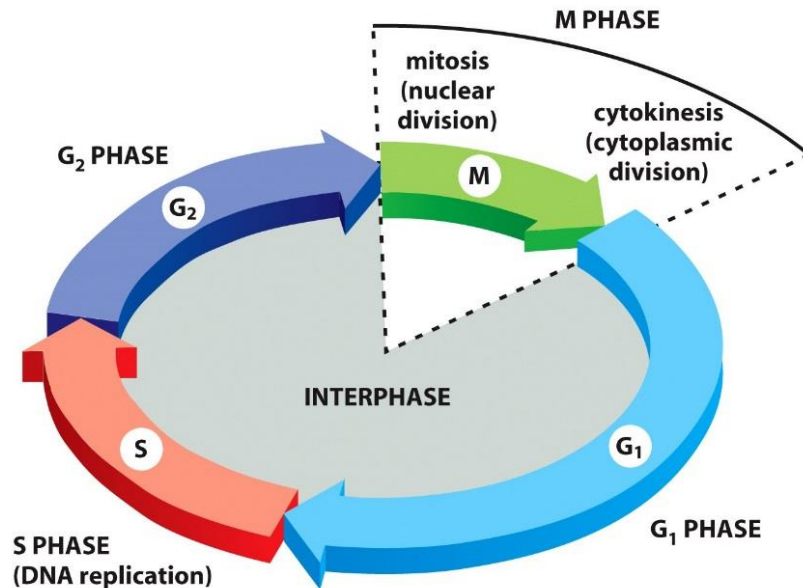


**Figure 1.6: The phases of the cell cycle.** The cell cycle can be divided into G<sub>1</sub> (gap 1), S (synthesis), G<sub>2</sub> (gap 2) and M phase (mitosis). The gap phases mainly comprise cell growth, whereas in S phase the DNA replicates and in M phase the cell divides into two daughter cells (49).

A series of checkpoints, which are located in G<sub>1</sub> phase, at the transition from G<sub>1</sub> to S phase, in S phase, at the transition from the G<sub>2</sub> to M phase and at the transition from meta- to anaphase (spindle assembly checkpoint), ensure that each stage of the cell cycle is successfully completed before the cell enters a new phase. The cell cycle progress is driven by cyclin-dependent kinases (CDKs), which require cyclin binding for their catalytic activity and substrate recognition. The expression levels of the different cyclins fluctuate during the cell cycle, thereby regulating CDK activation and cell cycle progression (49) (Figure 1.7).

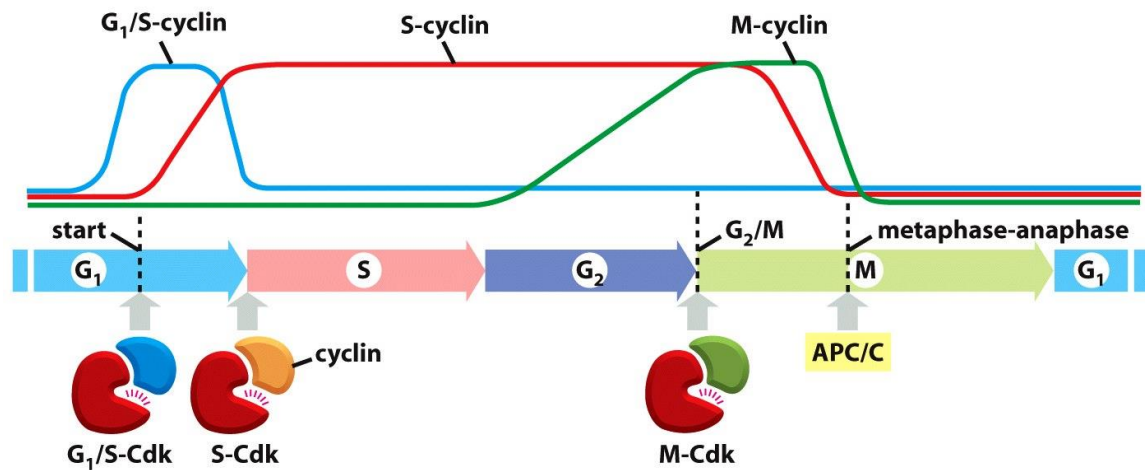


**Figure 1.7: Regulation of cell cycle progress via the formation of cyclin-CDK complexes.** The expression of different cyclins oscillates during the cell cycle, thereby regulating CDK activation and cell cycle progression, while the CDK concentration stays constant. In late G1 phase, the formation of G1/S-CDK complexes leads to the progression through the start checkpoint. S-CDK complexes trigger DNA replication, while M-CDK complexes trigger early events in mitosis (49).

As a member of the chromosomal passenger complex (CPC), Survivin acts as a key regulator during mitosis (59). The CPC plays a role in chromosome condensation, kinetochore-microtubule attachment, activation of the spindle assembly checkpoint and formation of the contractile ring during cytokinesis (60). Apart from Survivin, it consists of the kinase Aurora B and the two proteins INCENP and Borealin with which Survivin's C-terminal  $\alpha$ -helix forms a three helix bundle (20). In pro- and metaphase, the CPC localizes at the chromosome arms, where it phosphorylates Histone H3 on serine 10 and serine 28, and at the centromeres, where it plays a central role in kinetochore-microtubule attachment. It relocates to the spindle midzone in anaphase and is involved in the formation of the central spindle. In telophase, it is localized at the cleavage furrow, where it is required for the completion of cytokinesis. Survivin's interaction with the export receptor Crm1 is crucially involved in tethering the CPC to the centromeres in prophase and Survivin's BIR domain directly binds to Histone H3 phosphorylated at threonine 3 (21, 61). In addition to that, several post-translational modifications of Survivin play a role in CPC localization (ubiquitination at lysine 63 and phosphorylation at serine 20) and chromosome alignment (phosphorylation at threonine 117) (62–64) (Figure 1.8).

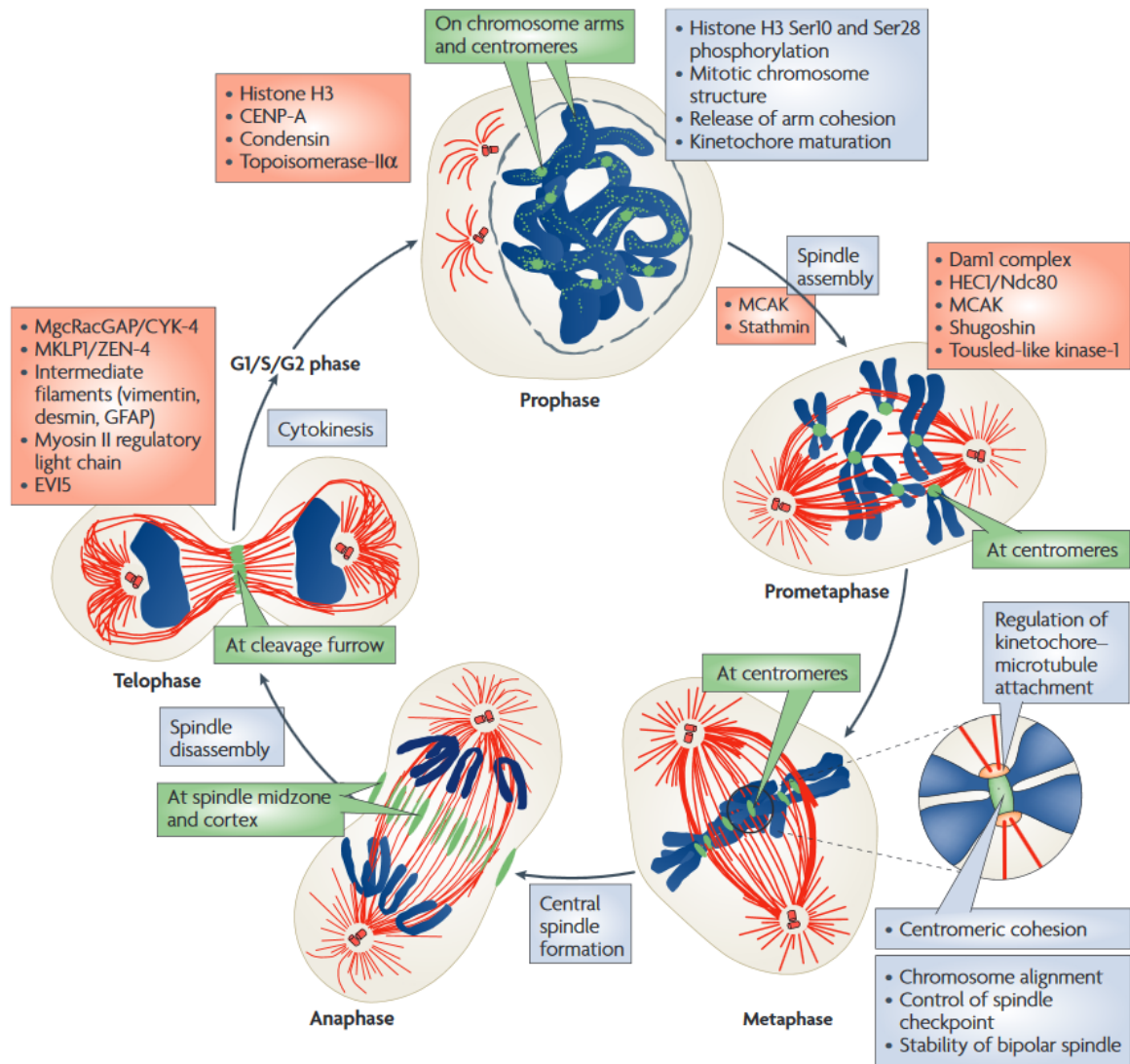


**Figure 1.8: Function and localization of the CPC during mitosis.** The CPC (green) localizes at the chromosome arms (blue) in prophase. In prometaphase, it accumulates at the centromeres, where it remains during metaphase. During anaphase, it relocates to the midzone of the mitotic spindle (red) and later in telophase to the midbody (61).

## 1.5 SURVIVIN'S ROLE IN APOPTOSIS

Apoptosis is the most common form of programmed cell death in multicellular organisms. In contrast to necrosis, which is caused by cellular trauma, apoptosis is a highly regulated process that is necessary to preserve the balance between cell proliferation and cell death (65). Apoptotic cells can be characterized by certain morphological changes like cell shrinkage, blebbing and DNA fragmentation. On a molecular level, apoptosis is induced by specific endopeptidases called caspases (cysteine-dependent aspartyl-specific proteases). Caspases are divided into two main groups: initiator and effector caspases. Initiator caspases (caspases 2, 8 and 9) are synthesized as inactive procaspases (zymogens) and are activated via dimerization following a death stimulus. Effector caspases are activated through cleavage, which leads to conformational changes and the formation of an active site. Effector caspases are responsible for the degradation of a variety of target proteins thereby triggering cell death (66–68). Apoptosis can be initiated through two main pathways, which trigger a caspase cascade (49).

The extrinsic pathway is triggered by extracellular ligands like tumor necrosis factor related apoptosis inducing ligand (TRAIL), which bind to death receptors (e.g. DR4 and DR5) on the surface of the cell (69, 70). This induces the assembly of the death-inducing signaling complex (DISC) together with the adaptor protein fas-associated death domain (FADD) and the initiator procaspases 8 and 10, which are then activated through dimerization. The caspases 8 and 10 are released into the cytoplasm and activate the effector caspases 3, 6 and 7, which then proteolytically degrade numerous intracellular protein targets to trigger cell death (67, 68). In addition, caspase 8 can process Bid into its truncated form (tBid), resulting in its translocation to the outer mitochondrial membrane where it induces oligomerization of Bax/Bak (71, 72). This results in pore formation and the release of cytochrome c and second mitochondria derived activator of caspases (Smac/DIABLO) into the cytosol (73, 74). From this point on, the intrinsic and extrinsic pathways coincide.

The intrinsic pathway is activated by cellular stress like radiation, viral infection, DNA damage or nutrient deprivation. In response to those stimuli, BH3-only proteins (BIM, Bad, Puma or Bid) directly bind Bax/Bak, thereby inducing pore formation and cytochrome c and Smac/DIABLO release from mitochondria (71). Cytochrome c initiates the formation of the apoptosome together with the adaptor protein Apaf-1 and caspase 9. Caspase 9 then activates the effector caspases 3, 6 and 7, which complete the cell death program. While cytochrome c directly induces caspase activation, Smac/DIABLO antagonizes members of the inhibitor of apoptosis family (IAP) like Survivin (75) (Figure 1.9).

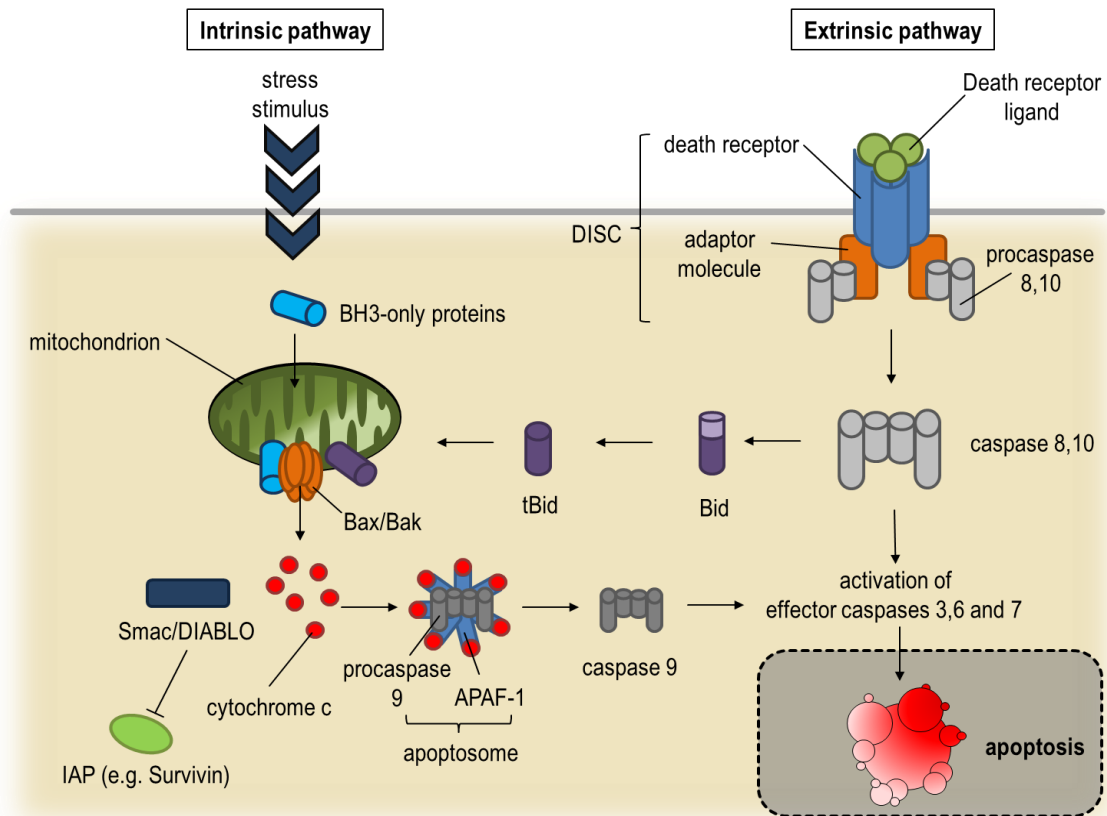


**Figure 1.9: The intrinsic and extrinsic apoptosis pathways.** In the extrinsic pathway ligands bind to death receptors on the surface of the cell. This induces the assembly of the DISC together with FADD and the procaspases 8 and 10. Caspases 8 and 10 activate the effector caspases 3, 6 and 7, which induce apoptosis. Caspase 8 can also process Bid into tBid, resulting in its translocation to the outer mitochondrial membrane where it induces oligomerization of Bax/Bak, pore formation and the release of cytochrome c and Smac/DIABLO into the cytosol. The intrinsic pathway is activated by cellular stress. BH3-only proteins directly bind Bax/Bak, thereby inducing cytochrome c and Smac/DIABLO release from mitochondria. Cytochrome c initiates the formation of the Apoptosome together with Apaf-1 and caspase 9, which activates the effector caspases 3, 6 and 7. Smac/DIABLO antagonizes members of the IAP family like Survivin (modified after (76)).

The human IAP family consists of eight proteins: Bruce/Apollon, neuronal apoptosis inhibitory protein (NAIP), cellular IAP1 (c-IAP1), cellular IAP2 (c-IAP2), X-linked inhibitor of apoptosis protein (XIAP), Livin, inhibitor of apoptosis protein-like protein 2 (ILP2) and Survivin (77). IAPs consist of one to three N-terminal baculovirus IAP repeat (BIR) domains, a 70–80 amino acid long zinc-binding domain and, in some cases, a C-terminal really interesting new gene (RING) domain with an E3-ubiquitin ligase activity and a caspase-associated recruitment domain (CARD) (77, 78). While all IAPs are able to prevent cell

death, only NAIP, c-IAP1, c-IAP2 and XIAP possess the upstream linker region to interact with caspases 3 and 7, and XIAP is the only IAP that is able to inhibit initiator caspase 9 via its BIR3 domain (78, 79) (Figure 1.10).

Survivin is the smallest member of the IAP family and contains only one BIR domain and no CARD or RING domain. Its anti-apoptotic function is not based on direct interaction with caspases (78, 80). Instead, several ways of indirect inhibition through interaction with partner proteins have been shown. An interaction with XIAP results in an increased stability of XIAP, which prevents its proteasomal degradation and increases its anti-apoptotic activity (81). By interacting with Smac/DIABLO, Survivin hinders the interaction of Smac/DIABLO and XIAP, which enables XIAP to inhibit caspases 3, 7 and 9 (75). Survivin is also able to form a complex with hepatitis B X-interacting protein (HBXIP), which is able to bind to procaspase 9 and prevents the recruitment of Apaf-1 and thereby apoptosome formation (82).

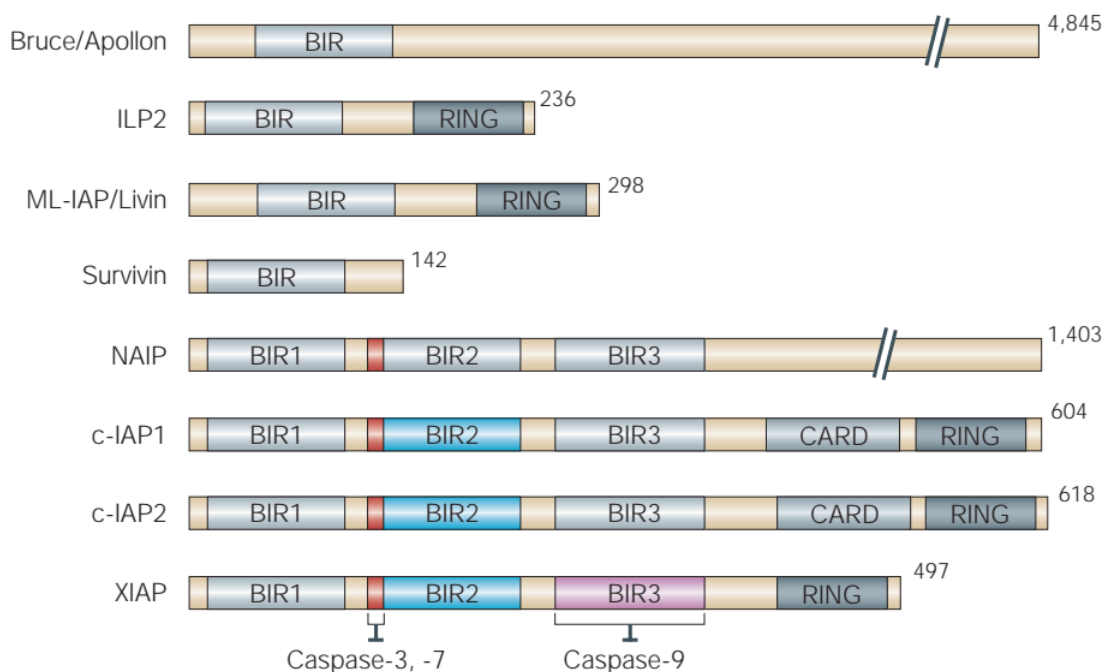


**Figure 1.10: The members of the inhibitor of apoptosis protein (IAP) family.** The IAP family consists of the proteins Bruce/Apollon, ILP2, Livin, Survivin, NAIP, c-IAP1, c-IAP2 and XIAP. All IAPs consist of one to three N-terminal BIR domains and, in some cases, an additional CARD and RING domain. Binding of caspases 3 and 7 occurs via the upstream linker of BIR2 (red) of NAIP, c-IAP1, c-IAP2 and XIAP. BIR3 of XIAP (violet) is able to inhibit caspase 9 (77).

## 1.6 HOMODIMERIZATION OF SURVIVIN

Survivin's dimerization interface comprises the mostly hydrophobic amino acids 6–10 and 89–102 (25). Dimer formation is stabilized by a central  $Zn^{2+}$  ion and supposed to be post-translationally regulated by acetylation and deacetylation of Lysine 129 by CREB-binding protein (CBP) and histone deacetylase 6 (HDAC6) (83). While acetylated Survivin is predominantly dimeric, deacetylated Survivin favours the monomeric state. Mutations of the amino acids phenylalanine 101 and leucine 102 are sufficient to prevent dimerization of Survivin (24). Recent studies indicate that both dimeric and monomeric Survivin have distinct functions within the cell. Monomeric Survivin interacts with the export receptor Crm1 during its nuclear export into the cytoplasm as well as with Smac/DIABLO and XIAP to fulfil its anti-apoptotic functions and with the members of the CPC during mitosis (18, 21, 84). It has been demonstrated that the homodimerization of Survivin antagonizes its nuclear export due to the overlap of the nuclear export signal (aa 89–98) and the dimer interface. Dimeric Survivin has been shown to stabilize microtubules and to inhibit the signal transducer and activator of transcription 3 (STAT3) (83). In addition to that, Survivin dimerization is important to prevent destabilization and degradation of the protein through the proteasome or autophagy (85).

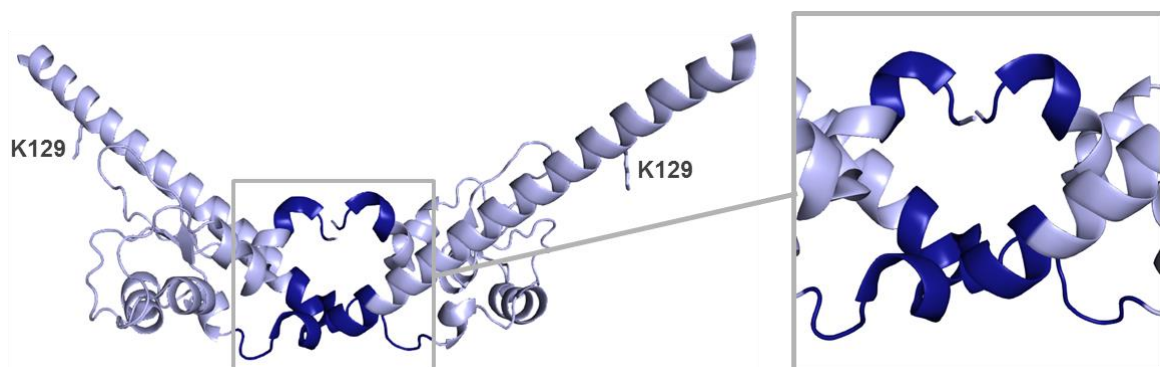


**Figure 1.11: Survivin's dimerization interface.** Survivin's dimerization interface (dark blue) consists of amino acids 6–10 and 89–102. An acetylation of lysine 129 (shown as sticks) within Survivin's C-terminal  $\alpha$ -helix by CREB-binding protein (CBP) is supposed to promote dimerization, while deacetylation by histone deacetylase 6 (HDAC6) inhibits dimerization (25, 83). (PDB: 1E31)

## 1.7 SURVIVIN AS A TARGET IN CANCER THERAPY

Survivin is overexpressed in almost all malignant tumors and is considered an early diagnostic and prognostic biomarker (6–10). In addition, it is associated with an increased resistance against chemo- and radiotherapy, an abbreviated patient survival and a faster disease progression (11–15). Due to its role as a cell cycle regulator and apoptosis inhibitor, it is involved in two key processes of carcinogenesis and therefore considered a promising target for cancer therapy.

Although Survivin is not a protein that is easy to address, having no enzymatic activity and not being expressed on the surface of the cell, various strategies to therapeutically target Survivin have been developed in recent years (86). Antisense oligonucleotides were designed to induce the degradation of Survivin's mRNA, which in turn inhibits Survivin expression resulting in decreased cell proliferation and apoptosis inhibition. The first oligonucleotide drug LY2181308 has by now reached phase II clinical trials (87, 88). Other approaches that managed to decrease Survivin expression by targeting its mRNA are ribozymes, which cleave Survivin mRNA due to their endonucleolytic activity as well as siRNAs, which both seem to show promising results in the first preclinical studies (89–91). As Survivin's cellular functions highly depend on different post-translational modifications, many potential inhibitors target Survivin on a post-translational level for example by inhibiting phosphorylation of Survivin at Threonine 34 during mitosis or by preventing the interaction with chaperone Hsp90 (91–93). Survivin has also been a target for the development of anti-cancer vaccination therapies, where HLA binding peptides were used to induce specific CD4+ T cell stimulation and cytotoxic T cell responses against cells overexpressing Survivin. Some vaccines like SurVaxM have already moved to phase II clinical trials (91, 94, 95). Gene therapy strategies are another promising approach to inhibit Survivin, for example by inducing the expression of cytotoxic genes driven by Survivin's promotor. This has the advantage that apoptosis is only induced in tumor cells, where the Survivin promotor is much more active than in normal cells, while there is only a minimal toxic effect in healthy cells (91, 96, 97). Moreover, several small molecule inhibitors for Survivin are currently evaluated in clinical studies. One of the most prominent examples is YM155, which binds to Survivin's promotor and inhibits Survivin expression, thereby inducing apoptosis and inhibiting cell proliferation. YM155 has already shown significant effects in several phase II studies (98–101).

Taken together, several strategies to address Survivin as a target in cancer therapy have shown promising results so far, even if none of the developed drugs have reached the clinic so far. Although toxicity on normal cells has been a concern in targeting Survivin therapeutically, no major systemic toxicity has been observed in clinical studies (86, 101).

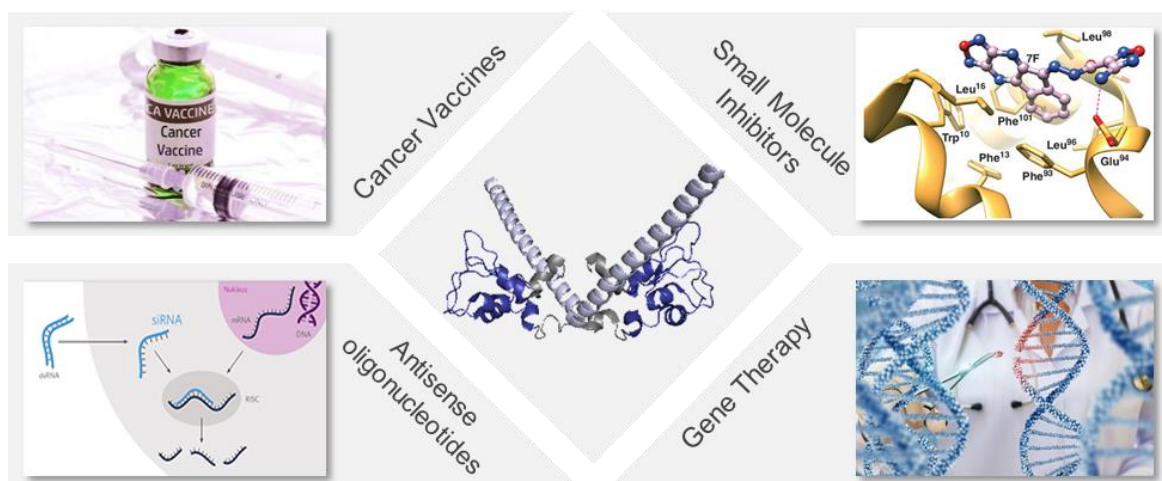


**Figure 1.12: Targeting Survivin in cancer therapy.** Survivin has been addressed as a target for novel cancer therapies in many different ways. It has been used as a target for the development of cancer vaccines to generate an immune response against cells overexpressing Survivin. Various small molecule inhibitors were designed to inhibit Survivin's cellular functions. Antisense oligonucleotides were used to induce Survivin degradation. Survivin also plays a role in the development of gene therapies, for example by using its promoter for the expression of cytotoxic genes (25, 91) (modified after (85, 102–104)).

## 1.8 AIM OF THIS THESIS: TARGETING SURVIVIN'S CELLULAR FUNCTIONS WITH SUPRAMOLECULAR LIGANDS

Survivin is highly upregulated in most cancers and has been associated with a resistance against chemo- and radiotherapy and a poor clinical outcome (11–15). The protein is considered a key player of carcinogenesis due to its anti-apoptotic function and its role in cell proliferation. As it is mainly expressed during embryonic development but mostly absent in terminally differentiated adult tissues, it might be one of the most cancer-specific proteins identified so far (105). However, as Survivin possesses no enzymatic activity, it is challenging to address the protein as a drug target. Current therapeutic strategies include antisense oligonucleotides, siRNAs, small molecule inhibitors, gene therapy and immunotherapy but none of those approaches has reached the clinic yet (86). This thesis thus explores a novel approach by identifying ligands that interfere with Survivin's cellular functions by inhibiting the interaction with its binding partners instead of downregulating its expression. This not only allows a better understanding of Survivin's biological role but moreover contributes to the development of novel anticancer drugs.

The modulation of protein-protein interactions (PPIs) has recently become more and more promising. Twenty years ago, PPIs were still thought to be “intractable” as PPI interfaces are, in contrast to the deep cavities that typically bind small molecules, flat and large (106–108). Thus, high-throughput screenings mostly did not provide validated hits. However, during the last decade, more advanced computational and biophysical methods allowed it to design and identify PPI inhibitors, which are typically larger and more hydrophobic than regular small molecule inhibitors (109). More than 40 PPIs have been targeted, and several inhibitors have reached clinical trials (108, 110).

This thesis is part of the collaborative research project “Supramolecular Chemistry on Proteins” (CRC1093), which focuses on the development of supramolecular ligands to manipulate PPIs. Supramolecular chemistry specializes in non-covalent interactions like van der Waals forces,  $\pi$ - $\pi$  interactions, cation- $\pi$  interactions, hydrogen bonding or ion-dipole interactions (111, 112). In collaboration with the Schmuck group (Supramolecular Chemistry, University of Duisburg-Essen), the aim was to develop highly selective supramolecular ligands to target PPIs between Survivin and its binding partners. To identify such ligands, rational design ideas derived from known structural data of the target protein were combined with combinatorial approaches. The ligands are based on the guanidiniocarbonyl pyrrole cation (GCP), which is a highly specific anion binder. Hence, they target mainly anionic hot spots on the protein surface, which are rich in glutamic and

aspartic acids. Previous work has already shown that the GCP group is able to form specific interactions with target proteins and that the hydrophobic character of the group facilitates cellular uptake (113–115).

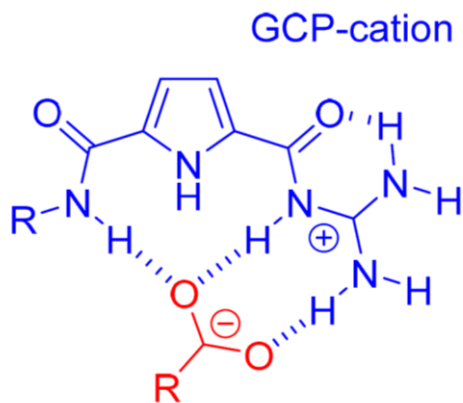


**Figure 1.13: Guanidiniocarbonyl pyrrole group for binding anionic hot spots on proteins.**

Survivin possesses two anionic hot spots that are surface exposed and functionally relevant and can be addressed with this kind of supramolecular ligands. One possibility is to target Survivin's Histone H3 binding site <sup>51</sup>EPDLAQCFFCFKELEGWEPDDDPIEEHKH<sup>80</sup>. The interaction between Survivin and Histone H3 is crucial for Survivin to fulfil its role as a member of the CPC during mitosis. Survivin's BIR domain directly binds to Histone H3 during pro- and metaphase and thereby tethers the CPC to the chromosome arms. Inhibiting the protein-protein interaction between Survivin and Histone H3 would therefore hamper Survivin's role in cell proliferation. Another possibility is to target Survivin's NES <sup>89</sup>VKKQFEELTL<sup>98</sup> with which the protein interacts with the export receptor Crm1. The interaction between Survivin and Crm1 is not only necessary for Survivin's Crm1-mediated nuclear export into the cytoplasm, where it acts as an inhibitor of apoptosis, but also to tether the CPC to the centromeres during mitosis. Impeding the protein-protein interaction between Survivin and Crm1 would therefore interfere with Survivin's role in cell proliferation as well as with its anti-apoptotic functions.

The Schmuck group developed several supramolecular GCP ligands that were designed to specifically target one of Survivin's anionic hot spots. The effect of two of those ligands on Survivin's cellular function is going to be analyzed in detail in this thesis: MM138, which consists of two GCP groups and is supposed to bind to Survivin's Histone H3 binding site and DA162, which is a four-armed ligand that was designed to interfere with the Survivin-

Crm1 binding. This project aims to validate MM138 and DA162 as potential protein-protein inhibitors of the Survivin-Histone H3 or Survivin-Crm1 interaction. This thesis focused on the establishment of different microscopy-based assays to analyze the effect of MM138, DA162 or similar inhibitors on Survivin's cellular functions. This would allow a better understanding of Survivin's biological role and contribute to the development of novel therapeutic strategies.

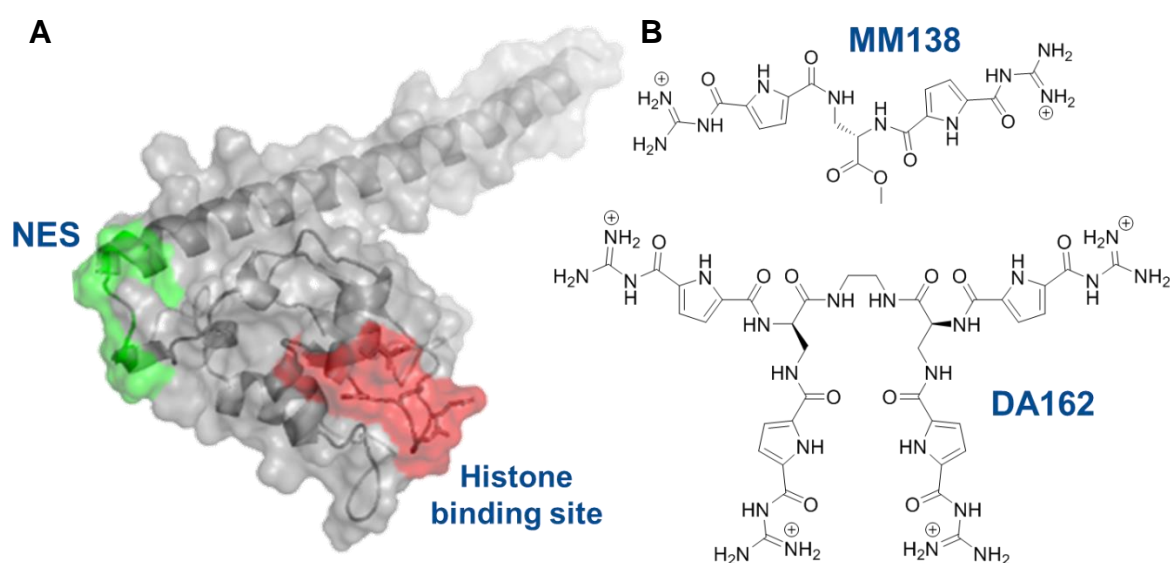


**Figure 1.14: Targeting Survivin's anionic hot spots.** **A)** The NES (aa 89–98) and the Histone H3 binding site of Survivin (aa 51–80) are surface exposed anionic hot spots that can be targeted with supramolecular GCP ligands. **B)** The supramolecular GCP ligands MM138 and DA162 were designed to target Survivin's Histone H3 binding site (MM138) or NES (DA162).

## 2 MATERIAL AND METHODS

### 2.1 MATERIAL

#### 2.1.1 INSTRUMENTS

All instruments and devices used in this work are listed in Table 2.1.

**Table 2.1: Instruments and devices**

<b>instrument</b>	<b>manufacturer</b>
Avance Ultrashield NMR spectrometer	Bruker Corporation, Billerica
Agarose gel electrophoresis chamber	Peqlab Biotechnologie GmbH, Erlangen
BioPhotometer Plus	Eppendorf AG, Hamburg
Calorimeter MicroCal iTC200	Malvern Panalytical GmbH, Kassel
Centrifuge 5417 C/R	Eppendorf AG, Hamburg
Centrifuge ROTINA 380/380 R	Andreas Hettich GmbH & Co. KG, Tuttlingen
Centrifuge Sorvall™ RC 6 Plus	Thermo Fisher Scientific, Waltham
ChemiDoc™ MP Imaging System	Bio-Rad Laboratories GmbH, Munich
CO <sub>2</sub> incubator	Binder GmbH, Tuttlingen
CO <sub>2</sub> incubator INC153	Memmert GmbH & Co. KG, Schwabach
Confocal laser scanning microscope TCS SP8	Leica Microsystems GmbH, Mannheim
Film processor Cawomat 2000 IR	CAWO, Schrobenhausen
Freezer (-20 °C) Liebherr Premium BioFresh	Liebherr GmbH, Biberach
Freezer (-80 °C) Forma 900S-RIFS	Thermo Fisher Scientific, Waltham
Gel caster	Bio-Rad Laboratories GmbH, Munich
Gel documentation system E-Box VX2	Vilber Lourmat GmbH, Eberhardzell
GloMax®-Multi+ Microplate Multimode Reader	Promega Corporation, Fitchburg
GrantBio 360° vertical multi-function rotator PTR-30	Grant Instruments Ltd, Cambridge
GrantBio orbital shaking platform POS-300	Grant Instruments Ltd, Cambridge
Heating plate	Medax GmbH & Co. KG, Rendsburg

<b>instrument</b>	<b>manufacturer</b>
Magnetic stirrer HI 180	Hanna Instruments Deutschland GmbH, Kehl
Microscope Primo Vert	Carl Zeiss, Oberkochen
Mini centrifuge Spectrafuge	Labnet International Inc, Edison
Multichannel Pipette Plus	Eppendorf AG, Hamburg
NMR spectrometer (700 MHz Ultrashield)	Bruker Corporation, Rheinstetten
Orbital benchtop shaker MaxQTM 4000	Thermo Fisher Scientific, Waltham
Orbital shaker POS-300	Grant Instruments Ltd, Royston
Orbital tabletop shaker Forma 420 Series	Thermo Fisher Scientific, Waltham
PAGE chamber Mini-PROTEAN® Tetra Cell	Bio-Rad Laboratories GmbH, Munich
pH meter	Hanna Instruments Deutschland GmbH, Kehl
PIPETMAN® P/Neo	Gilson International B.V., Limburg-Offheim
Pipettes Research Plus	Eppendorf AG, Hamburg
Power supply peqPOWER 300	PEQLAB Biotechnologie GmbH, Erlangen
Power supply PowerPac Basic	Bio-Rad Laboratories GmbH, Munich
Precision balance	Kern & Sohn GmbH, Balingen
Refrigerator Liebherr Comfort	Liebherr GmbH, Biberach
Refrigerator Liebherr Medline	Liebherr GmbH, Biberach
Rotator PTR-30	Grant Instruments Ltd, Royston
Safety cabinet NuAire NU-437-400E	Integra Biosciences GmbH, Fernwald
Safety cabinets HERAsafe	Thermo Fisher Scientific, Waltham
Spectrophotometer NanoDrop™ 2000c	Thermo Fisher Scientific, Waltham
Thermal mixer MHR 11	HLC BioTech, Bovenden
Thermal mixer ThermoMixer Comfort	Eppendorf AG, Hamburg
Thermal printer DPU-414	Seiko Instruments GmbH, Neu-Isenburg
Thermal printer P95D	Mitsubishi Chemical Europe GmbH, Düsseldorf
Thermocycler TProfessional gradient 96	Biometra GmbH, Göttingen
Trans-Blot® SD Semi-Dry Transfer Cell	Bio-Rad Laboratories GmbH, Munich
Ultrasonic homogenizer mini20	Bandelin electronic GmbH & Co. KG, Berlin

<b>instrument</b>	<b>manufacturer</b>
UV Sterilizing PCR Workstation	Peqlab Biotechnologie GmbH, Erlangen
Vacuum removal system AZ 02	HLC BioTech, Bovenden
Vortexer PV-1	Grant Instruments Ltd, Royston
Water bath 1002-1013	Gesellschaft für Labortechnik mbH, Burgwedel
Water purification system Milli-Q®	Merck KGaA, Darmstadt

### 2.1.2 CONSUMABLES

Consumables used in this thesis are listed in Table 2.2.

**Table 2.2: Consumables**

<b>item</b>	<b>supplier</b>
96-well cell culture plates	Sarstedt AG & Co., Nümbrecht
96-well opaque-walled glass bottom plates	Corning, Inc., Corning
Bottle top vacuum filter (0.45 µm)	Sarstedt AG & Co., Nümbrecht
Cell culture dish (6/10 cm)	Sarstedt AG & Co., Nümbrecht
Cell culture flask (T-25, T-75)	Sarstedt AG & Co., Nümbrecht
Cell scraper	Sarstedt AG & Co., Nümbrecht
Cryogenic tubes	Sarstedt AG & Co., Nümbrecht
Erlenmeyer flask (25/50/250/500 ml)	DURAN Group GmbH, Wertheim
Film Super RX	FUJIFILM Europe GmbH, Düsseldorf
Glass bottom dishes (35 mm)	MatTek Corporation, Ashland
Mr. Frosty™ Storage Container	Thermo Fisher Scientific, Waltham
PCR tubes (0.2 ml)	Bio-Rad Laboratories GmbH, Munich
Pipette tips (10/20/200/1250 µl)	Sarstedt AG & Co., Nümbrecht
PVDF membrane Amersham Hybond P 0.2	GE Healthcare Life Sciences, Freiburg
Reaction tubes (1.5/2 ml)	Sarstedt AG & Co., Nümbrecht
Reaction tubes (15/50 ml)	Sarstedt AG & Co., Nümbrecht

item	supplier
Rotilabo®-Blotting Papers	Carl Roth GmbH & Co. KG, Karlsruhe
Serological pipettes (2/5/10/25 ml)	Sarstedt AG & Co., Nümbrecht
UV cuvette	Sarstedt AG & Co., Nümbrecht
μ-Slide 8 well	ibidi GmbH, Planegg

### 2.1.3 CHEMICALS

Chemicals and reagents used in this thesis are listed in Table 2.3.

**Table 2.3: Chemicals and reagents**

chemical/reagent	supplier
Acetic acid	Applichem GmbH, Darmstadt
Acrylamide solution (30 %)	Applichem GmbH, Darmstadt
Agarose	Applichem GmbH, Darmstadt
Ammonium persulfate (APS)	Applichem GmbH, Darmstadt
Antibiotic-Antimycotic	Life Technologies GmbH, Darmstadt
Bio-Rad Protein Assay Dye Reagent (5x)	Bio-Rad Laboratories GmbH, Munich
Bovine serum albumin (BSA)	Applichem GmbH, Darmstadt
Bromophenol blue sodium salt	Applichem GmbH, Darmstadt
Carbenicillin (Carb) disodium salt	Applichem GmbH, Darmstadt
Coomassie Brilliant Blue G-250	Applichem GmbH, Darmstadt
Deoxynucleotide triphosphate (dNTP) Mix	New England BioLabs GmbH, Frankfurt a. M.
Dithiothreitol (DTT)	Applichem GmbH, Darmstadt
Dulbecco's Modified Eagle Medium (DMEM),	Life Technologies GmbH, Darmstadt
Dulbecco's Phosphate-Buffered Saline (DPBS)	Life Technologies GmbH, Darmstadt
Ethanol	VWR International GmbH, Darmstadt
Ethanol technical grade	Applichem GmbH, Darmstadt
Fetal calf serum (FCS)	Life Technologies GmbH, Darmstadt
Glycerol 87 %	Applichem GmbH, Darmstadt
HCS CellMask™ Deep Red Stain	Life Technologies GmbH, Darmstadt

<b>chemical/reagent</b>	<b>supplier</b>
HDGreen™ Plus	INTAS Science Imaging Instruments GmbH,
Hoechst 33342	Applichem GmbH, Darmstadt
Hydrochloric acid 1 M	Applichem GmbH, Darmstadt
Isopropanol	Applichem GmbH, Darmstadt
Kanamycin (Kan) sulfate	Applichem GmbH, Darmstadt
LB medium powder	Applichem GmbH, Darmstadt
Leptomycin B (LMB)	Enzo Life Sciences, Lörrach
Lipofectamine 2000	Life Technologies GmbH, Darmstadt
Luria-Bertani (LB) agar powder	Applichem GmbH, Darmstadt
Magnesium chloride hexahydrate	Applichem GmbH, Darmstadt
Methanol	Applichem GmbH, Darmstadt
Milk powder	Applichem GmbH, Darmstadt
N,N,N',N'-Tetramethylethylenediamine	Applichem GmbH, Darmstadt
Nonidet P-40 (NP-40)	Applichem GmbH, Darmstadt
Normal goat serum	Dako Deutschland GmbH, Hamburg
Optimized Minimum Essential Medium (Opti-	Life Technologies GmbH, Darmstadt
Phenylmethanesulfonylfluoride (PMSF)	Applichem GmbH, Darmstadt
Polyethylenimine (PEI)	Sigma-Aldrich Chemie GmbH, Munich
Potassium chloride	Applichem GmbH, Darmstadt
Potassium dihydrogen phosphate	Applichem GmbH, Darmstadt
Protease inhibitor cocktail tablets Complete	Roche, Mannheim
Roti-Histofix 4 %	Carl Roth GmbH & Co. KG, Karlsruhe
Sodium azide	Applichem GmbH, Darmstadt
Sodium chloride	Carl Roth GmbH & Co. KG, Karlsruhe
Sodium dihydrogen phosphate monohydrate	Carl Roth GmbH & Co. KG, Karlsruhe
Sodium dodecyl sulfate (SDS)	Applichem GmbH, Darmstadt
Tris hydrochloride (Tris-HCl)	Applichem GmbH, Darmstadt
Tris(hydroxymethyl)aminomethane (Tris)	Applichem GmbH, Darmstadt
Triton X-100	Applichem GmbH, Darmstadt
TrypLE Express	Life Technologies GmbH, Darmstadt
Tween 20	Applichem GmbH, Darmstadt

### 2.1.4 BUFFERS, SOLUTIONS AND MEDIA

The compositions of buffers, solutions and media used in this work are listed in Table 2.4. Unless stated otherwise, ingredients were dissolved in ultra-pure water (ddH<sub>2</sub>O).

**Table 2.4: Buffers solutions and media**

<b>buffer/solution/medium</b>	<b>ingredients</b>	<b>final concentration</b>
APS		10 % (w/v)
Carbenicillin		100 mg/ml
Coomassie destaining solution	Acetic acid	10 % (v/v)
	Ethanol	40 % (v/v)
Coomassie staining solution	Acetic acid	10 % (v/v)
	Ethanol	40 % (v/v)
	Coomassie brilliant blue G250	0.1 % (w/v)
DMEM+++	Antibiotic-Antimycotic	1x
	FCS	10 % (v/v) in DMEM
DNA loading dye (10x)	Bromophenol blue	0.25 % (w/v)
	EDTA	100 mM
	Glycerol	20 % (w/v)
	Xylene cyanol	0.25 % (w/v)
Kanamycin		50 mg/ml
LB agar	LB agar powder	40 g/l
		pH 7.5
LB medium	LB medium powder	25 g/l
		pH 7.5

<b>buffer/solution/medium</b>	<b>ingredients</b>	<b>final concentration</b>
HEPES buffer	HEPES	2.5 mM
	TCEP	0.05 mM
	MgCl <sub>2</sub>	1 mM
	NaCl	10 mM
		pH 6.5
NEB antibody dilution buffer	BSA	1 % (w/v)
	Triton X-100	0.3 % (v/v)
		in PBS
NEB blocking buffer	Normal goat serum	5 % (v/v)
	Triton X-100	0.3 % (v/v)
		in PBS
NMR buffer	KPi	50 mM
	KCl	90 mM
	DTT	2 mM
		pH 6.5
PEI		10 mM
		pH 6.8
Phosphate-buffered saline (PBS)	Disodium hydrogen phosphate	10 mM
	Potassium chloride	2.7 mM
	Potassium dihydrogen phosphate	2 mM
	Sodium chloride	137 mM
		pH 7.4
PMSF		0.2 M
		in ethanol

<b>buffer/solution/medium</b>	<b>ingredients</b>	<b>final concentration</b>
SDS sample buffer (5x)	Bromophenol blue	0.1 % (w/v)
	EDTA	5 mM
	Glycerol	30 % (v/v)
	$\beta$ -Mercaptoethanol	7.5 % (v/v)
	SDS	15 % (w/v)
	Tris-HCl	60 mM
		pH 6.8
SDS-PAGE running buffer	Glycine	192 mM
	SDS	0.1 % (w/v)
	Tris	25 mM
Separation gel buffer (4x)	SDS	0.8 % (w/v)
	Tris	1.5 M
		pH 8.8
Sodium azide		0.1 % (w/v)
		in PBS
Stacking gel buffer (4x)	SDS	0.8 % (w/v)
	Tris-HCl	0.5 M
		pH 6.8
Transfer buffer	Glycine	192 mM
	Methanol	20 % (v/v)
	SDS	0.01 % (w/v)
	Tris	25 mM
		pH 8.3
Tris-buffered saline (TBS)	Sodium chloride	150 mM
	Tris-HCl	50 mM
		pH 7.4

buffer/solution/medium	ingredients	final concentration
Tris-buffered saline and Tween 20 (TBST)	Sodium chloride	150 mM
	Tris-HCl	50 mM
	Tween 20	0.1 % (v/v)
		pH 7.4
Washing buffer	DTT	1 mM
	Sodium chloride	150 mM
	Tris-HCl	50 mM
		pH 7.5
WB blocking buffer	Milk powder	5 % (w/v) in TBST

### 2.1.5 BACTERIAL STRAINS

All bacterial strains used in this work are listed in Table 2.5.

**Table 2.5: Bacterial strains.**

strain	genotype	supplier
E. coli XL2-Blue	<i>endA1 supE44 thi-1 hsdR17 recA1 gyrA96 relA1 lac</i> [F' <i>proAB lacI<sup>q</sup>Z<math>\Delta</math>M15 Tn10</i> (TetR) Amy CamR]	Agilent Technologies, Waldbronn
E. coli SoluBL21	F <sup>-</sup> <i>ompT hsd SB</i> (rB- mB-) <i>gal dcm</i> (DE3) + further uncharacterized mutations	Genlantis, San Diego

### 2.1.6 EUKARYOTIC CELLS

The eukaryotic cell lines used in this thesis are listed in Table 2.6.

**Table 2.6: Eukaryotic cell lines.**

cell line	origin	property	reference
A549	<i>Homo sapiens</i> , lung carcinoma	adherent	Research resource identifier: CVCL_0023
HCT 116	<i>Homo sapiens</i> , colorectal carcinoma	adherent	Research resource identifier: CVCL_0291
HEK 293T	<i>Homo sapiens</i> , embryonic kidney	adherent	Research resource identifier: CVCL_1926
HeLa Kyoto	<i>Homo sapiens</i> , cervical adenocarcinoma	adherent	Research resource identifier: CVCL_1922
MDA-MB-231	<i>Homo sapiens</i> , mammary gland/breast adenocarcinoma	adherent	Research resource identifier: CVCL_0062

### 2.1.7 PLASMIDS

The plasmids used in this work are listed in Table 2.7.

**Table 2.7: Eukaryotic expression plasmids.**

plasmid	features	reference
pc3-Cerulean	Blue fluorescent Cerulean	Knauer group, University of Essen
pc3-Cerulean-Citrine	Blue fluorescent Cerulean C-terminally fused with the yellow fluorescent Citrine	Knauer group, University of Essen
pc3-Cerulean-Survivin	Survivin wildtype N-terminally fused with Cerulean	Knauer group, University of Essen

<b>plasmid</b>	<b>features</b>	<b>reference</b>
pc3-Cerulean-SurvivinDIM	Dimerization-deficient SurvivinF101AL102A mutant N-terminally fused with Cerulean	Knauer group, University of Essen
pc3-Citrine	Yellow fluorescent Citrine	Knauer group, University of Essen
pc3-Citrine-Survivin	Survivin wildtype N-terminally fused with Citrine	Knauer group, University of Essen
pc3-Citrine-SurvivinDIM	Dimerization-deficient SurvivinF101AL102A mutant N-terminally fused with Citrine	Knauer group, University of Essen
pc3-Crm1-GFP	Crm1 C-terminally fused with green fluorescent GFP	Knauer group, University of Essen
pc3-GFP	Green fluorescent GFP	Knauer group, University of Essen
pc3-myc-Survivin	Survivin wildtype N-terminally fused with myc	Knauer group, University of Essen
pc3-Survivin-HA	Survivin wildtype C-terminally fused with HA	Knauer group, University of Essen
pcDNA3.1(+)	cloning vector with amp <sup>r</sup> , neo <sup>r</sup>	Invitrogen, Karlsruhe
SRV100 NESmut	Crm1-binding deficient Survivin1-100 L96/98A NES mutant biosensor, kan <sup>r</sup>	Rodriguez group, University of the Basque Country, Spain
SRV100 WT	Survivin 1-100 biosensor, kan <sup>r</sup>	Rodriguez group, University of the Basque Country, Spain

### 2.1.8 SEQUENCING PRIMERS

Sequencing primers (Table 2.8) were synthesized by LGC Genomics, Berlin.

**Table 2.8: Sequencing primers.**

<b>name</b>	<b>sequence (5' → 3')</b>
CMV-F	CGCAAATGGGCGGTAGGCGTG
pcDNA3.1-R	TAGAAGGCACAGTCGAGGCT

### 2.1.9 ANTIBODIES

The primary (Table 2.9) and secondary antibodies (Table 2.10) were used for western blotting (WB, section 2.2.3.4), immunofluorescence (IF, section 2.2.4.7) and Proximity ligation assays (PLA, section 2.2.4.8).

**Table 2.9: Primary antibodies.**

<b>antigen</b>	<b>origin</b>	<b>dilution</b>			<b>manufacturer</b> (order number)
		WB	IF	PLA	
Centromere (Crest)	Human serum		1:400		Antibodies Incorporated (15-234)
CRM1	Mouse monoclonal	1:1000	1:500	1:500	Santa Cruz Biotechnology Inc, Heidelberg (sc-74454)
CRM1	Rabbit polyclonal	1:10000	1:1000	1:1000	Novus Biologicals Ltd, Cambridge (NB100-79802)
Flag-tag	Mouse monoclonal	-	1:300	-	Sigma-Aldrich Chemie GmbH, Munich (F3165)
HA-tag	Mouse monoclonal	1:1000	1:1000	-	BioLegend Inc, Koblenz (901501)
HA-tag	Rabbit polyclonal	1:10000	-	-	Abcam PLC, Cambridge (AB9110)
Histone H3	Mouse monoclonal	1:1000	1:500	1:500	Abcam PLC, Cambridge (AB195277)

antigen	origin	dilution			manufacturer (order number)
		WB	IF	PLA	
Histone H3 (T3p)	Rabbit polyclonal	1:500	1:500	1:500	Abcam PLC, Cambridge (AB130940)
Myc-tag	Mouse monoclonal	1:1000	1:500	-	BioLegend Inc, Koblenz (901501)
Myc-tag	Rabbit polyclonal	1:10000	-	-	Abcam PLC, Cambridge (AB9110)
Survivin	Mouse monoclonal	1:1000	1:100	1:100	OriGene Technologies Inc, Herford (TA502236)
Survivin	Rabbit polyclonal	1:1000	1:300	1:250	Novus Biologicals Ltd, Cambridge (NB500-201)
$\alpha$ -Tubulin	Mouse monoclonal	1:8000	1:4000	-	Sigma-Aldrich Chemie GmbH, Munich (T6074)
$\gamma$ -Tubulin	Rabbit polyclonal	1:1000	1:1000	-	Novus Biologicals Ltd, Cambridge (NB120-11318)

**Table 2.10: Secondary antibodies.**

antibody	origin	dilution			manufacturer (order number)
		WB	IF	PLA	
Anti-mouse IgG- AF 488	Goat	-	1:1000	-	Life Technologies GmbH, Darmstadt (A11001)
Anti-mouse IgG- AF568	Goat	-	1:1000	-	Life Technologies GmbH, Darmstadt (A11004)
Anti-rabbit IgG- AF488	Goat	-	1:1000	-	Life Technologies GmbH, Darmstadt (A11008)
Anti-rabbit IgG- AF568	Goat	-	1:1000	-	Life Technologies GmbH, Darmstadt (A11011)
Anti-mouse IgG- HRP	Sheep	1:10000	-	-	GE Healthcare Life Sciences, Freiburg (NXA931)
Anti-rabbit IgG- HRP	Donkey	1:10000	-	-	GE Healthcare Life Sciences, Freiburg (NA934)

### 2.1.10 DNA AND PROTEIN STANDARDS

All DNA and protein standards used in this work are listed in Table 2.11.

**Table 2.11: DNA and protein standards.**

<b>name</b>	<b>supplier</b>
GeneRuler 1 kb DNA Ladder	Thermo Fisher Scientific, Waltham
GeneRuler 1 kb Plus DNA Ladder	Thermo Fisher Scientific, Waltham
Spectra Multicolor Broad Range Protein Ladder	Thermo Fisher Scientific, Waltham

### 2.1.11 KITS

Kits that were used in this work are listed in Table 2.12.

**Table 2.12: Kits**

<b>kit</b>	<b>supplier</b>
ApoLive-Glo™ Multiplex Assay	Promega Corporation, Madison
CellTiter 96® AQueous One Solution Cell Proliferation Assay	Promega Corporation, Madison
Duolink® In Situ Detection Reagents Orange	Sigma-Aldrich Chemie GmbH, Munich
Duolink® In Situ PLA® Probes Mouse/Rabbit	Sigma-Aldrich Chemie GmbH, Munich
Expand High Fidelity PLUS PCR System	Roche, Mannheim
NucleoBond Xtra Midi kit	Macherey-Nagel GmbH & Co. KG, Düren
NucleoSpin 8 Plasmid kit	Macherey-Nagel GmbH & Co. KG, Düren
NucleoSpin Gel and PCR Clean-up kit	Macherey-Nagel GmbH & Co. KG, Düren
Pierce ECL Plus Western Blotting Substrate kit	Thermo Fisher Scientific, Waltham
TaKaRa DNA ligation kit	Clontech, Saint-Germain-en-Laye

### 2.1.12 SOFTWARE

The software used in this thesis is listed in Table 2.13.

**Table 2.13: Software.**

<b>software</b>	<b>manufacturer</b>
Adobe Illustrator CS4	Adobe Systems GmbH, Munich
Adobe Photoshop CS4	Adobe Systems GmbH, Munich
A plasmid Editor (ApE)	Wayne Davis (University of Utah), Salt Lake City
Canvas 11	ACD Systems International Inc., Seattle
Cell Profiler	Carpenter Lab (Broad Institute of Harvard and MIT), Cambridge
Citavi 5	Swiss Academic Software GmbH, Wädenswil
Clustal Omega	EMBL-EBI, Cambridge
Gene Construction Kit 3.0	Textco BioSoftware, Inc., New Hampshire
GraphPad Prism 5	GraphPad Software, Inc., La Jolla
ImageJ	U.S. National Institutes of Health, Bethesda
Instinct Software	Promega Corporation, Madison
Leica Application Suite X (LAS-X)	Leica Microsystems GmbH, Mannheim
Maestro Elements	Schrödinger, LLC, New York
MicroCal iTC200	Malvern Panalytical GmbH, Kassel
Microsoft Office	Microsoft Corporation, Redmond
NanoDrop 2000/2000c software	Thermo Fisher Scientific, Waltham
PyMOL	Schrödinger LCC, Portland
Top Spin	Bruker Corporation, Billerica

## 2.2 METHODS

### 2.2.1 MOLECULAR BIOLOGY

#### 2.2.1.1 POLYMERASE CHAIN REACTION (PCR)

Polymerase chain reaction (PCR) is a method to amplify DNA fragments using a DNA template, a sequence-specific pair of primers, a DNA polymerase and deoxynucleotide triphosphates (dNTPs) (116). One PCR cycle consists of three steps that are repeated 30 to 40 times. First, the double-stranded DNA template and primers are denatured at 94 °C, then the primers anneal to the DNA template at 2 to 5 °C below the melting temperature of the primers and finally DNA polymerase elongates the new DNA strand at 72 °C by incorporating free dNTPs.

PCR was performed using the Expand High Fidelity PLUS PCR System (Roche Diagnostics) according to the manufacturer's protocol. 50 µl of reaction mixture (see Table 2.14) were prepared and the PCR program (see Table 2.15) was carried out by a Thermocycler TProfessional standard gradient 96 from Biometra.

**Table 2.14: PCR reaction mixture**

Reagent	Volume
Buffer 2 (5x)	10 µl
Primer 1 (10 µM)	2 µl
Primer 2 (10 µM)	2 µl
dNTPs (10 mM each)	1 µl
DNA polymerase	0.5 µl
DNA template (10 ng/µL)	2 µl
H <sub>2</sub> O	32.5 µl

Table 2.15: PCR program

Step	Temperature	Time	
Initial denaturation	94 °C	2 min	
Denaturation	94 °C	30 s	x 30
Annealing	50–70 °C	30 s	
Elongation	72 °C	45 s	
Final elongation	72 °C	5 min	
Storage	15 °C	hold	

### 2.2.1.2 AGAROSE GEL ELECTROPHORESIS

Agarose gel electrophoresis is used to separate DNA by size. Negatively charged DNA moves through an agarose gel that is placed in an electric field. Small DNA fragments migrate faster through the pores of the gel than larger ones, thereby achieving size separation. DNA bands can then be visualized with fluorescent DNA-binding dyes.

Agarose gels were made by solving 1–2 % (w/v) agarose in 1 x TAE buffer, heating the mixture to boiling point and supplementing DNA-staining dye HDGreen™ PLUS from INTAS in a 10,000-fold dilution before casting the gel. After polymerization, the gel was inserted into a gel chamber filled with TAE buffer. Samples were mixed with 10 x DNA loading dye and loaded on the gel. Additionally, a DNA ladder (GeneRuler™ 1 kb PLUS from Thermo Scientific) was loaded on the gel. Electrophoretic separation occurred at 90–120 V for 45–90 min using a power supply peqPOWER 300 from PEQLAB. DNA bands were visualized with UV light in an E-Box VX2 documentation system from Vilber Lourmat.

### 2.2.1.3 PURIFICATION OF DNA FRAGMENTS

The NucleoSpin Gel and PCR Clean-Up kit (Macherey-Nagel) was used according to the manufacturer's protocol to remove contaminations like PCR additives, DNA dyes and enzymes from DNA. For this, the DNA was bound to a silica membrane, washed several times and eluted in 30 µl elution buffer.

#### **2.2.1.4 PHOTOMETRIC DETERMINATION OF DNA CONCENTRATION**

DNA concentration was measured using a NanoDrop™ 2000c from Thermo Fisher Scientific. The concentration was determined by measuring the absorbance at 260 nm, which is the absorption maximum of nucleic acids. An absorbance of 1 corresponds to a concentration of 50 ng/μl of DNA. Absorbance was also measured at 230 nm and 280 nm to determine DNA purity. The  $A_{260}/A_{230}$  ratio reveals contamination with organic substances and should ideally be 2.0 if the DNA is pure. The  $A_{260}/A_{280}$  ratio shows protein or RNA contamination and should lie between 1.8 and 2.0.

#### **2.2.1.5 RESTRICTION DIGEST**

Plasmids and PCR products were cut at distinct sites with restriction enzymes from NEB. The restriction enzymes, which mostly belong to the type II endonucleases, cut dsDNA within their palindromic recognition site by catalyzing the hydrolysis of phosphodiester bonds of the DNA backbone.

For analytical digests 200–500 ng DNA were digested with 4 units of restriction enzymes in the recommended buffer for 1 h at 37 °C. Preparative digests were performed using 5–10 μg DNA and 40 units of restriction enzymes for 1–4 h at 37 °C. Fragments were then separated by agarose gel electrophoresis (section 2.2.1.2) and afterwards purified (section 2.2.1.3).

#### **2.2.1.6 LIGATION**

Ligation of digested DNA fragments was performed using the TaKaRa DNA ligation kit (version 2.1) from Clontech. The included T4 DNA ligase catalyzes the formation of phosphodiester bonds in the DNA backbone and is able to ligate blunt ends as well as cohesive ends. The ligation mix contained 0.5 μl vector, 2 μl insert and 2.5 μl Solution I of the kit and was incubated for 30 min at RT. Afterwards, the ligated construct was transformed into competent *E. coli* XL2-Blue cells (section 2.2.2.1).

### **2.2.1.7 DNA SEQUENCE ANALYSIS**

DNA sequencing was carried out by LGC Genomics using the Sanger or chain termination sequencing method (117). For this, 20 µl plasmid DNA with a concentration of 80–100 ng/µl were sent to LGC Genomics. Sequencing primers were provided by the company. Sequencing results were analyzed with ApE (Wayne Davis) and Clustal Omega (EMBL-EBI).

## **2.2.2 MICROBIOLOGY**

### **2.2.2.1 TRANSFORMATION OF COMPETENT *E. COLI* CELLS**

Transformation enables the uptake and incorporation of exogenous DNA into competent *E. coli* cells. 30 µl of XL2 Blue cells were incubated with 2 µl of ligation product or 0.2 µg of plasmid DNA for 20 min on ice. Then a heat shock was performed for 1 min at 42 °C in a water bath, followed by a 5 min incubation on ice. The cells were resuspended in antibiotic-free LB medium and incubated for 1 h at 37 °C and 180 rpm before they were plated on a LB agar plate containing the respective antibiotic and incubated over night at 37 °C.

### **2.2.2.2 LONG-TERM STORAGE OF TRANSFORMED *E. COLI* CELLS**

Transformed *E. coli* cells were stored as bacterial glycerol stocks. They were generated by mixing 800 µl of overnight bacterial culture with 200 µl of 87 % glycerol. The solution was then frozen in liquid nitrogen and stored at -80 °C.

### **2.2.2.3 PLASMID ISOLATION FROM *E. COLI* CELLS**

To isolate plasmid DNA from *E. coli* cells a mini or midi preparation was performed depending on the required amount of DNA. The plasmids were isolated using alkaline lysis with subsequent chromatographic purification (118).

For mini preparations, 8 ml LB medium containing the respective antibiotic (50 µg/ml kanamycine or 100 µg/ml carbenicillin) were inoculated with a bacterial colony from a LB agar plate and incubated over night at 37 °C and 200 rpm. Afterwards, 6 ml of the bacterial culture were centrifuged (2,000 x g, 5 min, RT) and the plasmids were isolated using the

NucleoSpin 8 Plasmid kit (Macherey-Nagel) according to the manufacturer's protocol. Plasmid DNA was eluted with 100 µl elution buffer.

For midi preparations, 300 ml LB medium containing the respective antibiotic were inoculated with 1 ml of bacterial culture and incubated over night at 37 °C and shaking at 120 rpm. Cells were then centrifuged (3900 x g, 15 min, 4 °C) and plasmids were isolated using the NucleoBond Xtra Midi kit (Macherey-Nagel). Following elution, plasmid DNA was precipitated with isopropanol, desalted in 70 % ethanol and after drying dissolved in H<sub>2</sub>O.

## **2.2.3 BIOCHEMISTRY**

### **2.2.3.1 DETERMINATION OF PROTEIN CONCENTRATION**

#### **2.2.3.1.1 BRADFORD-ASSAY**

The Bradford Assay, which is based on the binding of the dye Coomassie Blue G250 to proteins, was used to determine the protein concentration of whole cell lysates. For this, 1 µl of lysate was mixed with 200 µl of 5 x protein assay dyereagent (Bio-Rad) and 800 µl PBS in a cuvette. After incubation for 5 min at RT, absorption at 595 nm was measured with the Bio-Photometer Plus (Eppendorf AG). Protein concentration was determined by comparing the absorption to a predefined calibration curve of bovine serum albumin (BSA).

#### **2.2.3.1.2 NANODROP**

Protein concentration measurement with the NanoDrop™ 2000 c spectrophotometer (Thermo Scientific) is based on the absorbance of proteins at 280 nm due to the aromatic amino acids tryptophan and tyrosine. Prior to measurement, the extinction coefficient and molecular weight of the protein were entered and a blank measurement with the respective buffer was performed before 2 µl of the protein solution were measured.

### **2.2.3.2 SDS-POLYACRYLAMIDE GEL ELECTROPHORESIS**

SDS-polyacrylamide gel electrophoresis (SDS-PAGE) was used to separate proteins according to their size within an electric field. Depending on the amount of negatively charged sodium dodecyl sulfate (SDS) bound to the proteins, their electrophoretic mobility varies (119). Therefore, small proteins move faster through the pores of the gel than large

ones. Discontinuous gels consisting of a stacking and separation gel were used to improve the formation of protein bands. The pore size of the gels varied depending on polyacrylamide concentration as summarized in table Table 2.16. Gels were cast in a BioRad casting module. First, the separation gel was cast and after polymerization the stacking gel was added on top and a comb was inserted to form wells.

Protein samples were mixed with 5 x SDS sample buffer and denatured for 10 min at 95 °C before they were loaded onto the gel. In addition, 8 µl of the Spectra Multicolor Broad Range protein ladder (Thermo Scientific) was used as size standard. Electrophoresis was performed at 160–180 V for 60–90 min. Afterwards, gels were either stained with Coomassie (section 2.2.3.3) or used for Western blotting (section 2.2.3.4).

**Table 2.16: Composition of SDS-polyacrylamid gels with a thickness of 1.5 mm**

Component	separation gel		stacking gel
	12.5 %	15 %	4 %
ddH <sub>2</sub> O (ml)	1.6	1.2	2.5
4 x separation gel buffer (ml)	1.3	1.3	-
4 x stacking gel buffer (ml)	-	-	1.3
30 % polyacrylamide (ml)	2.1	2.5	0.65
10% APS (µl)	50	50	50
TEMED (µl)	5	5	5

### **2.2.3.3 COOMASSIE-STAINING OF POLYACRYLAMIDE GELS**

Coomassie was used for unspecific protein staining, as it binds to basic amino acids under acidic conditions. Polyacrylamide gels were incubated with Coomassie brilliant blue G-250 staining solution for 30 min on a shaker platform and then washed several times with H<sub>2</sub>O before they were incubated in destaining solution for 2 h to remove background staining.

#### **2.2.3.4 WESTERN BLOTTING**

Western blotting is a method to transfer proteins from a polyacrylamide gel onto a membrane on which they can be detected with specific antibodies. By applying an electric field, the negatively charged proteins migrate towards the anode. The membrane is placed between the polyacrylamide gel and the anode, allowing the proteins to be immobilized due to hydrophobic and electrostatic interactions. On the membrane, the proteins can be visualized through antigen-antibody interaction.

In this work, the semi-dry blot technique was applied. An Amersham Hybond P 0.2 PVDF membrane was activated in methanol for 1 min and afterwards equilibrated in Western Blot buffer for 15 min together with the polyacrylamide gel and four pieces of blotting paper (Carl Roth). The blot sandwich was assembled from anode to cathode and consisted of two pieces of blotting paper, the PVDF membrane, the polyacrylamide gel and two additional pieces of blotting paper. The electrophoretic transfer was performed using a Trans-Blot<sup>®</sup> SD Semi-Dry Transfer Cell (Bio-Rad) applying 100 mA per gel for 90 min. After successful transfer, unspecific binding sites were blocked by incubating the membrane for 1 h in WB blocking buffer on a shaking platform. The membrane was then incubated in primary antibody solution at 4 °C over night. Following three washing steps with TBST for 5 min each, the membrane was incubated with a HRP-conjugated secondary antibody for 1 h at RT. After two additional washing steps with TBST and one with TBS, proteins were detected using Pierce<sup>™</sup> ECL Plus Western Blotting Substrate or SuperSignal<sup>™</sup> West Femto Maximum Sensitivity Substrate (both Thermo Scientific) and the film processor CAWOMAT 2000 IR (CAWO) or the ChemiDoc<sup>™</sup> MP Imaging System (Bio-Rad).

#### **2.2.3.5 ISOTHERMAL TITRATION CALORIMETRY**

Isothermal titration calorimetry (ITC) was used to determine binding constants of potential ligands to Survivin. It is based on the measurement of temperature changes produced by, in this case, ligand binding. By stepwise titration of Survivin 1-120 to the ligand, data-points are collected that reveal information about binding affinity and stoichiometry of the reaction.

ITC experiments were carried out using the MicroCal iTC200 calorimeter in combination with the MicroCal iTC200 software (Malvern Panalytical). Measurements were performed at 25 °C using HEPES buffer (pH 6.5). 300 µl of 100 µM ligand solution were inserted into the sample cell and subjected to stepwise titration with 30 x 1 µl of a 380 µM solution of Survivin 1-120 (provided by Sandra Bäcker, Knauer group, University of Duisburg-Essen).

The reference power was set to 5  $\mu\text{cal/s}$ , the initial delay to 60 s and the stirring speed to 750 rpm. Injections took place every 3 s.

Blank titrations of either the ligand or the protein solution into buffer were performed as a control. Data was analyzed with the AFFINImeter software for Isothermal Titration Calorimetry by S4SD-AFFINImeter.

ITC experiments were conducted and ligands were provided by Dennis Aschmann, Schmuck group, University of Duisburg-Essen.

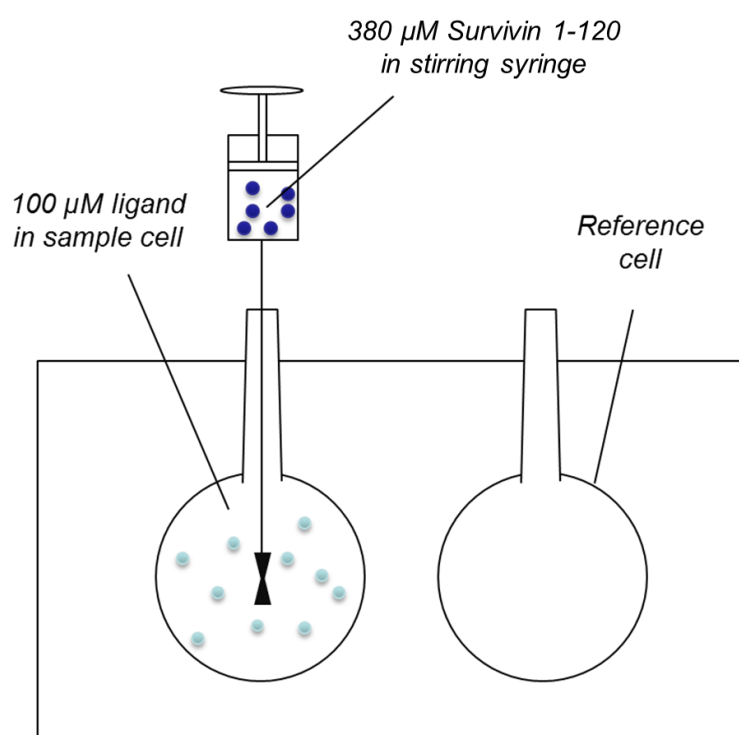


**Figure 2.1: Setup for ITC experiments.** 100  $\mu\text{M}$  ligand solution were inserted into the sample cell and subjected to stepwise titration with 380  $\mu\text{M}$  solution of Survivin 1-120 from the stirring syringe.

### 2.2.3.6 NMR SPECTROSCOPY

$^{15}\text{N}$ -Survivin (1-120) for NMR experiments was expressed as GST fusion protein with a PreScission Protease site in *E. coli* SoluBL21 (Genlantis) cells using M9 minimal media with  $^{15}\text{N}$  ammonium chloride as the sole nitrogen source. The protein was purified using a GSH affinity column. Subsequently, the GST tag was cleaved by addition of PreScission protease and the tagless  $^{15}\text{N}$ -Survivin was isolated using a Superdex S75 size exclusion column in

tandem with a GSH affinity column to separate the Survivin dimer (27.7 kDa) from the free GST (28.0 kDa).

NMR experiments were recorded at 25 °C on a Bruker 700 MHz Avance Ultrashield NMR spectrometer (Bruker) equipped with a 5 mm TCI  $^1\text{H}/^{13}\text{C}/^{15}\text{N}/\text{D}$  cryoprobe with z-gradient. The  $^1\text{H},^{15}\text{N}$ -BEST-TROSY pulse sequence is part of the NMRlib 2.0 pulse sequence tools from IBS (Grenoble, France; <http://www.ibs.fr/research/scientific-output/software/pulse-sequence-tools/>) (120). Spectra were processed with Topspin 3.5 and analyzed in CARA (121). The assignments of Survivin (1-120) were obtained from the BMRB database (BMRB # 6342) (122).

NMR samples were prepared in NMR buffer (50 mM  $\text{KPi}$  pH 6.5, 90 mM KCl, 2 mM DTT) containing 10 %  $\text{D}_2\text{O}$  with a final protein concentration of 300  $\mu\text{M}$ . A 10 mM stock of MM138 in DMSO- $d_6$  was added stepwise, yielding a final ligand concentration of 400  $\mu\text{M}$  in the presence of at most 4% DMSO- $d_6$ .  $^1\text{H},^{15}\text{N}$ -BEST-TROSY spectra were recorded for each titration step. To account for slight shifting of signals due to the presence of DMSO, a control titration with the corresponding volumes of DMSO- $d_6$  without ligand was performed.

The amide chemical shift perturbation  $\Delta\delta_{\text{total}}$  was calculated from the  $^1\text{H}$ - and  $^{15}\text{N}$ -shifts according to equation 1 using the spectra with no and 400  $\mu\text{M}$  of ligand.  $\Delta\delta_{\text{N}}$  and  $\Delta\delta_{\text{H}}$  represent the chemical shift perturbation value of the amide nitrogen and proton relative to the corresponding DMSO control spectrum without ligand (123):

$$\Delta\delta_{\text{total}} = \sqrt{\Delta\delta_{\text{H}}^2 + (0.154 \cdot \Delta\delta_{\text{N}})^2} \quad [1]$$

Furthermore, the relative intensities  $I/I_0$  were evaluated. A more than average decrease in intensity also indicates ligand binding due to intermediate exchange kinetics.

All NMR experiments including  $^{15}\text{N}$ -Survivin (1-120) expression were performed by Dr. Christine Beuck, Bayer group, ZMB, University of Duisburg-Essen.

## **2.2.4 CELL BIOLOGY**

### **2.2.4.1 CULTIVATION OF EUKARYOTIC CELLS**

The adherent eukaryotic cell lines used in this work were cultivated in DMEM+++ growth medium at 37 °C, 5 % CO<sub>2</sub> and 90 % relative humidity. They were passaged twice a week in a ratio of 1:20 to regulate cell density and to supply the cells with fresh growth medium. For this, growth medium was aspirated and the cells were rinsed with 5 ml DPBS. Afterwards, 2 ml of TrypLE Express (Life Technologies) were added to the cells to allow enzymatic detachment from the cell culture flask. The cells were incubated on a heating plate until all of them were detached before 8 ml of new DMEM+++ were added. 0.5 ml of the cell suspension were then added to a new culture flask together with 9.5 ml of fresh DMEM+++.

### **2.2.4.2 FREEZING AND THAWING CELLS**

For long term conservation, cells were centrifuged at 300 x g for 5 min at RT and resuspended in FCS with 10% DMSO at a cell density of approximately  $2 \times 10^6$  cells / ml. 1 ml aliquots were transferred into cryo tubes and frozen in a Mr. Frosty™ freezing container at -80 °C, which allows cooling of -1 °C per minute. Cells were then put into a liquid nitrogen tank for long-term storage.

Cells were thawed by heating the cryo tube in a 37 °C water bath and adding the cells to a reaction tube containing 9 ml of pre-warmed culture medium. The suspension was centrifuged at 300 x g for 5 min at RT and the cells were resuspended in 10 ml fresh culture medium before they were transferred into a culture flask.

### **2.2.4.3 TRANSIENT TRANSFECTION OF EUKARYOTIC CELLS**

Transient transfection enables the temporal introduction of exogenous DNA into eukaryotic cells. In this work, the transport of the DNA through the cell membrane was achieved chemically by using the cationic polymer Polyethylenimine (PEI) or the liposomal transfection reagent Lipofectamine 2000 (Life Technologies). PEI binds to the negatively charged DNA and thereby facilitates cellular uptake via endocytosis while Lipofectamine 2000 forms liposomes around the DNA, which can fuse with the cell membrane.

For the transfection with PEI, cells were seeded in 3 cm dishes in 2 ml of DMEM+++ growth medium. Transfection took place after a 24 h incubation of the cells at 37 °C and 5 % CO<sub>2</sub>. For this purpose, two transfection solutions were generated. Solution A contained 10 µl of 10 mM PEI and 60 µl PBS and solution B consisted of 2 µg of DNA and 60 µl of PBS. Solution A and B were mixed, incubated for 5 min at RT to allow complex formation and added to the cells. Following transfection, the cells were incubated for 24 h at 37 °C and 5 % CO<sub>2</sub> before they were used in further experiments.

For Lipofectamine 2000 transfection, cells were also seeded 24 h in advance. Again, two transfection solutions were prepared. Solution A consisted of 3 µl of Lipofectamine 2000 and 100 µl of Opti-MEM whereas solution B contained 2 µg of DNA and 100 µl of Opti-MEM. Both solutions were vortexed and combined. The transfection mix was then vortexed again and incubated for 5 min at RT before it was added to the cells. After 24 h at 37 °C and 5 % CO<sub>2</sub> the cells were used for further experiments.

If the transfection took place in other cell culture dishes or in a different volume of growth medium, the volumes of the transfection reagents were adjusted accordingly.

#### **2.2.4.4 PREPARATION OF WHOLE CELL LYSATES FROM EUKARYOTIC CELLS**

Whole cell lysates were generated by chemically lysing cells with RIPA buffer containing the detergents sodium deoxycholate and NP40. Cells were first detached from the 6 cm cell culture dish with a cell scraper. The cell suspension was then centrifuged at 500 x g for 5 min at 4 °C and washed with PBS before it was resuspended in 300 µl RIPA buffer. After incubating the cells for 30 min on ice, they were sonicated twice with a Sonopuls mini20 ultrasonic homogenizer for 10 s and an amplitude of 90 %. After centrifugation at 20,000 x g for 20 min at 4 °C, the supernatant was transferred into a new reaction tube and stored at -80 °C after freezing it in liquid nitrogen.

#### **2.2.4.5 IMMUNOPRECIPITATION**

Immunoprecipitation is a method to precipitate proteins from eukaryotic cell lysates. A specific antibody coupled to magnetic beads was used to separate the target protein from the lysate by applying a magnetic field. This allowed the investigation of protein-protein interactions, as binding partners were still bound to the precipitated target protein (Co-IP).

Immunoprecipitation was performed using the  $\mu$ MACS isolation kits (Miltenyi Biotec). Eukaryotic cells were transiently transfected with a plasmid coding for the tagged target protein. 24 h after transfection, cell lysates were generated (section 2.2.4.4) using interaction buffer instead of RIPA buffer. Before adding 50  $\mu$ l Tag antibody-coupled magnetic beads to the lysates, input samples were taken. The lysates were incubated on the beads for 1 h on ice and then transferred onto a  $\mu$  column that had been placed into a  $\mu$ MACS separator and equilibrated with 200  $\mu$ l interaction buffer. The column was washed four times with 200  $\mu$ l interaction buffer and once with 100  $\mu$ l wash buffer 2 from the kit. Elution was achieved by adding 20  $\mu$ l preheated (95 °C) elution buffer from the kit onto the column and incubating for 5 min before adding another 50  $\mu$ l of preheated elution buffer. The eluates were collected in 1.5 ml reaction tubes and input and eluate samples were analyzed by SDS-PAGE (section 2.2.3.2) and Western Blot (section 2.2.3.4).

#### **2.2.4.6 CONFOCAL FLUORESCENCE MICROSCOPY**

A fluorescence microscope uses laser light of distinct wavelengths to excite fluorophores, causing them to emit light of a longer wavelength that can then be detected by the microscope to create a fluorescence image. Confocal microscopy is a special form of fluorescence microscopy, where only a small layer of the sample is excited, thereby increasing contrast and lateral resolution of the pictures.

Confocal fluorescence microscopy images were taken with the scanning microscope TCS SP8 (Leica Microsystems) equipped with four lasers (Argon: 458/476/488/496/514 nm; DPSS: 561 nm; Helium Neon: 633 nm; UV Diode: 405 nm), two PMT confocal imaging detectors and one sensitive imaging hybrid detector. The samples were imaged with a HCX PL APO CS 63.0 x / 1.20 water objective or a HCX PL APO 63 x / 1.4–0.6 oil objective. The microscope was operated with the Leica Application Suite X (LAS X) software (Leica Microsystems).

#### **2.2.4.7 IMMUNOFLUORESCENCE STAINING**

Immunofluorescence is a technique to visualize proteins in cells with fluorophore-conjugated antibodies. In this work, the indirect immunofluorescence (IF) staining was applied, where two different antibodies, a target specific primary antibody and a fluorophore-conjugated secondary antibody, were used. Cells were seeded in culture dishes suitable for microscopy and prior to IF staining fixed with 4 % Roti<sup>®</sup>-Histofix for 20 min at RT.

Following three washing steps with PBS, the cells were permeabilized and unspecific binding sites were blocked for 30 min at 37 °C with NEB blocking buffer containing TritonX-100 and normal goat serum. Afterwards, the cells were incubated with primary antibodies diluted in NEB Ab dilution buffer at 4 °C over night. After washing three times with PBS, the secondary antibody solution was added onto the cells and incubated for 1 h at RT in the dark. The secondary antibody was again diluted in NEB Ab dilution buffer and was supplemented with 10 µg/ml Hoechst33342 and HCS CellMask™ Deep Red Stain (Thermo Scientific) if needed. Following three final washing steps with PBS, the samples were stored at 4 °C in 0.1% (w/v) sodium azide/PBS before they were analyzed with the confocal fluorescence microscope (section 2.2.4.6).

#### **2.2.4.8 PROXIMITY LIGATION ASSAY**

The *in situ* proximity ligation assay (PLA) is a method to analyze protein-protein interactions in cells on an endogenous level. Two primary antibodies bind to the two potentially interacting targets. These antibodies are then recognized by secondary antibodies, which are conjugated to a matched pair of short single-stranded oligonucleotides (PLA probes). If the two targets interact and are in close proximity (<40 nm), the oligonucleotide probes will hybridize and ligate with two additional connector oligonucleotides to form a continuous circular DNA structure. DNA polymerase then amplifies these circular structures through rolling-circle amplification with fluorescent nucleotides that can be detected as PLA signals with fluorescence microscopy (Figure 2.2).

PLA staining was performed with the Duolink® In Situ Orange PLA Kit Mouse/Rabbit together with the Duolink® In Situ PLA® Probes and Detection Reagents from Sigma-Aldrich. Cells were seeded in 35 mm glass bottom dishes (MatTek) and fixed with 4 % Roti®-Histofix for 20 min at RT prior to PLA staining. Following three washing steps with PBS, the cells were permeabilized and unspecific binding sites were blocked for 30 min at 37 °C with NEB blocking buffer containing TritonX-100 and normal goat serum. Afterwards, the cells were incubated at 4 °C over night with two primary antibodies derived from mouse and rabbit, which were diluted in NEB Ab dilution buffer. Duolink® In Situ PLA probes Anti-Rabbit PLUS and Anti-Mouse MINUS were added after washing three times with PBS and incubated for 1 h at 37°C. Following three additional washing steps, the ligation solution was incubated on the cells for 30 minutes at 37°C. After another three washing steps, the amplification reagents were added and incubated for 100 minutes at 37°C. Cells were then stained with 10 µg/ml Hoechst33342 and HCS CellMask™ Deep Red Stain (Thermo Scientific) in a

dilution of 1:5000 in PBS for 20 min at RT in the dark before they were stored at 4 °C in 0.1% (w/v) sodium azide / PBS until they were microscopically analyzed.

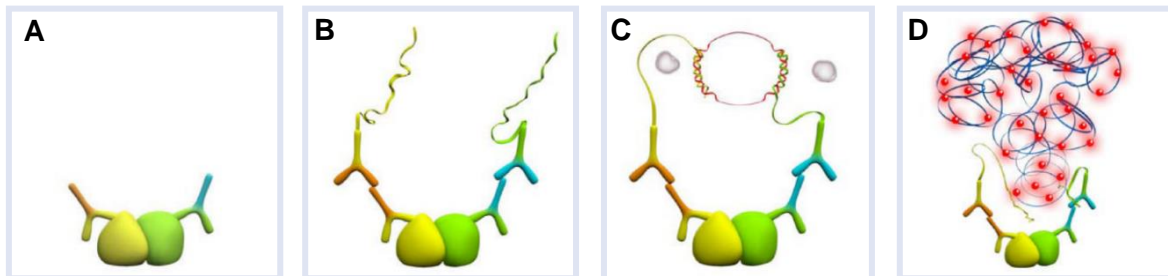


**Figure 2.2: The PLA enables the analysis of endogenous protein-protein interactions. A)** Primary antibodies bind to two potentially interacting targets. **B)** These antibodies are recognized by secondary antibodies, which are conjugated to a matched pair of short single-stranded oligonucleotides (PLA probes). **C)** If the two targets interact and are in close proximity (<40 nm), the oligonucleotide probes hybridize and ligate with two additional connector oligonucleotides to form a continuous circular DNA structure. **D)** DNA polymerase amplifies these circular structures through rolling-circle amplification with fluorescent nucleotides (modified after (124)).

Subsequently, maximum projection images of z-stacks were analyzed with Cell Profiler. The outlines of the nuclei were defined based on Hoechst 33342 staining (primary objects) and the outlines of the entire cells were encircled based on Cell Mask staining and defined as secondary objects. PLA foci within the cells were then detected and assigned to the respective parental cells.

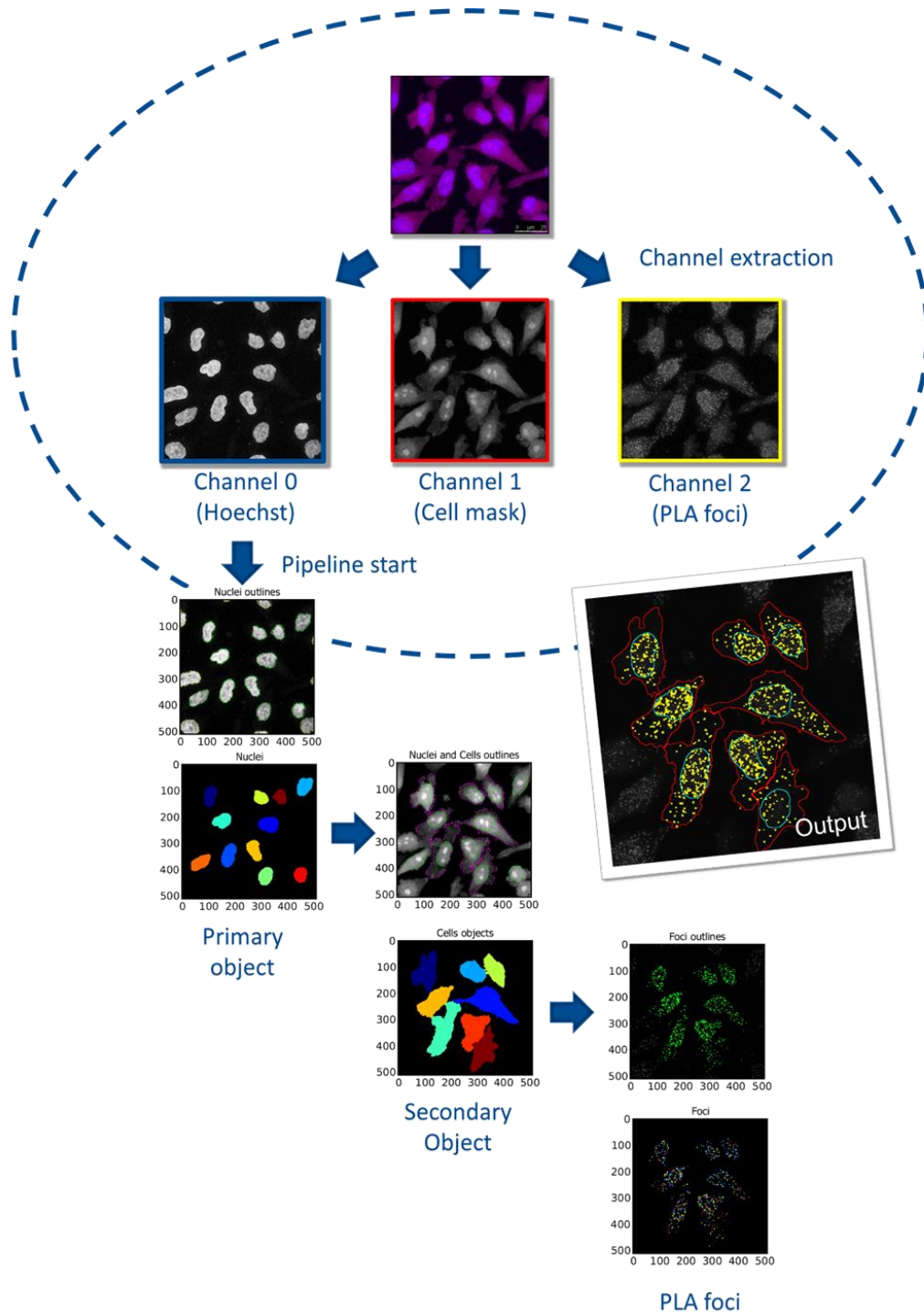


**Figure 2.3: PLA analysis conducted with Cell Profiler.** For quantification, Hoechst 33342 stained nuclei were defined as primary objects (blue). Cell Mask was used to define the entire cells as secondary objects (red). Finally, PLA foci (yellow) within the respective cells were counted and assigned to the parental cells. Cells which were partly out of the field of view were not included into the analysis (modified after (76)).

#### **2.2.4.9 SRV100 BIOSENSOR ASSAY**

The SRV100 biosensor assay was used to analyze the export activity of Crm1 in the presence or absence of potential Survivin-Crm1 inhibitors in a cellular context (125). The biosensor (SRV100) is composed of a shortened version of Survivin (1–100), which contains the NES responsible for the interaction with the export receptor Crm1 and in addition two nuclear localization signals (NLS) and a 3 x Flag-tag. The NLS sequences ensure a nuclear localization of the biosensor in case it is not actively exported by Crm1. If no inhibitor is added, Crm1 is able to export the biosensor into the cytoplasm. If an inhibitor is able to prevent Survivin from interacting with Crm1, the biosensor would remain in the nucleus (Figure 2.4).

293T cells were seeded in 8 well  $\mu$ -slides (ibidi) 24 h before they were transfected with 300 ng of the plasmids SRV100 (biosensor) and Crm1-GFP (section 2.2.4.3). 4 h after transfection the respective Survivin-Crm1 inhibitors were added to the culture medium. 24 h after transfection, the Flag-tag of the biosensor was stained (AF568) via immunofluorescence (section 2.2.4.7). Cells were additionally stained with 10  $\mu$ g/ml Hoechst33342 and HCS CellMask™ Deep Red Stain (Thermo Scientific) in a dilution of 1:5000 in PBS for 20 min at RT in the dark before they were stored at 4 °C in 0.1% (w/v) sodium azide/PBS until they were microscopically analyzed.

Biosensor plasmids used in this assay were kindly provided by the group of Jose A. Rodríguez, University of the Basque Country, Spain.

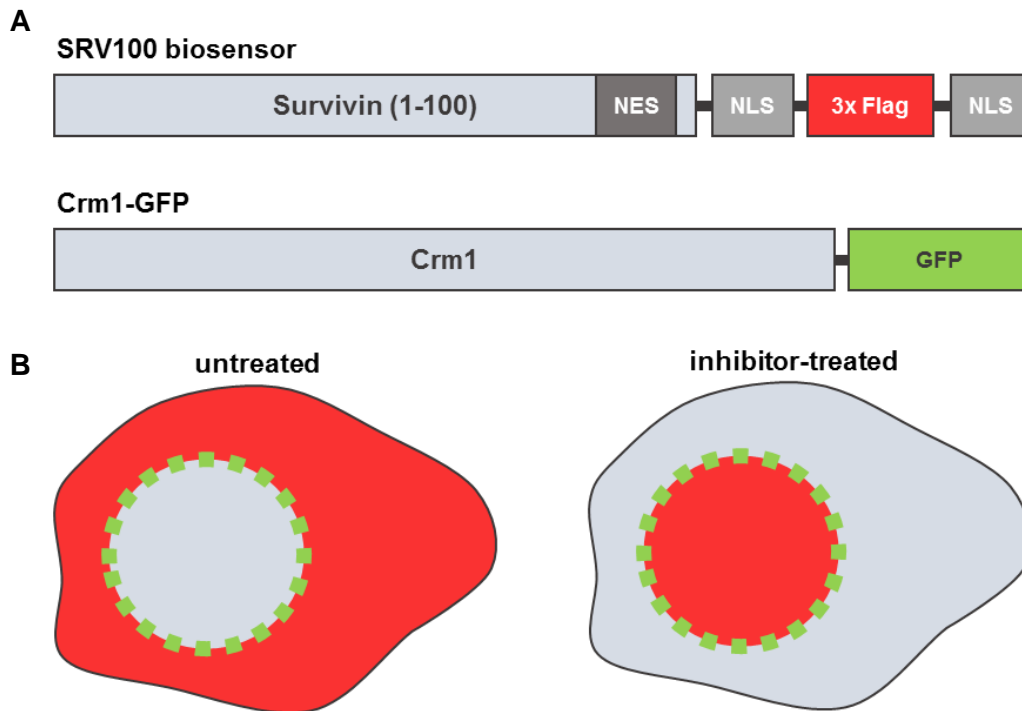


**Figure 2.4: The SRV100 biosensor assay enables the analysis of Crm1's export activity in a cellular system. A)** The SRV100 biosensor is composed of a shortened version of Survivin (1–100), two nuclear localization signals (NLS) and a 3 x Flag-tag. It was co-transfected with Crm1-GFP. **B)** If no inhibitor is added, Crm1 (green) is able to export the biosensor (red) into the cytoplasm. If an inhibitor is able to prevent Survivin from interacting with Crm1 (green), the biosensor (red) would remain in the nucleus.

#### 2.2.4.10 FÖRSTER RESONANCE ENERGY TRANSFER (FRET)

Förster resonance energy transfer (FRET) is based on the principle of radiation-free energy transfer between two fluorophores (126). One fluorophore is called the donor fluorophore and the other one the acceptor fluorophore. The donor absorbs light of a higher frequency than the acceptor. If donor and acceptor are in close proximity (<10 nm), a radiation-free energy transfer from the donor to the acceptor occurs. Therefore, the emission spectrum of the donor has to overlap with the absorption spectrum of the acceptor.

FRET can be used to analyze protein-protein interactions in a cellular context. In this work, it was performed to investigate Survivin's dimerization behavior by coupling Survivin to a donor fluorophore (Cerulean-Survivin) and an acceptor Fluorophore (Citrine-Survivin, Figure 2.5). Both constructs were transfected into HeLa cells (section 2.2.4.3). 24 h after transfection, cells were fixed and analyzed with the FRET Ab wizard of the SP8 confocal microscope (Leica Microsystems). FRET was measured using the acceptor photobleaching technique, where the donor fluorescence is measured before and after destroying the

acceptor via photobleaching. If donor and acceptor were in close proximity, an increase in donor fluorescence can be observed.

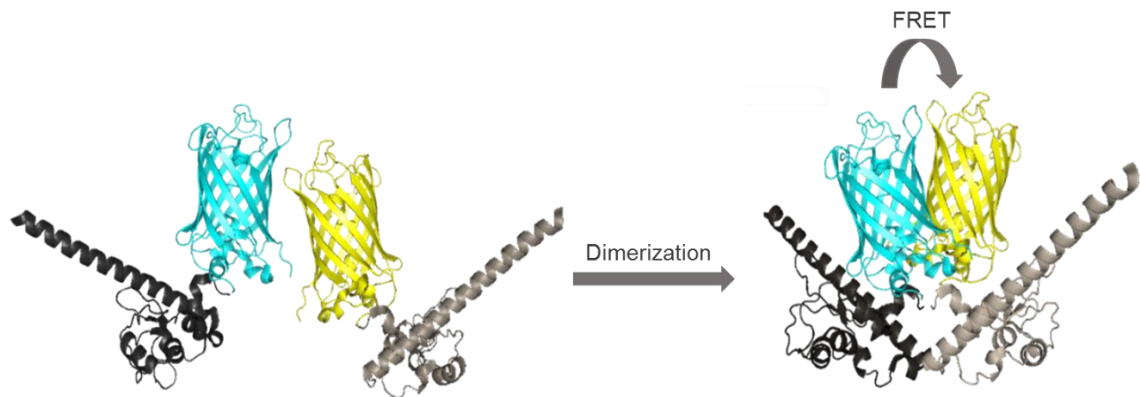


**Figure 2.5: FRET between Cerulean-Survivin and Citrine-Survivin.** If Cerulean-Survivin (donor) and Citrine-Survivin (acceptor) dimerize, a radiation-free energy transfer from the donor to the acceptor occurs, which is called FRET.

#### **2.2.4.11 CELL PROLIFERATION, VIABILITY AND APOPTOSIS ASSAYS**

##### **2.2.4.11.1 CELLTITER 96® AQUEOUS ONE CELL PROLIFERATION ASSAY**

The CellTiter 96® Aqueous One Cell Proliferation Assay (Promega) was used to observe cell proliferation after treatment with different ligand concentrations. The assay determines the number of viable cells per well by using the MTS tetrazolium compound (Owen's reagent) that is bioreduced by NADPH or NADH in living cells into a colored formazan product (Figure 2.6).

The assay was performed according to the manufacturer's protocol by adding 20 µl of CellTiter 96® Aqueous One Solution Reagent directly into each culture well and incubating for 4 h. Afterwards, the absorption was measured at 490 nm with a GloMax®-Multi plate reader (Promega).

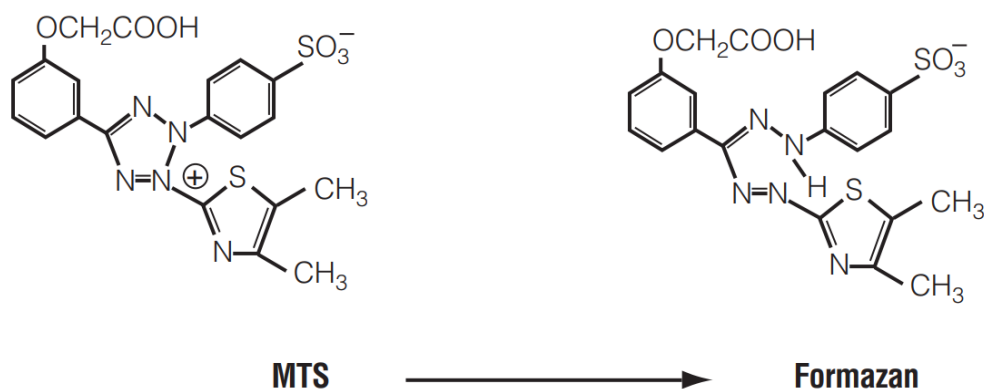


**Figure 2.6: Structures of the MTS substrate and the product formazan.** MTS is bioreduced by NADPH or NADH produced by dehydrogenase enzymes in metabolically active cells into the coloured product formazan (127).

#### 2.2.4.11.2 APOlive-GLO™ MULTIPLEX ASSAY

The ApoLive-Glo™ Multiplex Assay (Promega) enables to assess cell viability and caspase activation in a combined assay. Cell viability is measured by adding a substrate for the live-cell protease. The substrate enters intact cells and gets cleaved by the live-cell protease generating a fluorescent signal proportional to the number of living cells (128). In the second part of the assay, caspase activity, a marker for apoptosis, is detected by adding a luminogenic caspase-3/7 substrate to the cells (Figure 2.7).

The assay was performed according to the manufacturer's protocol. Briefly, cells were seeded in opaque-walled 96 well glass bottom plates (Corning) and treated with the respective ligands at different time points. Cells were then treated with the viability reagent and incubated for 2 h at 37 °C and 5 %CO<sub>2</sub> before fluorescence was measured at 400<sub>Ex</sub>/505<sub>Em</sub> with a GloMax®-Multi plate reader (Promega). Afterwards, the Caspase-Glo® 3/7 reagent was added and the cells were incubated for 2 h at RT before luminescence was measured with the plate reader.

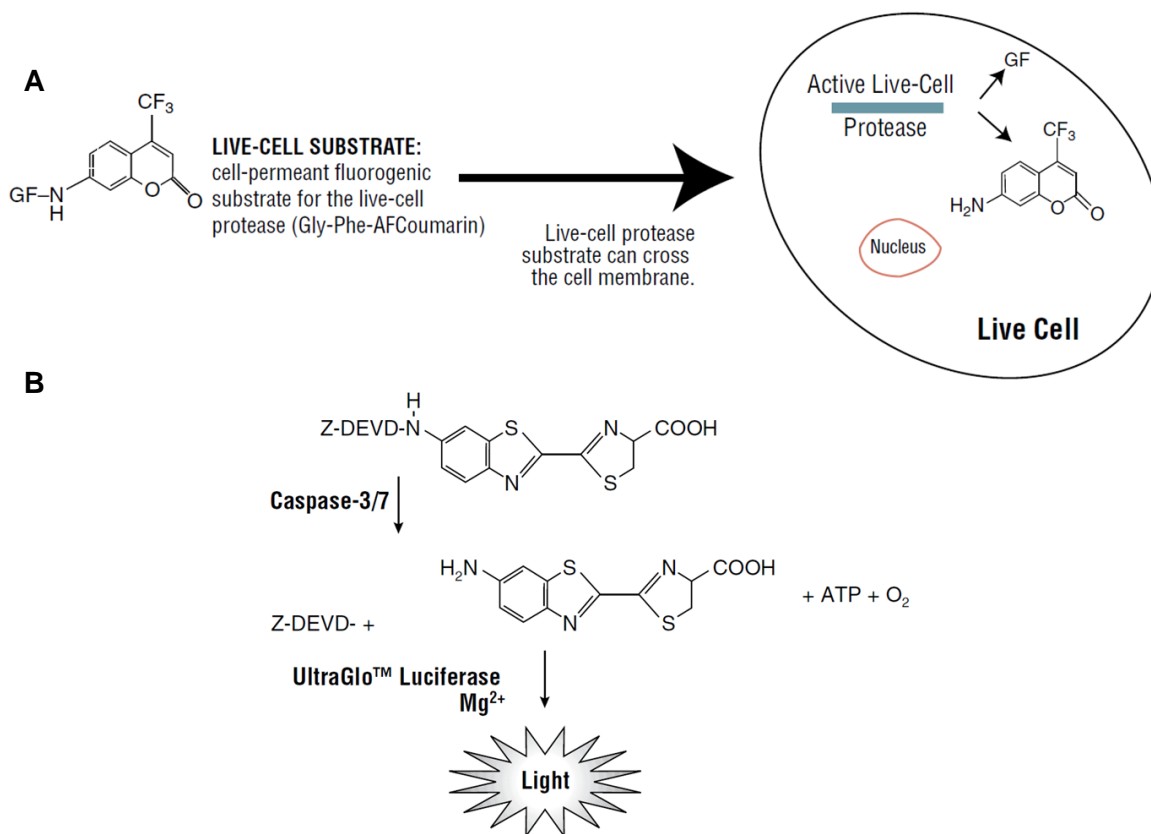


**Figure 2.7: Detection of cell viability and caspase 3/7 activation using the ApoLive-Glo™ Multiplex Assay from Promega. A)** Cell viability measurement via a substrate for live-cell protease that is cleaved into the fluorescent AFC. **B)** Detection of apoptosis via a caspase 3/7 substrate that is cleaved into a substrate for luciferase that generates a luminescent signal (128).

## 2.2.5 BIOINFORMATICS

### 2.2.5.1 DOCKING

Docking was performed using the program Maestro Elements (Schrödinger) and setting up a Glide Ligand Docking Calculation. In advance, ligands were prepared with LigPrep. The crystal structure of Survivin (pdb: 1XOX) was repaired with the “Protein Preparation” tool prior to running “Glide Grid Generation” and “Glide Ligand Docking”. Calculations took place with either the Survivin monomer or dimer.

All docking studies were performed by Matthias Killa, Schmuck group, University of Duisburg-Essen.

## 3 RESULTS

Survivin is highly upregulated in most cancers and has been associated with a resistance against chemo- and radiotherapy and a poor clinical outcome (11–15). The protein is considered a key player of carcinogenesis due to its anti-apoptotic function and its role in cell proliferation (3–5). This thesis explores a novel approach to interfere with Survivin's cancer-promoting functions by using supramolecular ligands that were designed to specifically target either Survivin's Histone H3 or its Crm1 binding site.

### 3.1 TARGETING THE SURVIVIN-HISTONE H3 INTERACTION WITH SUPRAMOLECULAR GCP LIGANDS

The interaction between Survivin and Histone H3 is crucial for Survivin to fulfil its role within the CPC during mitosis. Survivin's BIR domain directly binds to Histone H3 during pro- and metaphase and thereby tethers the CPC to the chromosome arms. MM138 was designed to target Survivin's Histone H3 binding site and inhibit the interaction between the two proteins to interfere with Survivin's role in cell proliferation. This part of the project aims to establish different cellular and *in vitro* assays to validate MM138 as a potential protein-protein inhibitor of the Survivin-Histone H3 interaction.

#### 3.1.1 DOCKING STUDIES PREDICT BINDING OF MM138 TO SURVIVIN'S HISTONE H3 BINDING SITE

In collaboration with the Schmuck group, the supramolecular ligand MM138 was designed to specifically target the interaction between Survivin and Histone H3. Preliminary docking studies revealed that MM138 seems to bind to Survivin's Histone H3 binding site <sup>51</sup>EPDLAQCFKCFKELEGWEPDDDDPIEEHKKH<sup>80</sup>. The anionic hot spot is surface accessible and rich in glutamic and aspartic acids.

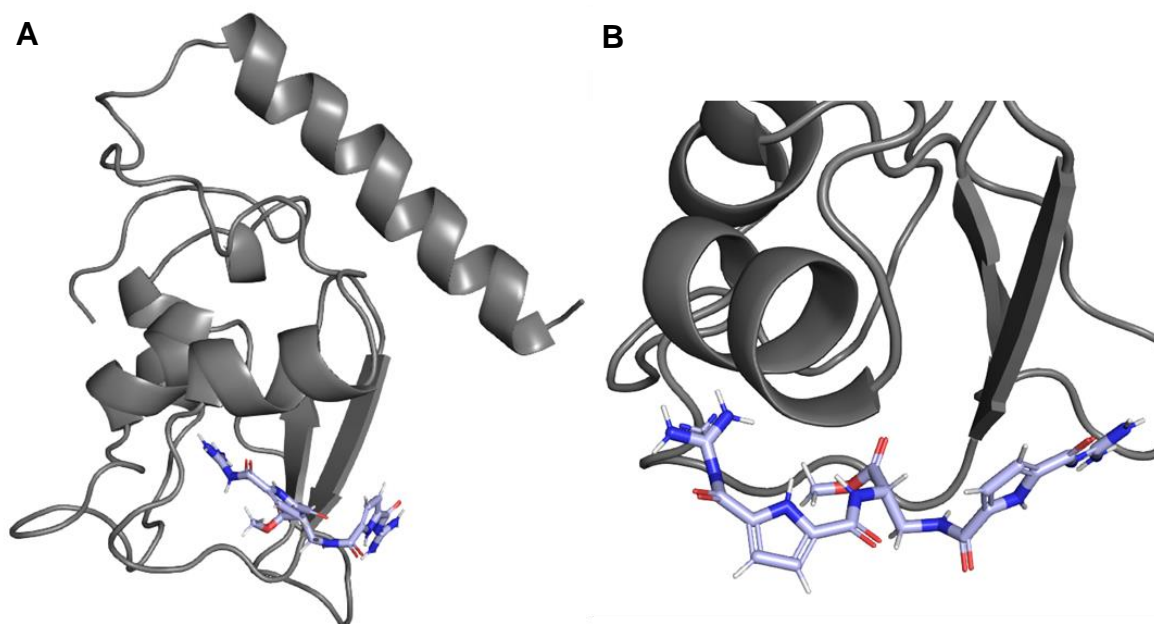


**Figure 3.1: Docking predicts binding of MM138 to Histone H3 binding site. A)** Docking of MM138 to Survivin monomer. **B)** Close-up of MM138 interacting with Survivin's Histone H3 binding site. Docking was performed by Matthias Killa, Schmuck group, University of Duisburg-Essen (PDB:1XOX) (25).

The 2D model of the docking results highlights how the GCP ligand MM138 presumably interacts with Survivin. MM138 consists of two GCP groups. The amino groups of the cationic GCP ligand seem to interact with the anionic glutamic acids 65 and 76 as well as aspartic acids 71 and 72.

All docking studies were conducted by Matthias Killa, Schmuck group, University of Duisburg-Essen.

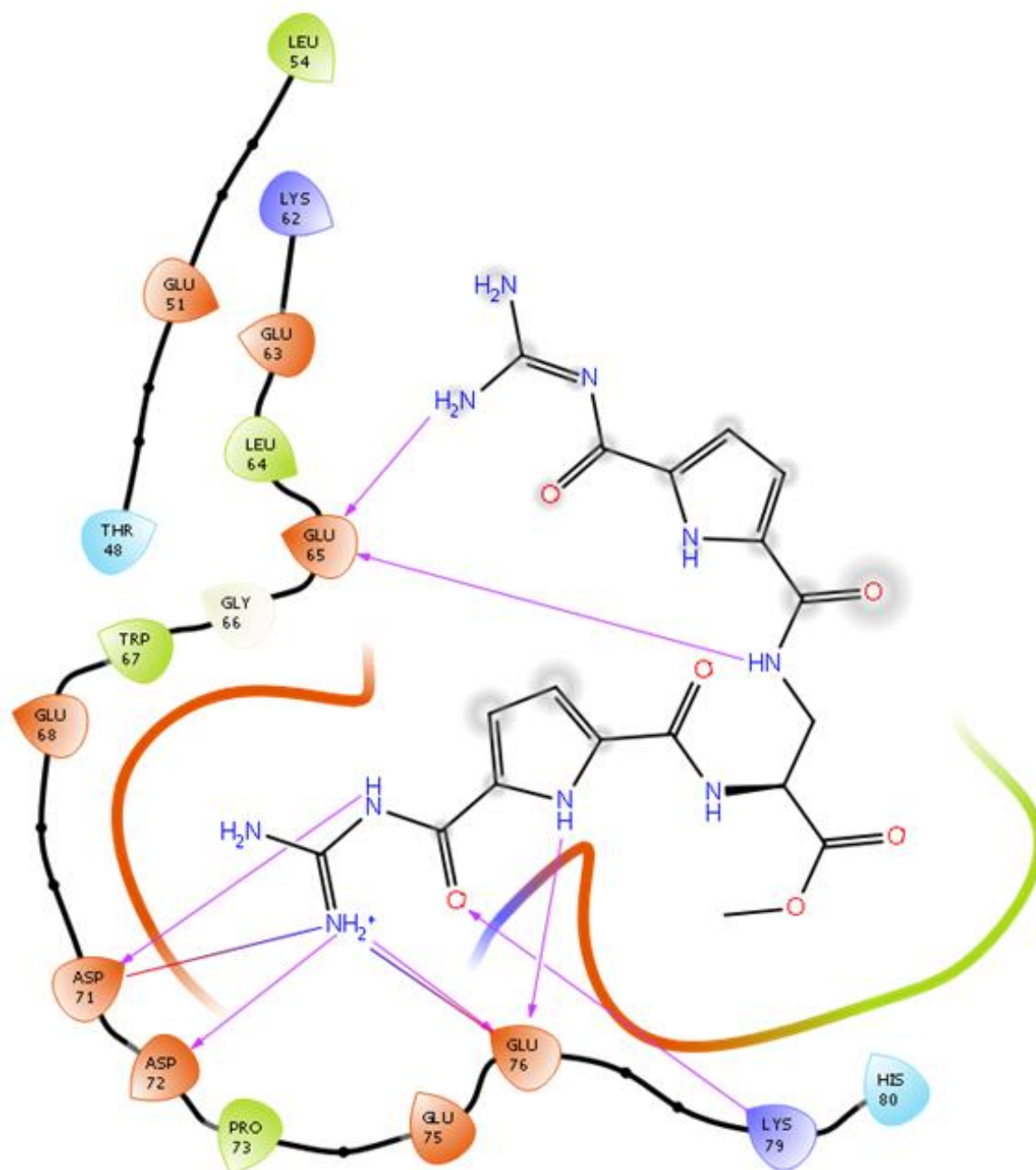


**Figure 3.2: 2D model predicts interactions with glutamic and aspartic acids within Survivin's Histone H3 binding site.** The amino groups of the cationic GCP ligand MM138 seem to interact with glutamic acids 65 and 76 as well as with aspartic acids 71 and 72. Docking was performed by Matthias Killa, Schmuck group, University of Duisburg-Essen (PDB:1XOX) (25).

### 3.1.2 NMR TITRATION EXPERIMENTS CONFIRM BINDING OF MM138 TO SURVIVIN'S HISTONE H3 BINDING SITE

NMR experiments were used to verify the predicted binding site of MM138 to Survivin. As the full length version of Survivin did not provide proper NMR signals and the only published NMR structure of Survivin is of a truncated version of the protein (aa 1–120), *in silico* analysis was performed prior to NMR titration experiments to find out whether the C-terminal  $\alpha$ -helix might destabilize the protein (127).

Dynamic simulations of monomeric and dimeric Survivin were calculated over time (Fig.3.1). The simulations revealed that Survivin's  $\alpha$ -helix of both the monomer and dimer seemed to be unstable and bending in multiple directions, especially around amino acid 120, while the rest of the protein was structurally stable. This confirmed the assumption that the  $\alpha$ -helix destabilizes the protein, which is why the following NMR experiments were performed using truncated Survivin 1-120.

Dynamic simulations were performed by Dr. Jean-Noël Grad, Hoffmann group, University of Duisburg-Essen (129).

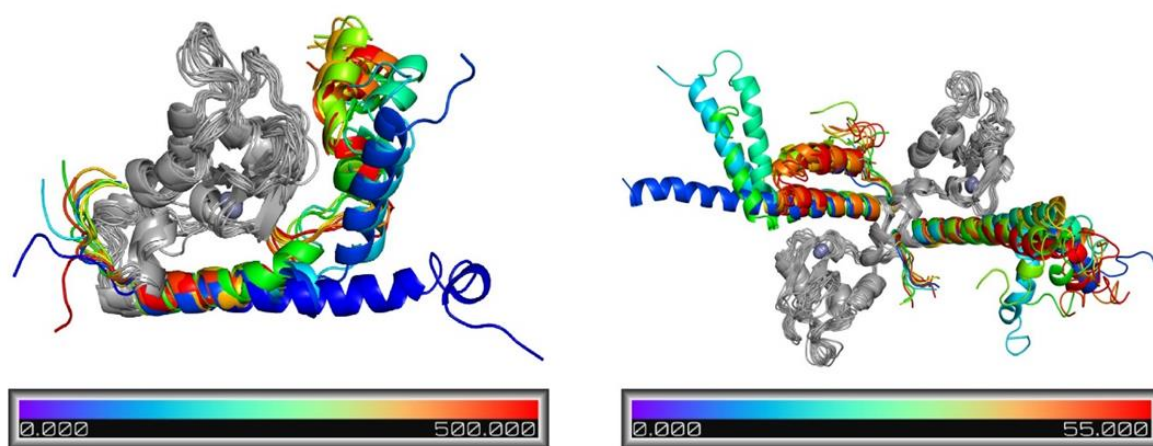


**Figure 3.3: Survivin's C-terminal  $\alpha$ -helix destabilizes the protein.** Dynamic simulations of the Survivin monomer (left) and dimer (right) over time revealed an instability of the  $\alpha$ -helix. Structurally stable regions are shown in grey, while instable regions are shown in colour. The colour bar indicates the different colours used to depict the instable regions of the protein over time (ns). *In silico* experiments were performed by Dr. Jean-Noël Grad, Hoffmann group, University of Duisburg-Essen (129).

A  $^1\text{H}$ - $^{15}\text{N}$ -BEST-TROSY-HSQC NMR spectrum of  $300\ \mu\text{M}$   $^{15}\text{N}$ -labeled Survivin 1-120 was recorded, before MM138 was added stepwise from a  $10\ \text{mM}$  stock solution in DMSO up to a final ligand concentration of  $300\ \mu\text{M}$ . Additional  $^1\text{H}$ - $^{15}\text{N}$ -BEST-TROSY spectra were recorded for each titration step (Fig.3.2). A comparison of the spectra with and without ligand concerning signal intensities and chemical shift perturbations was used to map binding of MM138 to specific amino acids of Survivin.

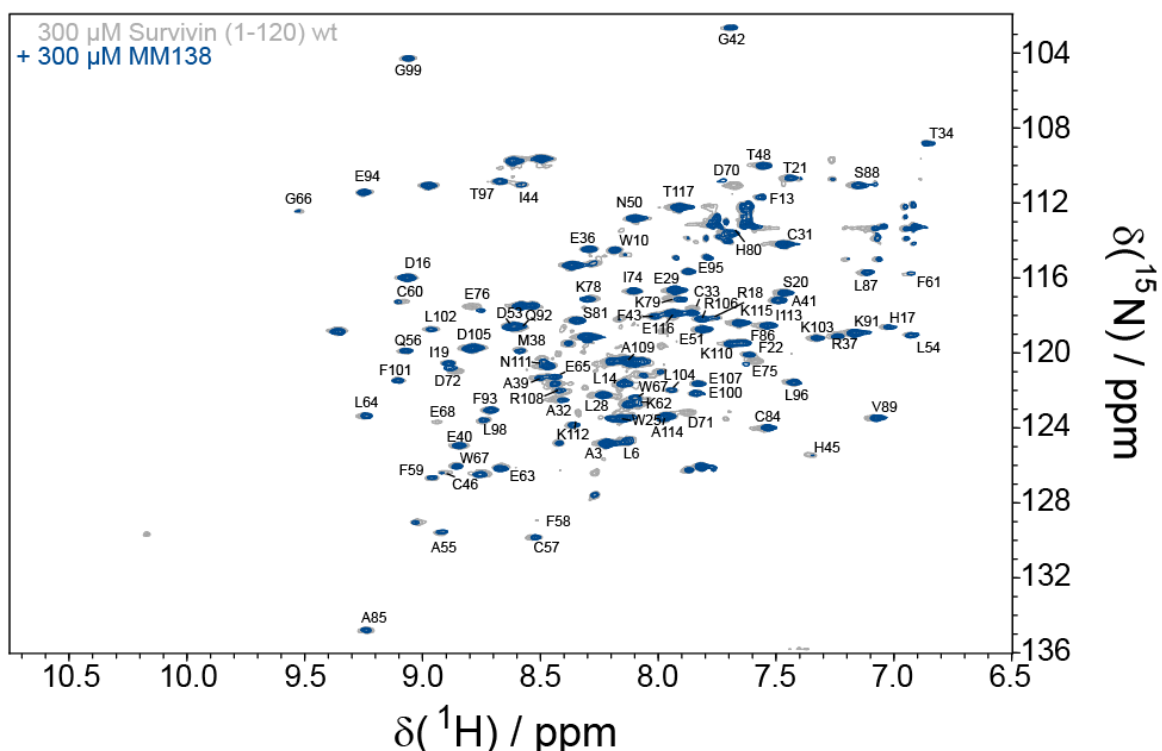


**Figure 3.4: NMR titration reveals binding of MM138 to Survivin's Histone H3 binding site.**

$^1\text{H}$ - $^{15}\text{N}$ -BEST-TROSY-HSQC spectra of  $300\ \mu\text{M}$   $^{15}\text{N}$ -labeled Survivin 1-120 with (blue) and without (grey) titration of up to  $300\ \mu\text{M}$  MM138. NMR samples contained a final protein concentration of  $300\ \mu\text{M}$  Survivin 1-120. A  $10\ \text{mM}$  stock of MM138 in DMSO- $d_6$  was added stepwise, yielding a final ligand concentration of  $300\ \mu\text{M}$  in the presence of at most 3 % DMSO- $d_6$ .  $^{15}\text{N}$ -labeled protein purification and NMR measurements were performed by Dr. Christine Beuck, Bayer group, University of Duisburg-Essen.

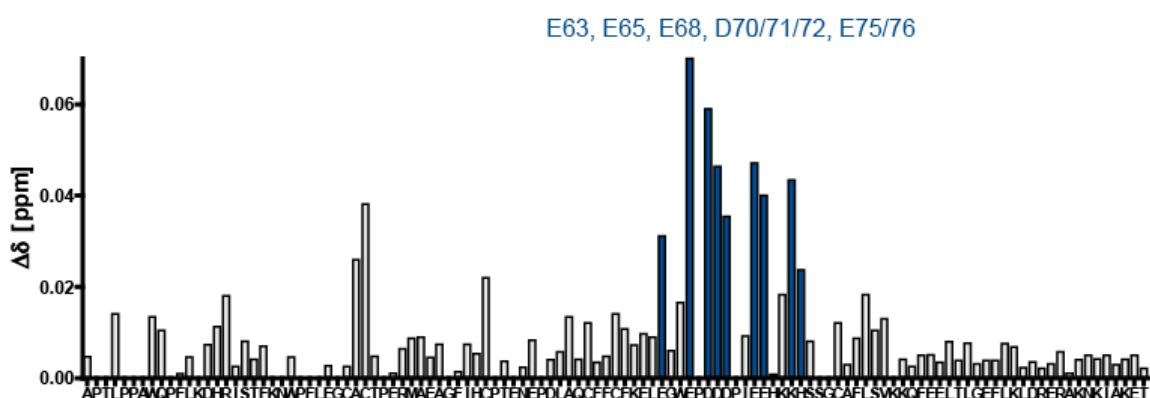
MM138 titration caused chemical shift perturbations of up to  $0.07\ \text{ppm}$  at glutamic acids (E) 63, 65 and 68, aspartic acids (D) 70, 71 and 72 and glutamic acids (E) 75 and 76 (Fig.3.3 A). Those amino acids correspond to the known Histone H3 binding site of Survivin, which comprises amino acids 51 to 80 (130). Since chemical shift perturbations can also occur when ligands interact with the protein for only a short period of time without actually binding

to it, signal intensities were evaluated in addition, as a decrease in signal intensity indicates a robust and stable interaction between ligand and protein.

Indeed, also the relative intensities  $I/I_0$  show a more than average decrease within Survivin's Histone H3 binding site, thereby indicating ligand binding within this region (Fig. 3.3 B). The intensities strongly decreased for glutamic acid (E) 68, aspartic acid (D) 70, 71 and 72 and glutamic acid (E) 75.

Taken together, NMR titration with MM138 confirmed binding of the ligand to Survivin's Histone H3 binding site, more precisely to glutamic and aspartic acids within this region. This is in line with the design and properties of the inhibitor, which is supposed to specifically target glutamic and aspartic acids.

### A 300 $\mu$ M Survivin (1-120) + 300 $\mu$ M MM138 (3% DMSO), Shifts



### B 300 $\mu$ M Survivin (1-120) + 300 $\mu$ M MM138 (3% DMSO), Intensities

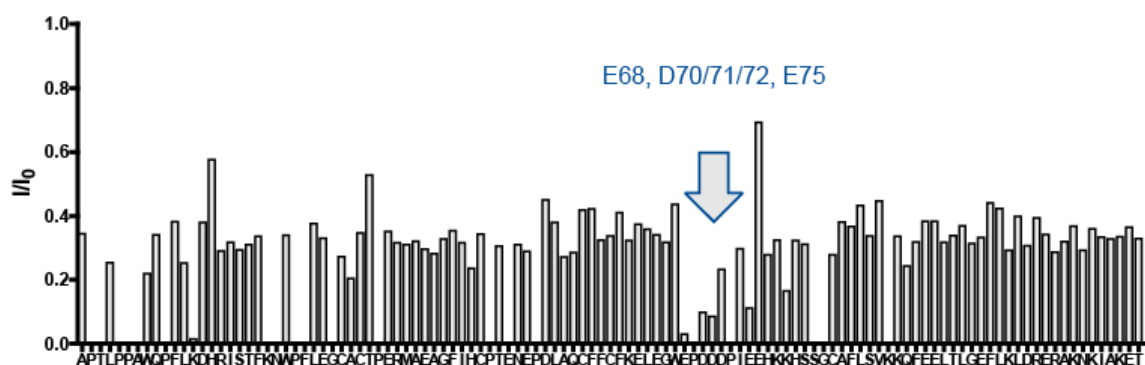


**Figure 3.5: Chemical peak shifts and a decrease in relative intensities confirms binding of MM138 to glutamic acid and aspartic acid residues within Survivin's Histone H3 binding site.**

$^1\text{H}$ - $^{15}\text{N}$ -BEST-TROSY-HSQC spectra of 300  $\mu\text{M}$   $^{15}\text{N}$ -labeled Survivin 1-120 titrated with and without up to 300  $\mu\text{M}$  MM138. **A)** Chemical peak shifts were identified for each signal and plotted against the Survivin sequence (blue). Aspartic acid and glutamic acid residues within the Histone H3 binding site of Survivin show prominent shift perturbations. **B)** The relative intensities show a more than average decrease in relative intensity  $I/I_0$  within Survivin's Histone H3 binding site indicating ligand binding within this region (blue arrow).  $^{15}\text{N}$ -labeled protein purification and NMR measurements were performed by Dr. Christine Beuck, Bayer group, University of Duisburg-Essen.

### 3.1.3 MM138 INHIBITS THE INTERACTION BETWEEN SURVIVIN AND HISTONE H3 DURING MITOSIS

As NMR experiments confirmed binding of MM138 to the Histone H3 binding site of Survivin, the next step was to investigate whether MM138 also interferes with the interaction between Survivin and Histone H3 in a cellular context. This was tested via immunoprecipitation in HeLa cell lysates overexpressing Survivin-HA as well as by performing a Proximity Ligation Assay (PLA) in HeLa cells expressing Survivin and Histone H3 only on an endogenous level.

For the immunoprecipitation, HeLa cells were transfected with Survivin-HA and treated with DMSO (control) or different concentrations of MM138 for 24 h before cell lysates were prepared. Survivin-HA was precipitated together with its interaction partners using magnetic HA-antibody-coupled beads. Survivin and Histone H3 were then detected via Western Blot in both input and eluate samples using specific antibodies against the HA-tag of Survivin-HA and against Histone H3 (Fig. 3.4 A). The amount of Histone H3 binding to Survivin was quantified by normalizing the Histone H3 signal in the eluate to the respective Survivin-HA signal (Fig. 3.4 B).

Quantification of the Western Blot revealed that the interaction between Survivin and Histone H3 seems to be decreased by MM138 in a concentration-dependent manner. A treatment of HeLa cells with 10  $\mu\text{M}$  MM138 for 24 h led to a 50 % decrease in Survivin-Histone H3 interaction, while 50  $\mu\text{M}$  MM138 reduced the interaction even by 65 % compared to the DMSO control (Fig. 3.4 C).

This confirms that MM138 does not only bind to Survivin's Histone H3 binding site, but that it is also able to decrease the interaction between the two proteins inside the cell.

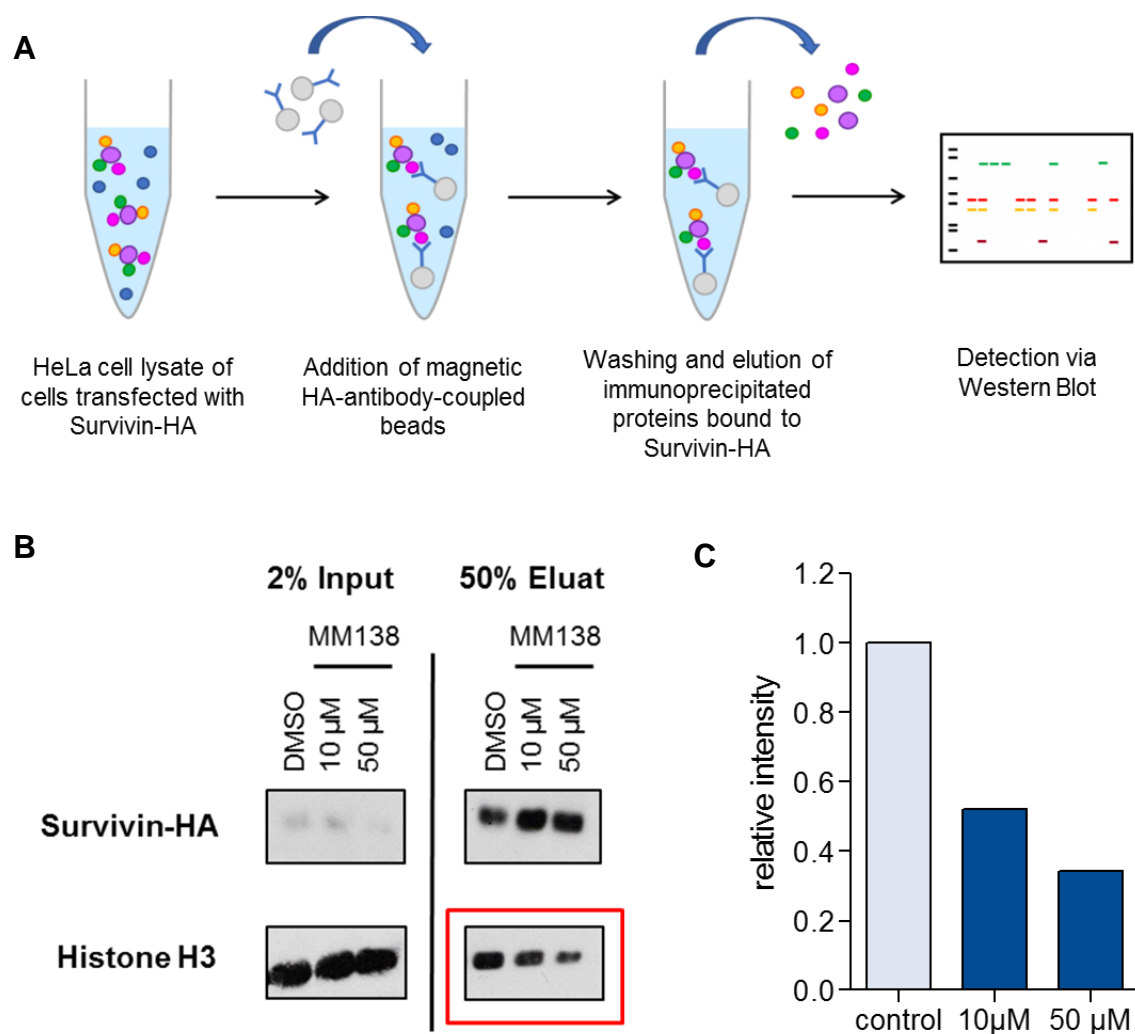


**Figure 3.6: Immunoprecipitation experiments reveal a concentration-dependent inhibition of the Survivin-Histone H3 interaction by MM138.** **A)** Experimental setup for immunoprecipitation (IP) experiments. **B)** Western Blot analysis of IP samples. HeLa cells were transfected with Survivin-HA and treated with different concentrations of MM138 or DMSO (control). After 24 h, HeLa cell lysates were generated and incubated with magnetic HA-antibody-coupled beads. Survivin-HA and its interaction partners were eluted through  $\mu$ MACS columns. Input and eluate samples were analyzed via immunoblotting and detected with HA and Histone H3 specific antibodies. **C)** Quantitative analysis of the Western Blot shows the intensity of the Histone H3 signal in the eluate normalized to the respective Survivin-HA signal of HeLa cells treated with either 10  $\mu$ M MM138, 50  $\mu$ M MM138 or DMSO (control).

To investigate whether the effect of MM138 is not only observable in cell lysates overexpressing Survivin-HA but also in HeLa cells expressing endogenous levels of Survivin and Histone H3, a PLA was performed. The PLA enables the visualization of protein-protein interactions within cells on an endogenous level. If two target proteins are in close proximity (<40 nm), the oligonucleotides connected to the secondary antibodies ligate and a rolling circle amplification with fluorescent nucleotides generates a PLA signal that can be detected with the fluorescence microscope.

As the interaction between Histone H3 and Survivin takes place during the early phases of mitosis, where it is crucial to tether the CPC to the centromeres, HeLa cells were analyzed in prophase and metaphase (21, 61). The cells were first treated with either 50  $\mu$ M MM138 or the respective amount of DMSO for 48 h and synchronized with the CDK1 inhibitor RO-3306. Cells were fixed when the majority of them had reached metaphase before a PLA staining was performed prior to microscopic analysis. As Survivin specifically interacts with Histone H3 phosphorylated at threonine 3 (H3T3p) during mitosis, primary antibodies against Survivin and H3T3p were used for the staining.

To verify the accuracy of the PLA staining, the Survivin-Histone H3 interaction was first examined in all mitotic phases. As expected, an interaction could only be detected during prophase and metaphase, while no PLA foci were visible during anaphase or telophase, when the CPC relocates at the spindle midzone and later at the midbody (Fig. 3.5 A). This confirmed the suitability of the assay to analyze the interaction of Survivin with Histone H3 during mitosis.

The influence of MM138 on the Survivin-Histone H3 interaction was analyzed by comparing the number of foci per cell in treated versus untreated cells. The quantification was performed automatically with a Cell Profiler pipeline that counted all foci within the border of the respective cells. Only prophase and metaphase cells were included into the analysis. The quantification revealed that MM138 treatment significantly reduced the interaction between Survivin and Histone H3 (Fig. 3.5 C). The average number of foci per cell was 26 in DMSO-treated cells and only 23 in cells treated with 50  $\mu$ M MM138 (Fig. 3.5 B).

Unfortunately, only 50  $\mu$ M of MM138 could be tested on HeLa cells as higher concentrations of the ligand impaired cell proliferation and mitosis (section 3.1.6). In addition to that, the increasing amount of DMSO, which is used as solvent, has a considerable toxic effect on the cells. Nevertheless, immunoprecipitation and PLA allowed it to be demonstrated that MM138 is not only able to bind to Survivin's Histone H3 binding site, but that it is also capable of inhibiting the interaction between the two proteins inside the cell.

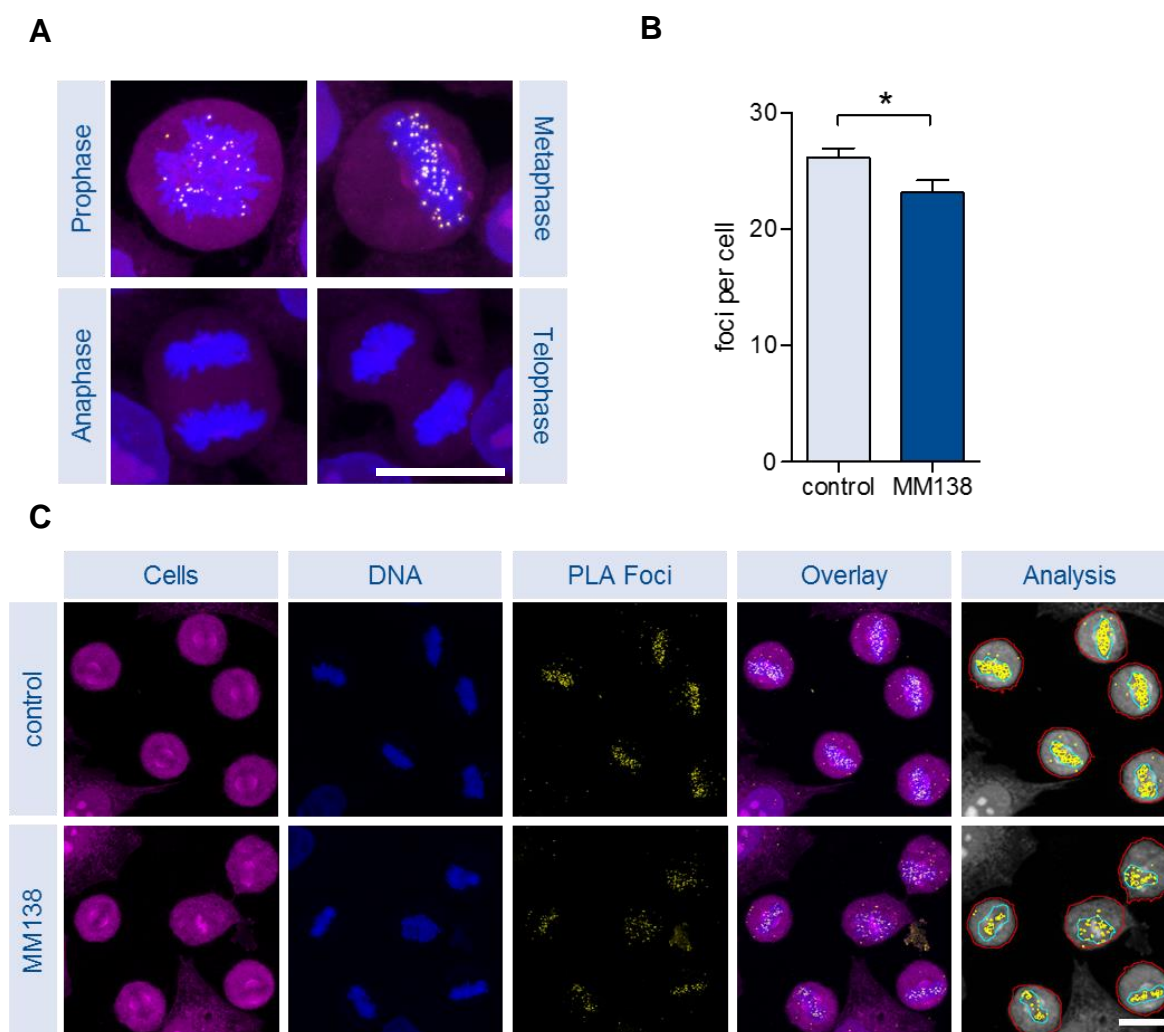


**Figure 3.7: MM138 inhibits the Survivin-Histone H3 interaction in HeLa cells.** **A)** Interaction of Survivin and Histone H3 phosphorylated at threonine 3 during the different phases of mitosis shown by PLA. Entire cells are depicted in magenta, DNA in blue and PLA foci in yellow. **B)** Quantitative analysis of the interaction between Survivin and Histone H3 during the early phases of mitosis (prophase and metaphase). HeLa cells were treated with either 50  $\mu$ M MM138 or the respective amount of DMSO (control) for 48 h and synchronized with RO-3306 prior to fixation and PLA staining. The bar graph shows the number of PLA foci per mitotic cell in treated cells vs. control cells. The number of cells analyzed with CellProfiler was 56 in control and 58 in MM138-treated cells. Data was analyzed by t test. One asterisk (\*) indicates p value smaller than 0.05 (99 % confidence interval). The error bars represent SEM. **C)** Representative images of PLA. Entire cells are depicted in magenta, DNA in blue and PLA foci in yellow. Scale bar: 20  $\mu$ m.

### 3.1.4 SURVIVIN DIMERIZATION IS INCREASED BY MM138 TREATMENT

Survivin forms homodimers in solution, while it seems to bind to most of its interaction partners inside the cell as a monomer. As dimerization and interaction with other binding partners seem to be competitive processes, the question was whether the inhibition of Survivin-Histone H3 interaction would have an influence on Survivin's dimerization behaviour inside the cell (18, 21, 84).

To examine Survivin dimerization inside the cell, an Acceptor Photobleaching FRET Assay was established, using Cerulean as a donor fluorophore and Citrine as an acceptor fluorophore. If donor and acceptor are in close proximity (<10 nm), the donor fluorescence is quenched by the acceptor. Bleaching of the acceptor results in an increase in donor fluorescence, which can be quantified and allows the calculation of a FRET efficiency.

HeLa cells were either cotransfected with Cerulean and Citrine on two separate plasmids as a negative control, as the two fluorophores alone do not specifically interact with each other, or transfected with a plasmid coding for a fusion protein of Cerulean directly linked to Citrine. This fusion protein served as a positive control since donor and acceptor are linked to each other, which maximizes the FRET efficiency (Fig. 3.6 A).

The determined FRET efficiencies for the positive and negative control were found to be significantly different from each other. The mean FRET efficiency in the positive control was 0.2, while it was only 0.006 in the negative control (Fig. 3.6 B). This suggests that this donor and acceptor pair is suitable to investigate protein dimerization inside the cell.

In addition to that, the assay was also validated by comparing the FRET efficiencies of Survivin wildtype (WT) to those of a known dimerization deficient mutant (F101AL102A). Cells were either cotransfected with Survivin wildtype linked to Cerulean (Cerulean-SurvivinWT) and to Citrine (Citrine-SurvivinWT) or with the Survivin mutant linked to Cerulean (Cerulean-SurvivinF101AL102A) and to Citrine (Citrine-SurvivinF101AL102A).

The FRET efficiencies revealed a significant difference between the wildtype (mean FRET efficiency of 0.17) and the dimerization deficient mutant (mean FRET efficiency of 0.10), thereby validating the Acceptor Photobleaching FRET assay for the analysis of Survivin dimerization (data not shown).

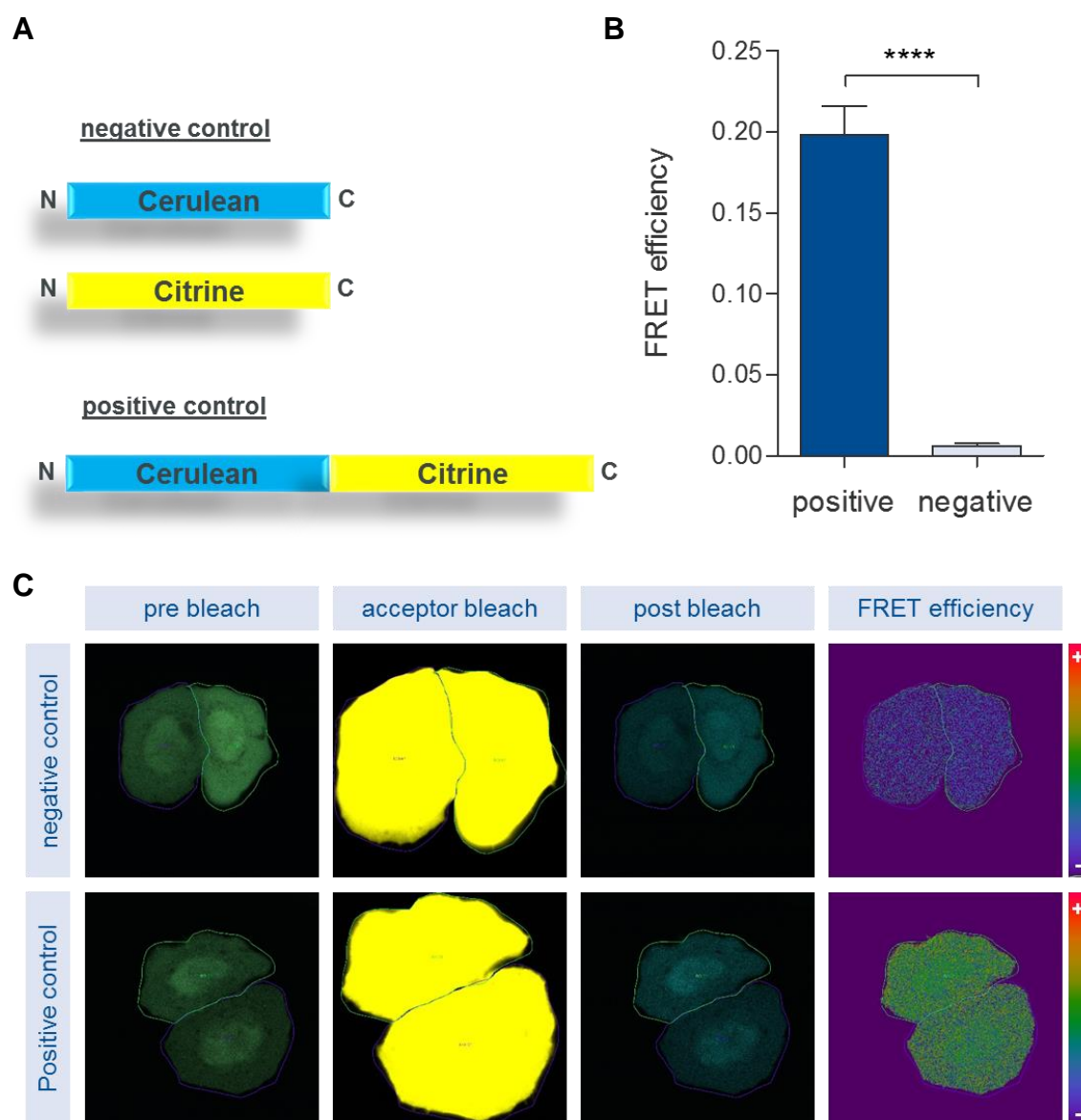


**Figure 3.8: Survivin dimerization can be analyzed with Acceptor Photobleaching FRET.** **A)** Transfection constructs for negative control (cotransfection of Cerulean and Citrine) and positive control (transfection of Cerulean directly linked to Citrine). **B)** FRET efficiencies of negative and positive controls measured by Acceptor Photobleaching FRET Assay. The experiment was performed in HeLa cells. Data was analyzed by t test. Four asterisks (\*\*\*\*) indicate p value smaller than 0.0001 (99 % confidence interval). The error bars represent SEM. **C)** Representative images of the FRET assay. Pre bleach and post bleach images show overlay of Cerulean (cyan) and Citrine (yellow) signals. Acceptor bleach image shows area of the cell that was bleached for 15 frames at a laser wavelength of 514 nm. FRET efficiencies are visualized by pseudo coloured images. N>25.

To investigate the influence of MM138 on Survivin dimerization, cells were transfected with Cerulean-Survivin and Citrine-Survivin and treated with 50  $\mu$ M MM138 or the respective amount of DMSO for 24 h before they were fixed and analyzed by Acceptor Photobleaching FRET assay (Fig 3.7 A).

The FRET efficiencies in MM138-treated cells were significantly different from those in control cells. MM138-treated cells had an average FRET efficiency of 0.19, while the average FRET efficiency in control cells was only 0.16 (Fig 3.7 B). This indicates that MM138 treatment increases Survivin dimerization in HeLa cells.

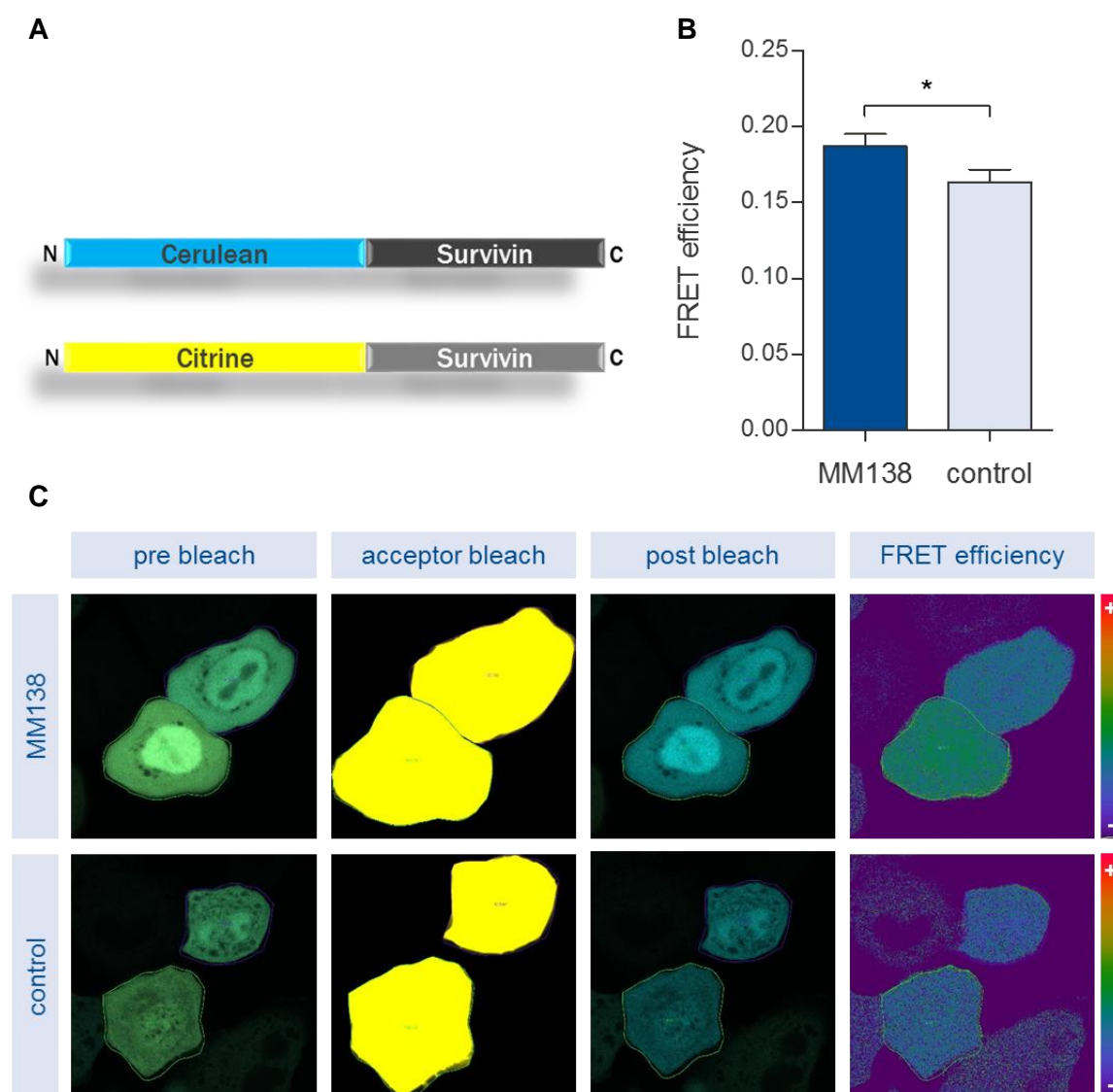


**Figure 3.9: MM138 increases Survivin dimerization in HeLa cells.** **A)** Transfection constructs Cerulean-Survivin and Citrine-Survivin used for Acceptor Photobleaching FRET Assay. **B)** FRET efficiencies in MM138-treated cells in comparison to DMSO-treated cells (control). HeLa cells were

cotransfected with Cerulean-Survivin (donor) and Citrine-Survivin (acceptor) and treated with 50  $\mu$ M MM138 or the respective amount of DMSO for 24 h before they were fixed and analyzed via Acceptor Photobleaching FRET Assay. Data was analyzed by t test. One asterisk (\*) indicates p value smaller than 0.05 (99 % confidence interval). The error bars represent SEM. **C)** Representative images of the FRET assay in MM138-treated vs. control cells. Pre bleach and post bleach images show overlay of Cerulean (cyan) and Citrine (yellow) signals. Acceptor bleach image shows area of the cell that was bleached for 15 frames at a laser wavelength of 514 nm. FRET efficiencies are visualized by pseudo coloured images. N>20.

### 3.1.5 MM138 CAUSES MITOTIC DEFECTS IN HELA CELLS

As the interaction between Survivin and Histone H3 is crucial for Survivin to fulfil its role within the CPC during mitosis, it is likely that an inhibition of this protein-protein interaction causes major mitotic defects or cell cycle arrest.

To investigate whether MM138 treatment has such effects, HeLa cells were treated with 50  $\mu$ M of the ligand for 48 h and synchronized with the CDK1 inhibitor RO-3306 to increase the mitotic fraction in the sample. Cells were then fixed and the DNA, the spindles and the centromeres were visualized via immunostaining to be able to identify the different mitotic defects.

Cells with mitotic defects were counted and assigned to one of the five following categories of mitotic defects according to the “Guide to classifying mitotic stages and mitotic defects in fixed cells” (Fig 3.8 A) (131):

- 1) Chromatin bridges: Chromatin bridges occur in anaphase or telophase and exhibit the feature of a “DNA bridge” between the two groups of segregating chromosomes. They can be connected to both groups of segregating chromosomes or disconnected on one or both ends. They might also break during anaphase and appear disconnected in the middle (131, 132).
- 2) Acentric fragments: Acentric fragments can be identified in metaphase as well as in anaphase and telophase. They appear as DNA fragments that are separated from the rest of the chromosomes but lack a centrosome (131).

- 3) Lagging chromosomes: Lagging chromosomes occur in anaphase or telophase. They stay behind at the spindle midzone, while the other chromosomes move towards the spindle poles. In contrast to acentric fragments, they possess a centrosome (131, 133, 134).
- 4) Multipolar ana-/telophase: A cell during anaphase or telophase, which has more than two spindle poles and where the chromosomes might be segregating in more than two groups (131).
- 5) Mutipolar prometa-/metaphase: A cell during prometaphase or metaphase with more than two spindle poles (131).

The analysis revealed that mitotic defects occurred more frequently in cells treated with MM138 than in control cells. While only 6.1 % of control cells had mitotic defects, 32.1 % of MM138-treated cells were affected (Fig 3.8 C). However, not only the percentage of cells with mitotic defects changed after MM138 treatment, but also the proportions of the different types of defects (Fig 3.8 B). In control cells, 60 % of mitotic defects consisted of acentric fragments and 40 % of lagging chromosomes. MM138-treated cells showed a larger variety of mitotic defects. Only 29 % were comprised of acentric fragments and 18 % of lagging chromosomes. In addition, 23 % belonged to the phenotype of multipolar ana-/telophase and 18 % to the phenotype of multipolar prometa-/metaphase. In 12 % of MM138-treated cells, chromatin bridges could be found.

Taken together, MM138 does not only seem to increase the amount of mitotic defects in HeLa cells, but also seems to cause different kinds of mitotic defects like multipolar spindles and chromatin bridges instead of only acentric fragments and lagging chromosomes.

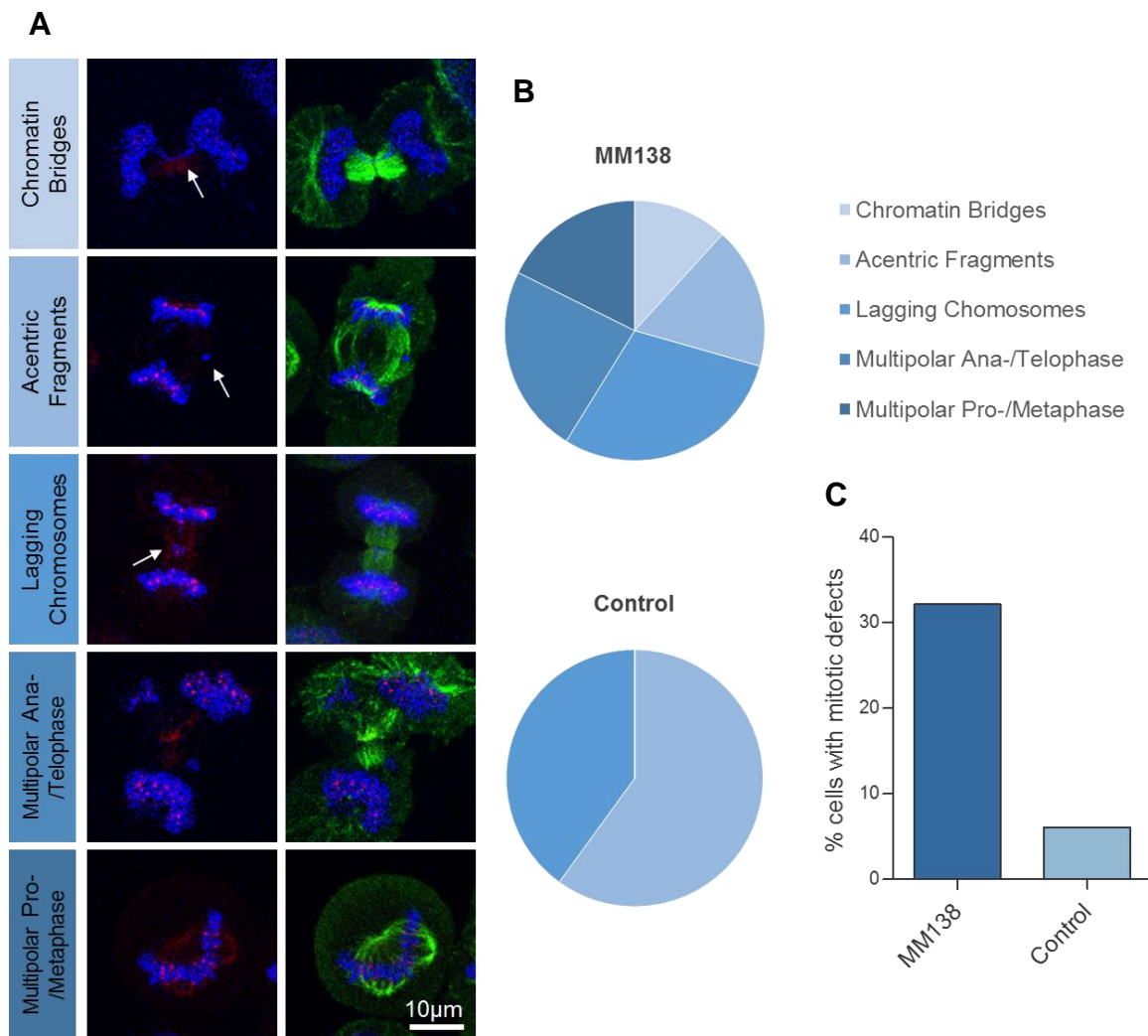


**Figure 3.10: MM138 causes mitotic defects in HeLa cells. A)** Types of mitotic defects found in HeLa cells treated with 50  $\mu\text{M}$  MM138 for 48 h and synchronized with RO-3306. Cells were fixed and immunostained. DNA is shown in blue, centromeres in red and  $\alpha$ -Tubulin in green. White arrows highlight chromosome segregation defects. **B)** Pie charts show proportions of mitotic defects in MM138-treated cells in comparison to DMSO-treated cells (control). **C)** Bar graph shows percentage of cells with mitotic defects in MM138-treated cells in comparison to control cells (131).  $N > 100$ .

### 3.1.6 MM138 REDUCES PROLIFERATION OF CANCER CELLS

As MM138 induced mitotic defects in HeLa cells it seems likely that it also has an effect on cell proliferation in general. This is why the influence of MM138 was tested on different types of cancer cells: HeLa cells that are derived from cervical cancer, A549 cells as a model for lung cancer, MDA-MB-231 cells originating from breast cancer and HCT 116 cells that serve as a model for colon cancer.

The cells were treated with different concentrations of MM138 or the respective amounts of DMSO (control) and incubated for 72 h before cell proliferation was measured using the CellTiter 96® AQueous One Cell Proliferation Assay (Promega). The assay determines the number of viable cells by using a tetrazolium compound that is added to the cells. After 4 h the quantity of formazan product, which is directly proportional to the number of living cells, can be measured at 490 nm (127).

It could be demonstrated that MM138 reduces cell proliferation in all cancer cell lines tested, but to different degrees. In addition to that, the inhibition was enhanced with increasing concentrations of the ligand (Fig. 3.9).

In HeLa cells, cell proliferation decreased only by 17 % in cells treated with the highest ligand concentration (200  $\mu$ M) compared to the DMSO control. Similar effects could also be observed in cells treated with 100  $\mu$ M (16 % decrease) and 50  $\mu$ M MM138 (14 % decrease). Treatment with 10  $\mu$ M and 5  $\mu$ M MM138 had only a minor effect on cell proliferation (8 % and 4 % decrease).

At a concentration of 200  $\mu$ M, MM138 had a stronger effect on cell proliferation in A549 cells than in HeLa cells. Cell proliferation was decreased by 31 % compared to only 17 % in HeLa cells. Nevertheless, at lower concentrations, the ligand had nearly no effect on A549 cells. It decreased cell proliferation only by 6 % at 100  $\mu$ M, by 5 % at 50  $\mu$ M, by 4 % at 10  $\mu$ M and had no effect at a concentration of 5  $\mu$ M.

The strongest effect on cell proliferation could be observed in MDA-MB-231 cells, where MM138 led to a 35 % decrease in cell proliferation at a concentration of 200  $\mu$ M and 38 % decrease at 100  $\mu$ M. Weaker effects could still be observed at 50  $\mu$ M (30 % decrease) and 10  $\mu$ M (19 % decrease).

In HCT 116 cells, the effect at 200  $\mu$ M was similar to the effect this concentration had in MDA-MB-231 cells. At this concentration, MM138 treatment decreased cell proliferation by 38 %. However, in contrast to MDA-MB-231 cells, MM138 had a notably weaker effect on HCT 116 cells in lower concentrations. It decreased cell proliferation only by 15 % at 100  $\mu$ M and 50  $\mu$ M, by 12 % at 10  $\mu$ M and by 2 % at 5  $\mu$ M.

To sum up, MM138 was able to decrease cell proliferation in several cancer cell lines from different origins. Due to the fact that MM138 needs to be solved in DMSO, it was not possible to test higher concentrations of the ligand, as larger amounts of DMSO had a severe toxic effect on the cells. Nevertheless, cell proliferation could be decreased by more than 30 % in three of the four cell lines tested.

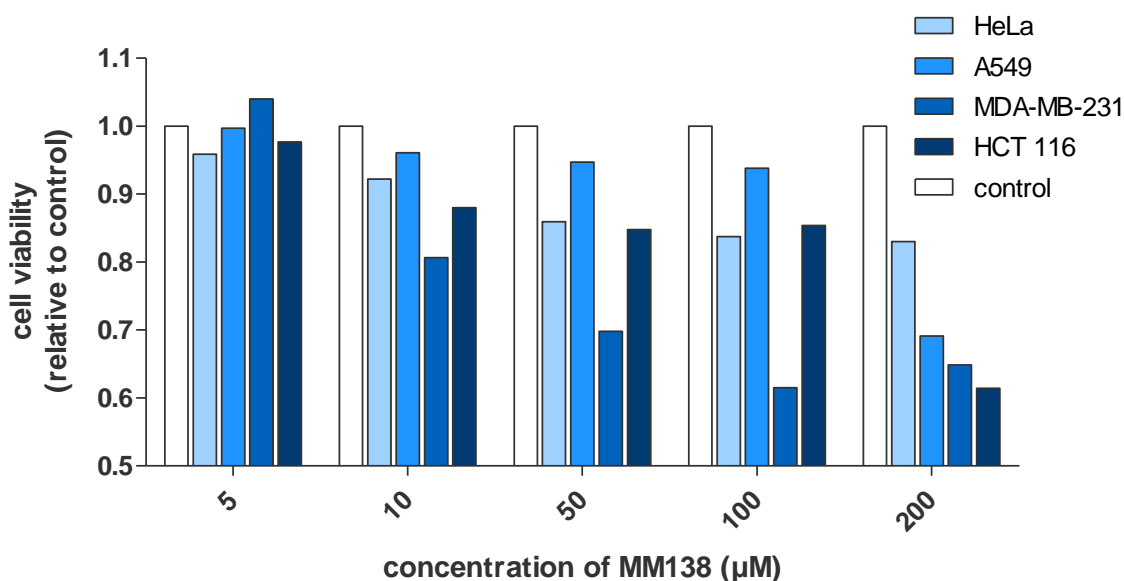


**Figure 3.11: MM138 treatment leads to a concentration-dependent inhibition of cell proliferation in different types of cancer cells.** HeLa, A549, MDA-MB-231 and HCT 116 cells were treated with different concentrations of MM138 or the respective amounts of DMSO and incubated for 72 h before cell proliferation was measured using the CellTiter 96® AQueous One Cell Proliferation Assay (Promega). The absorbance (490 nm) values of the samples were subtracted by a medium only control. Absorbance of MM138-treated cells is depicted relative to control.

In this part of the project, several cellular assays were successfully established to validate MM138 as a protein-protein inhibitor targeting the interaction between Survivin and Histone H3. It could be shown that MM138 binds to Survivin's Histone H3 binding site and is able to decrease the interaction between the two proteins, which affected Survivin's mitotic functions and reduced cell proliferation in several different cancer cell lines.

---

## 3.2 TARGETING THE SURVIVIN-CRM1 INTERACTION WITH SUPRAMOLECULAR GCP LIGANDS

Survivin functions as an inhibitor of apoptosis protein but is also necessary for proper chromosome segregation during mitosis. For both functions, an interaction with the export receptor Crm1 is mandatory (21). The supramolecular GCP ligand DA162 was designed to specifically target Survivin's Crm1 binding site to inhibit the interaction between the two proteins and thereby interfere with Survivin's functions in cell proliferation and apoptosis inhibition. This part of the project aims to establish different cellular and *in vitro* assays to validate DA162 as a potential protein-protein inhibitor of the Survivin-Crm1 interaction.

### 3.2.1 DOCKING STUDIES PREDICT BINDING OF DA162 TO SURVIVIN'S NUCLEAR EXPORT SIGNAL

In collaboration with the Schmuck group, the supramolecular ligand DA162 was designed to specifically target the interaction between Survivin and Crm1. Preliminary docking studies suggest that DA162 binds to Survivin's NES <sup>89</sup>VKKQFEELTL<sup>98</sup>, which contains two anionic glutamic acids. The four-armed GCP ligand seems to be able to interact not only with the NES of the Survivin monomer but also with both NESs of the Survivin dimer.

The 2D model of the docking results highlights how the GCP ligand DA162 presumably interacts with Survivin. Docking of DA162 to monomeric Survivin revealed that the amino groups of the cationic GCP ligand seem to interact with glutamic acids 94 and 95. Docking to dimeric Survivin suggests that the four-armed ligand is also able to interact with both NESs of the homodimer. While two of the ligand arms presumably interact with glutamic acids 94 and 95 of one monomer, the other two arms interact with glutamic acids 95 and 100 of the other monomer.

All docking studies were conducted by Matthias Killa, Schmuck group, University of Duisburg-Essen.

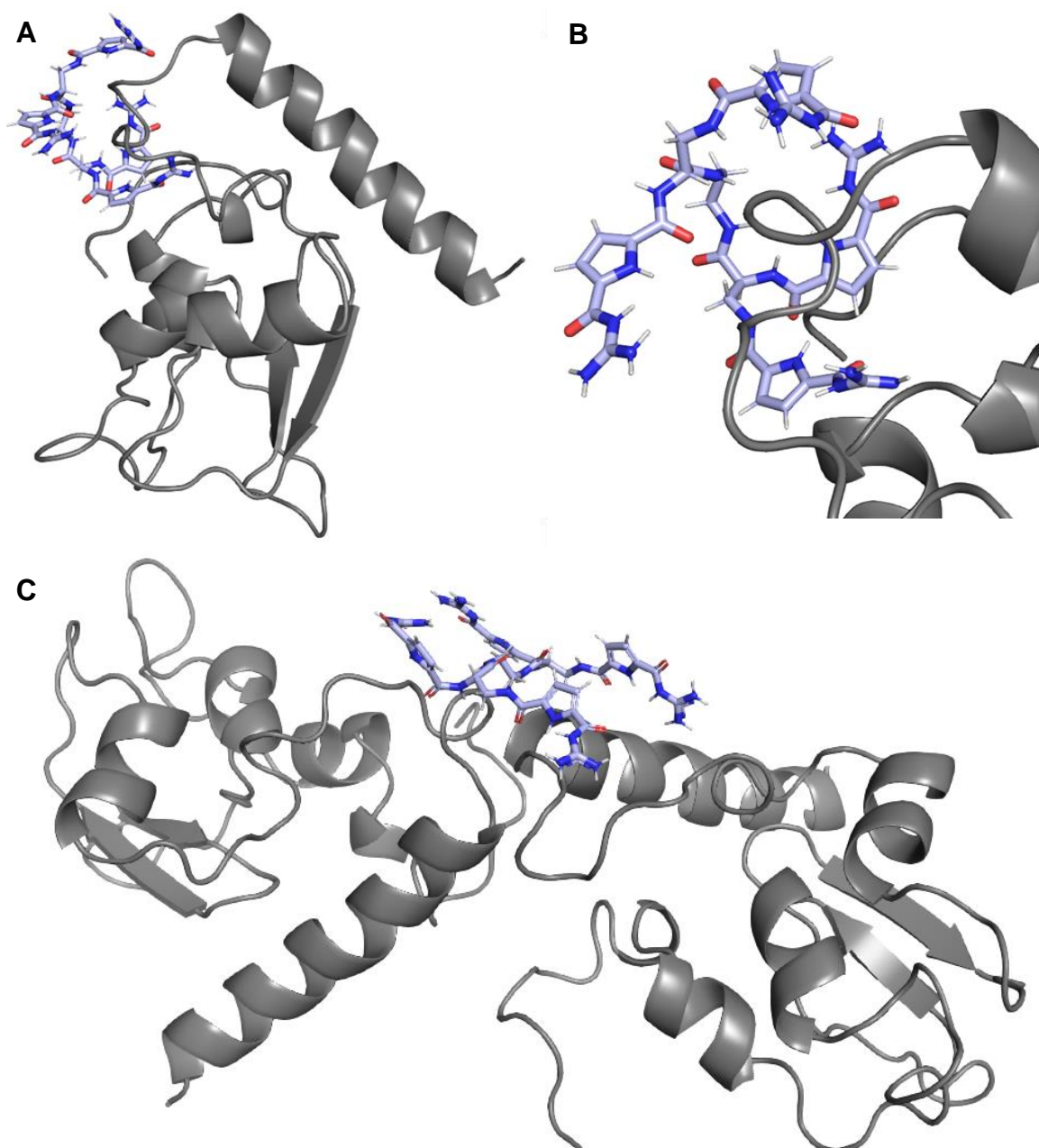


**Figure 3.12: Docking predicts binding of DA162 to Survivin's NES. A)** Docking of DA162 to Survivin monomer. **B)** Close-up of DA162 interacting with Survivin's NES. **C)** Docking of DA162 to Survivin dimer. Docking was performed by Matthias Killa, Schmuck group, University of Duisburg-Essen. (PDB:1XOX) (25)

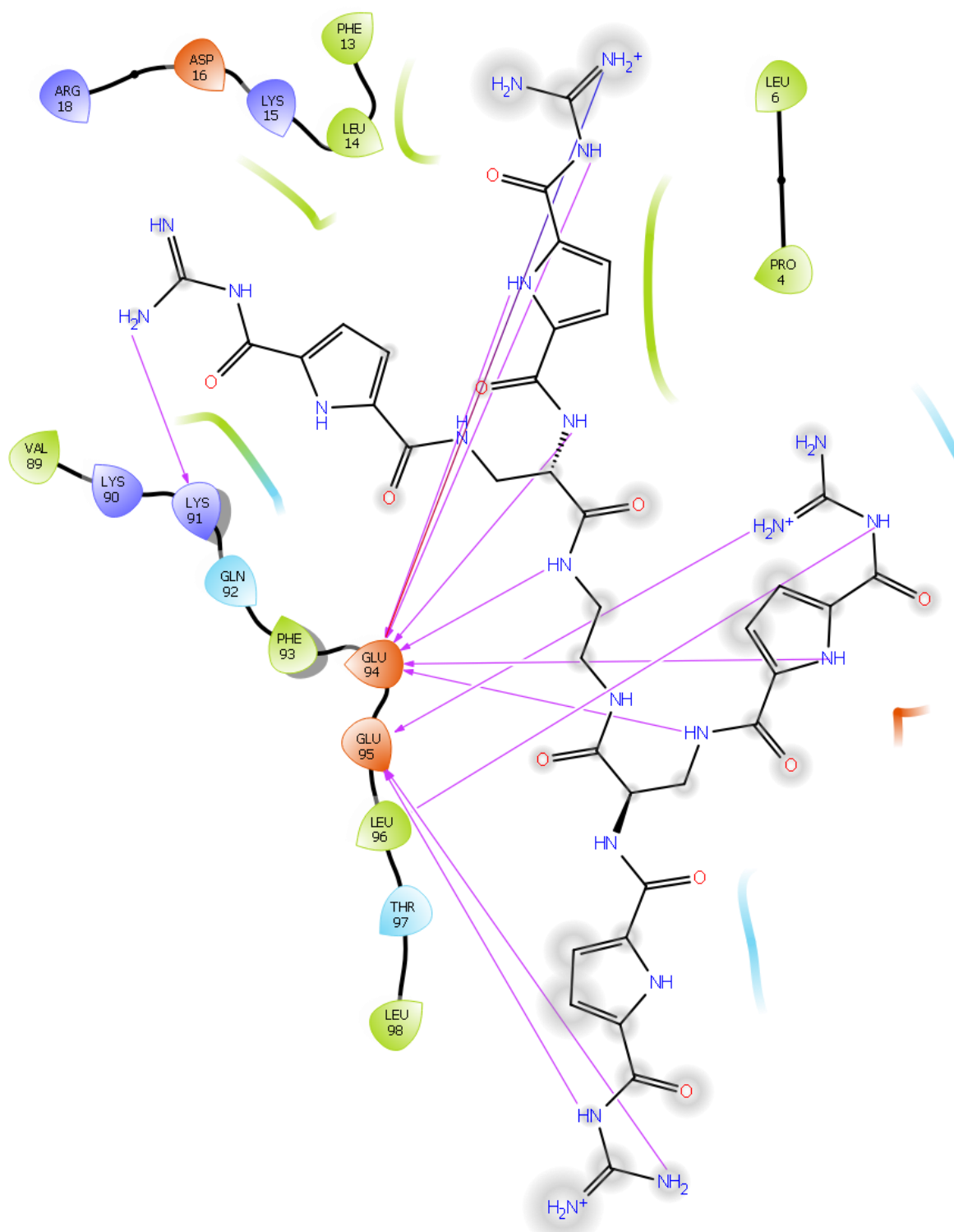


**Figure 3.13: 2D model of monomer predicts interactions with glutamic and aspartic acids within Survivin's NES.** The amino groups of the GCP ligand DA162 seem to interact with glutamic acids 94 and 95 of the Survivin monomer. Docking was performed by Matthias Killa, Schmuck group, University of Duisburg-Essen (PDB:1XOX) (25).

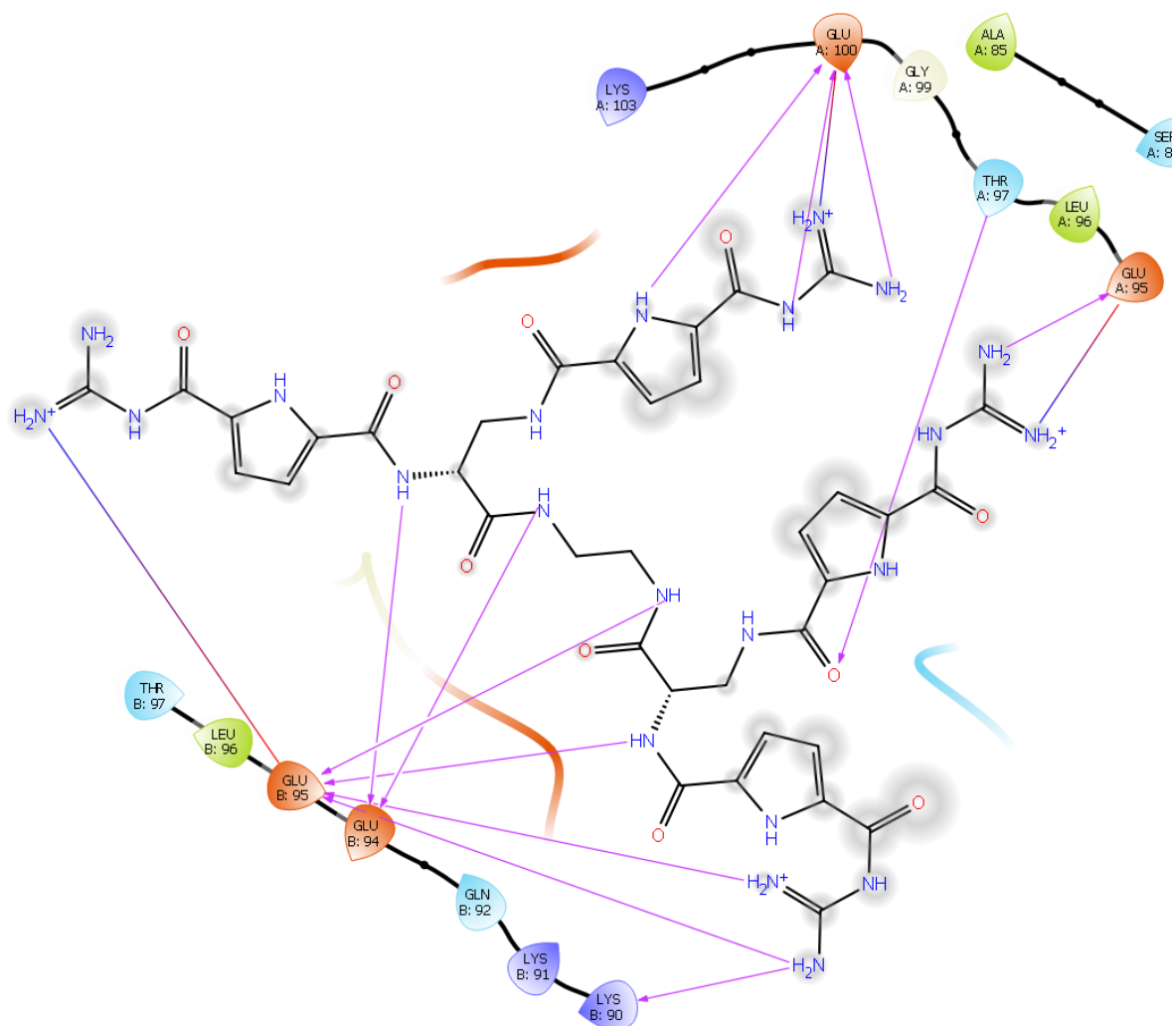


**Figure 3.14: 2D model of dimer predicts interactions with glutamic and aspartic acids within the NESs of both monomers.** Docking to dimeric Survivin suggests that the four-armed ligand is able to interact with both NESs of the homodimer. While two of the ligand arms presumably interact with glutamic acids 94 and 95 of one monomer, the other two arms interact with glutamic acids 95 and 100 of the other monomer. Docking was performed by Matthias Killa, Schmuck group, University of Duisburg-Essen (PDB:1XOX) (25).

### 3.2.2 ITC EXPERIMENTS CONFIRM BINDING OF DA162 TO SURVIVIN

To confirm direct binding of DA162 to Survivin and to determine the binding affinity of the ligand, ITC measurements were performed. A solution of 100  $\mu\text{M}$  DA162 was placed into the sample cell and 380  $\mu\text{M}$  Survivin 1-120 was added stepwise to the ligand solution.

Titration of Survivin 1-120 led to an exothermic binding reaction (Fig. 3.10). Fitting of the binding curve to a sequential four-site binding model revealed dissociation constants  $K_D$  of 62  $\mu\text{M}$ , 24  $\mu\text{M}$ , 9  $\mu\text{M}$  and 35  $\mu\text{M}$  and confirmed direct binding of DA162 to Survivin.

Ligand was provided and ITC measurements were performed by Dennis Aschmann, Schmuck group, University of Duisburg-Essen. Survivin 1-120 was provided by Dr. Sandra Bäcker, Knauer group, University of Duisburg-Essen.

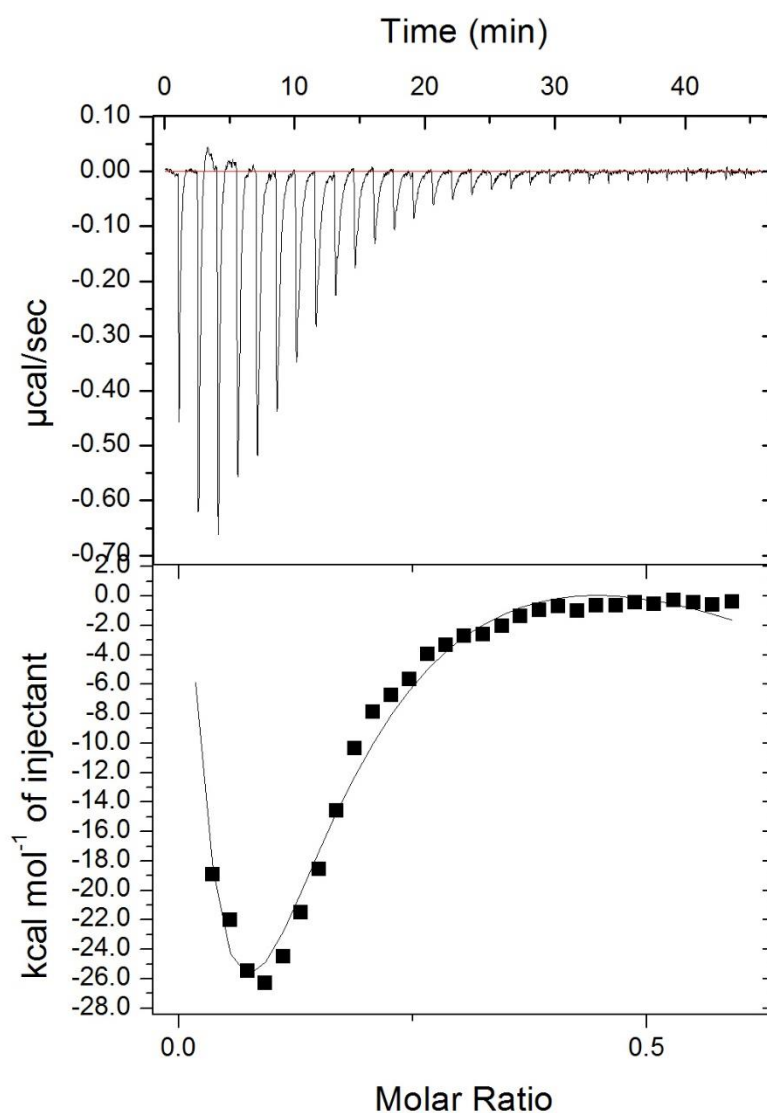


**Figure 3.15: DA162 binds to Survivin 1-120 with a nanomolar  $K_D$ .** 380  $\mu\text{M}$  Survivin 1-120 was titrated stepwise to a 100  $\mu\text{M}$  DA162 solution. The raw heating power over time subtracted by the heating power of Survivin 1-120 titrated into buffer alone is displayed at the top. The integrated energy values normalized to Survivin 1-120 are displayed at the bottom. Fitting of the ITC data to a sequential four-site binding model revealed dissociation constants  $K_D$  of 62  $\mu\text{M}$ , 24  $\mu\text{M}$ , 9  $\mu\text{M}$  and 35  $\mu\text{M}$ . Ligand was provided and ITC measurements were performed by Dennis Aschmann, Schmuck group, University of Duisburg-Essen; Survivin 1-120 was provided by Dr. Sandra Bäcker, Knauer group, University of Duisburg-Essen.

### 3.2.3 DA162 INHIBITS THE INTERACTION BETWEEN SURVIVIN AND CRM1

As ITC measurements confirmed binding of DA162 to Survivin, the next step was to test whether DA162 is also able to target Survivin inside the cell and inhibit its interaction with the export receptor Crm1. To do this, a PLA was performed, which is able to visualize protein-protein interactions inside the cell on an endogenous level.

HeLa cells were treated with either 50  $\mu\text{M}$  DA162 or the respective amount of  $\text{H}_2\text{O}$  (control) before they were fixed and a PLA staining was performed prior to microscopic analysis. The assay was quantified by comparing the number of foci in treated and control cells with the help of a Cell Profiler pipeline that counted all foci within the border of the respective cells (Fig. 3.11 A).

The quantification revealed that MM138 treatment significantly reduced the interaction between Survivin and Crm1. In control cells, the average number of foci per cells was 67, while it decreased to 40 in DA162-treated cells (Fig. 3.11 B). This suggests that DA162 indeed seems to be able to reduce the interaction between Survivin and the export receptor Crm1 in HeLa cells.

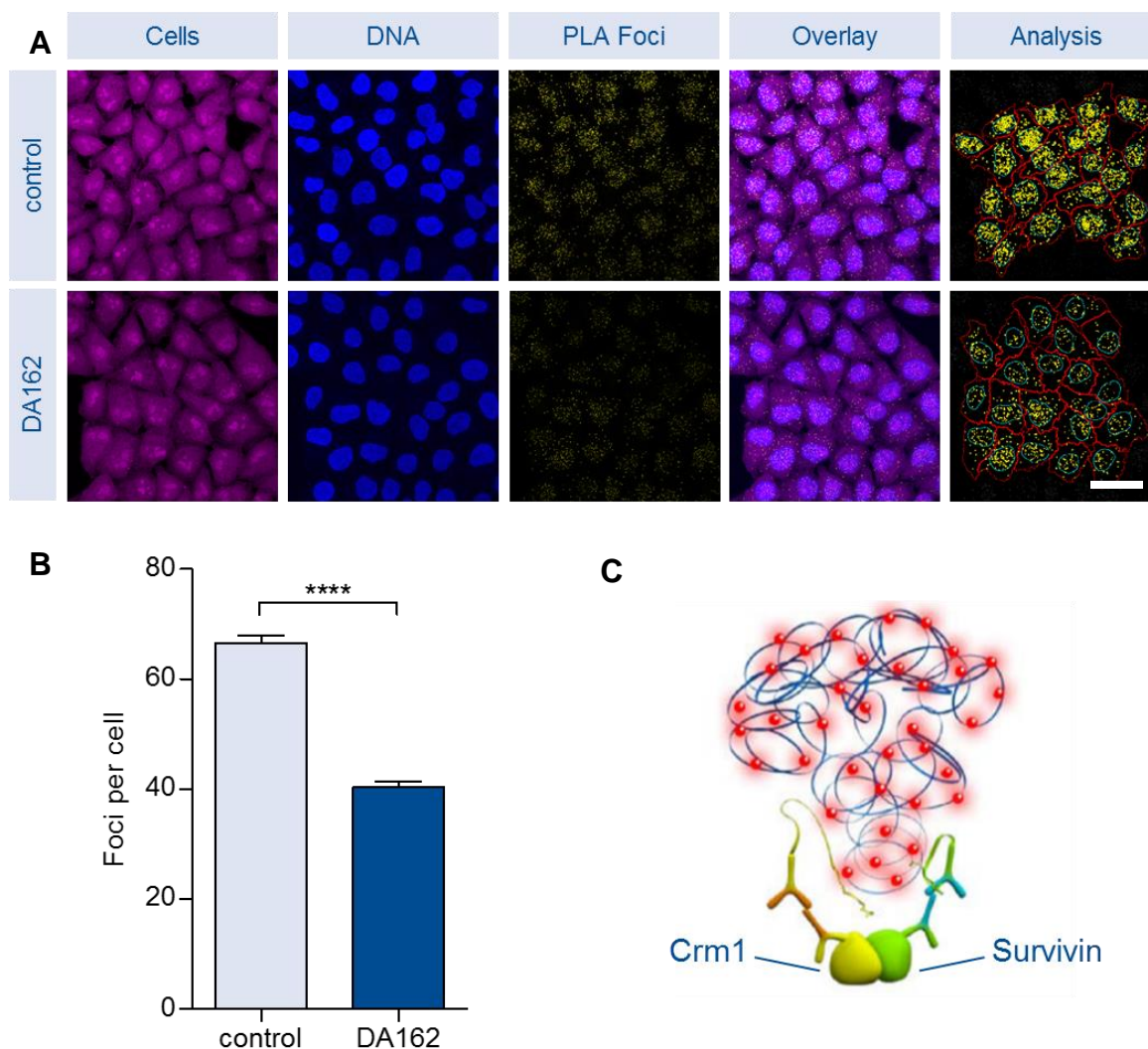
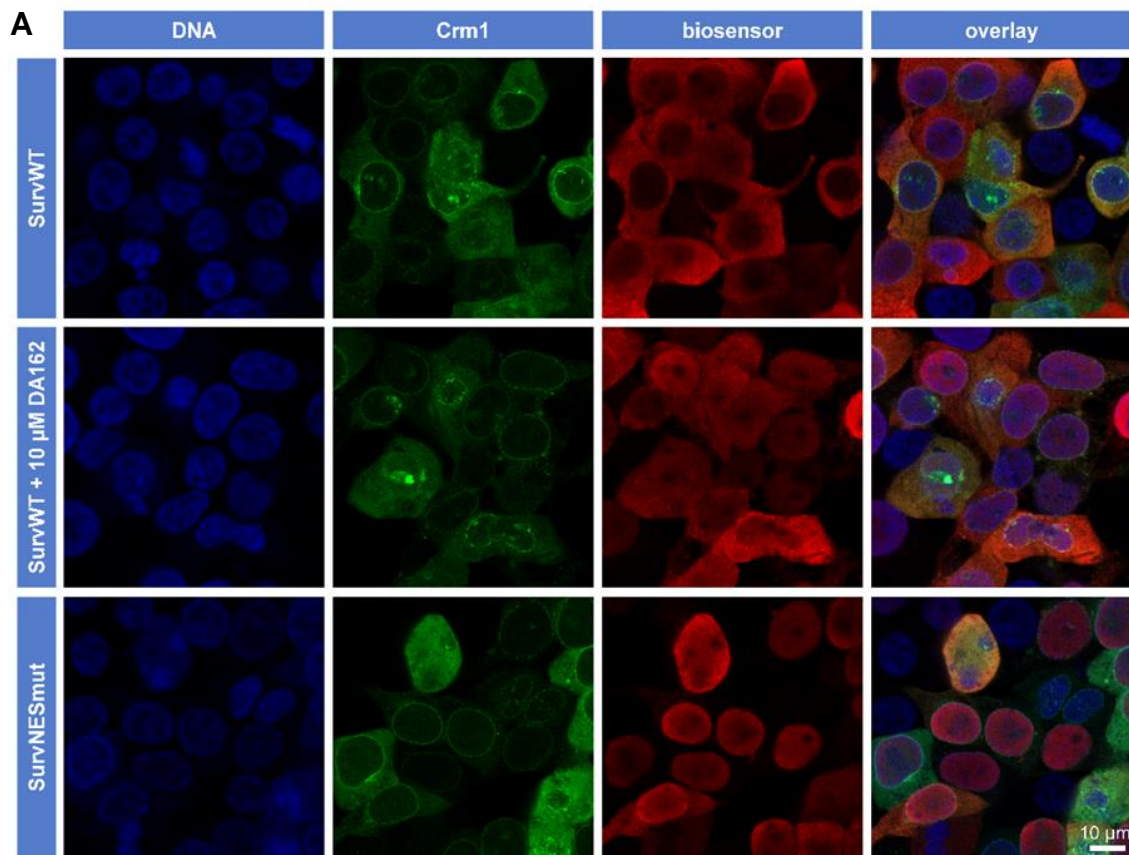


**Figure 3.16: DA162 inhibits the Survivin-Crm1 interaction in HeLa cells.** **A)** Representative images of PLA. Entire cells are depicted in magenta, DNA in blue and PLA foci in yellow. Scale bar: 20  $\mu\text{m}$ . **B)** Quantitative analysis of the interaction between Survivin and Crm1. HeLa cells were treated with either 50  $\mu\text{M}$  DA162 or the respective amount of  $\text{H}_2\text{O}$  (control) for 24 h prior to fixation and PLA staining. The bar graph shows the number of PLA foci per cell in treated cells vs. control cells. Data was analyzed by t test. Four asterisks (\*\*\*\*) indicate p value smaller than 0.0001 (99 % confidence interval). The error bars represent SEM. **C)** Functional principle of PLA with endogenous Survivin and Crm1. If the two proteins are in close proximity (<40 nm), the rolling circle amplification with fluorescent nucleotides will generate a PLA signal that can be detected with the fluorescence microscope (124). N>155.

### 3.2.4 CRM1-MEDIATED NUCLEAR EXPORT OF SURVIVIN IS REDUCED BY DA162

As the PLA revealed that DA162 is able to decrease the interaction between Survivin and Crm1 in HeLa cells, the question was whether this also affects Survivin's Crm1-mediated nuclear export. This was tested with a SRV100 biosensor assay that allows the analysis of Crm1's export activity in the presence or absence of a potential Survivin-Crm1 inhibitor in a cellular context. The biosensor contains two NLSs that ensure its nuclear localization in case it is not actively exported by Crm1, a shortened version of Survivin (1–100) and a 3 x Flag-tag. Without an inhibitor, Crm1 exports the biosensor into the cytoplasm. When an inhibitor is able to prevent Survivin's Crm1-mediated nuclear export, the biosensor remains in the nucleus. HEK 293T cells were cotransfected with Crm1-GFP and the Survivin wildtype (SurvWT) biosensor and either treated with 10  $\mu$ M DA162 or the respective amount of H<sub>2</sub>O. Alternatively, they were cotransfected with Crm1-GFP and the NESmut biosensor, containing a known export deficient NES mutant of Survivin (L96A, L98A). Cells were then fixed and immunostained prior to microscopic analysis.

It could be shown that, as expected, the biosensor localized predominantly to the cytoplasm in cells transfected with the SurvWT biosensor and almost exclusively to the nucleus in cells transfected with the NESmut biosensor confirming a properly functioning assay (Fig. 3.12 A). In cells that were treated with DA162, the biosensor localized to the nucleus in some cells, while it seemed rather evenly distributed or cytoplasmic in others, which suggests that DA162 decreases Survivin's Crm1-mediated nuclear export to some extent but that, at least at this concentration, a small proportion of Survivin is still exported into the cytoplasm (Fig. 3.12 A). To quantify the results, cells were assigned to one of three different groups: Cells with a predominantly nuclear localization of the biosensor, cells with an evenly distributed biosensor and cells with a predominantly cytoplasmic localization of the biosensor (Fig. 3.12 B and C). The analysis revealed that in 78 % of cells transfected with the SurvWT biosensor the biosensor had a predominantly cytoplasmic localization, while it was evenly distributed in 19 % of cells and predominantly nuclear in only 3 % of cells. A treatment with DA162 led to a decrease of the proportion of cells with a cytoplasmic localization of the biosensor and an increase of cells with a nuclear localization of the biosensor. In DA162-treated cells, only 55 % of cells showed a cytoplasmic localization of the biosensor, while it was evenly distributed in 16 % of cells and predominantly nuclear in 29 % of cells. In 100 % of cells transfected with the NESmut biosensor, the biosensor was located in the nucleus. This confirms the assumption that DA162 is able to decrease the Crm1-mediated nuclear export of Survivin, at least to a certain extend.



**B**

Nucleocytoplasmic localization	SurvivinWT untreated	SurvivinWT 10 μM DA162	SurvivinNESmut untreated
N<C	48	32	0
N=C	12	9	0
N>C	2	17	49

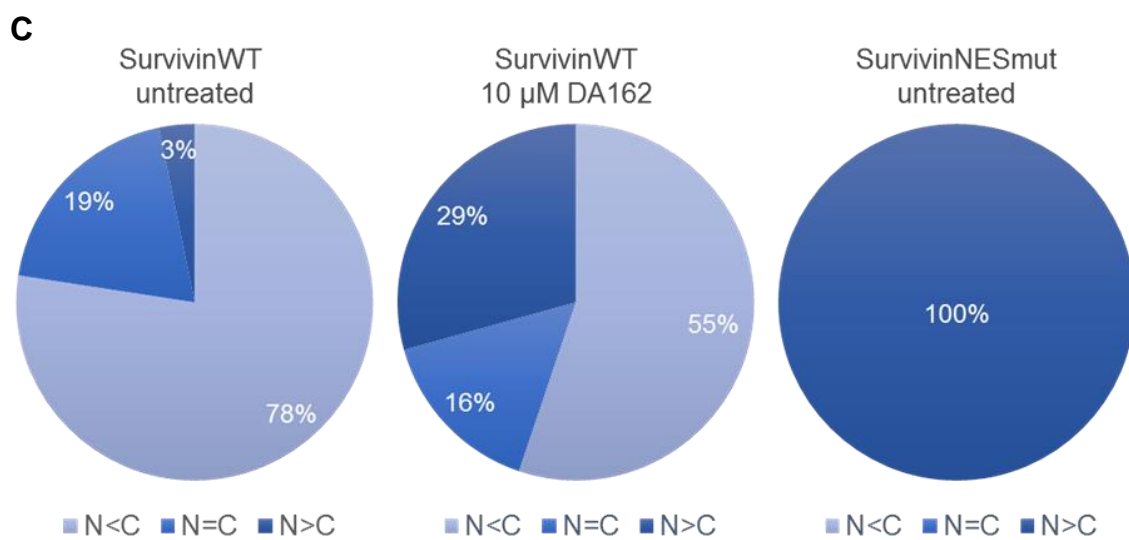


**Figure 3.17: DA162 decreases the Crm1-mediated nuclear export of Survivin.** **A)** Representative images of the biosensor assay in HEK 293T cells. Cells were cotransfected with Crm1-GFP and SurvWT or SurvNESmut (negative control) biosensor. One of the SurvWT samples was additionally treated with 10  $\mu$ M DA162 for 24 h before the samples were fixed and immunostained. DNA is shown in blue, Crm1-GFP in green and the biosensor in red. **B)** Quantification of nucleocytoplasmic localization of the biosensor. **C)** Percentages of nucleocytoplasmic localization in SurvWT, SurvWT+DA162 and SurvNESmut samples. N=nucleus, C=cytoplasm. N>50.

### 3.2.5 DA162 HAS NO SIGNIFICANT INFLUENCE ON SURVIVIN DIMERIZATION

As Survivin's NES overlaps with its dimerization site, nuclear export and homodimerization are thought to be competitive processes. Thus, it seems reasonable to suppose that an inhibition of the Survivin-Crm1 interaction might also affect homodimerization. To investigate the influence of DA162 on Survivin dimerization, cells were transfected with Cerulean-Survivin and Citrine-Survivin (Fig. 3.13 A) and treated with 10  $\mu$ M DA162 or the respective amount of H<sub>2</sub>O for 24 h before they were fixed and analyzed by Acceptor Photobleaching FRET assay.

FRET efficiencies in DA162-treated cells were not significantly different from those in control cells although DA162 seemed to slightly increase Survivin dimerization. DA162-treated cells had an average FRET efficiency of 0.20, while the average FRET efficiency in control cells was only 0.17 (Fig. 3.13 B). This indicates that DA162 might have a small effect on dimerization but that this effect is, maybe due to the rather small sample size (n=17 for each condition), not significant.

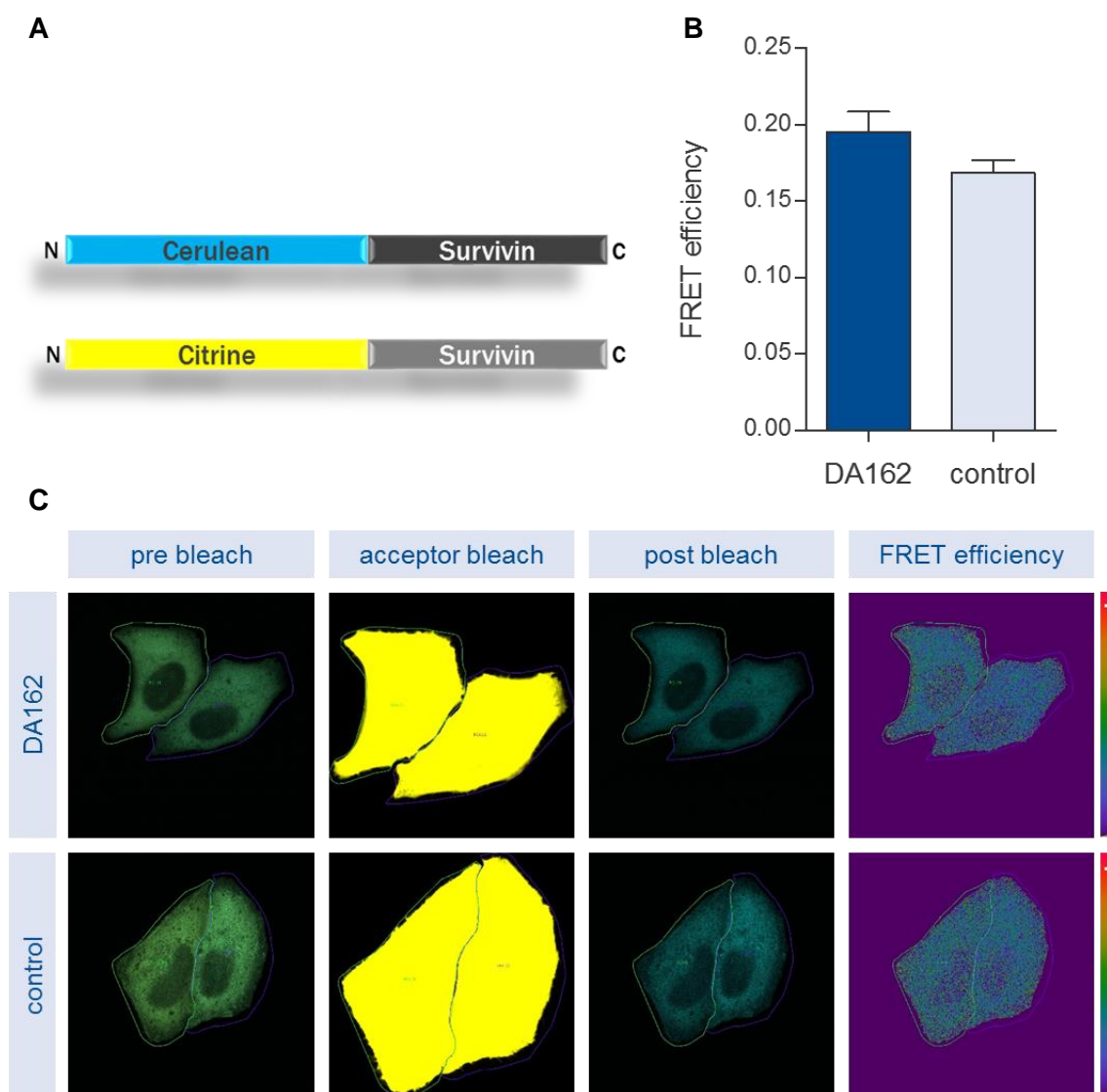


**Figure 3.18: DA162 treatment does not have a significant influence on Survivin dimerization in HeLa cells.** **A)** Transfection constructs Cerulean-Survivin and Citrine-Survivin used for Acceptor Photobleaching FRET Assay. **B)** FRET efficiencies in DA162-treated cells in comparison to H<sub>2</sub>O-treated cells (control). HeLa cells were cotransfected with Cerulean-Survivin (donor) and Citrine-Survivin (acceptor) and treated with 10  $\mu$ M DA162 or the respective amount of H<sub>2</sub>O for 24 h before they were fixed and analyzed via Acceptor Photobleaching FRET Assay. Data analysis via t test resulted in a p value larger than 0.05 (99 % confidence interval) and was therefore not significant. The error bars represent SEM. **C)** Representative images of the FRET assay in DA162-treated vs. control cells. Pre bleach and post bleach images show overlay of Cerulean (cyan) and Citrine (yellow) signals. Acceptor bleach image shows area of the cell that was bleached for 15 frames at a laser wavelength of 514 nm. FRET efficiencies are visualized by pseudo coloured images. N=17.

### 3.2.6 DA162 REDUCES PROLIFERATION OF CANCER CELLS

It could be shown that DA162 is able to decrease the interaction between Survivin and Crm1 and reduce Survivin's Crm1-mediated nuclear export into the cytoplasm. As the interaction with Crm1 is important for Survivin's mitotic as well as anti-apoptotic functions, it seems likely that DA162 treatment has an influence on cell proliferation. This is why the influence on cell proliferation was tested on different kinds of cancer cells: HeLa cells that are derived from cervical cancer, A549 cells as a model for lung cancer, MDA-MB-231 cells originating from breast cancer and HCT 116 cells that served as a model for colon cancer.

The cells were treated with different concentrations of DA162 or the respective amounts of H<sub>2</sub>O (control) and incubated for 72 h before cell proliferation was measured using the CellTiter 96<sup>®</sup> Aqueous One Cell Proliferation Assay (Promega). The assay determines the number of viable cells with the help of a tetrazolium compound that is added to the cells. After 4 h the quantity of formazan product, which is directly proportional to the number of living cells, can be measured at 490 nm (127).

It could be demonstrated that DA162 reduces cell proliferation in all cancer cell lines tested, albeit to different degrees. In addition to that, the effect was enhanced with increasing concentrations of the ligand (Fig. 3.14).

In HeLa cells, cell proliferation only decreased by 15 % in cells treated with the highest ligand concentration (200  $\mu$ M) compared to the control. Treatment with lower concentrations only had a small effect on proliferation (6 % decrease at 100  $\mu$ M, and 5 % decrease at 50  $\mu$ M and 10  $\mu$ M).

The strongest effect on cell proliferation could be observed in A549 cells, where the DA162 treatment led to a 53 % decrease in cell proliferation at a concentration of 200  $\mu$ M. Weaker effects could still be observed at 100  $\mu$ M (24 % decrease), 50  $\mu$ M (22 % decrease) and 10  $\mu$ M (16 % decrease).

In MDA-MB-231 cells, cell proliferation decreased by 47 % at a ligand concentration of 200  $\mu$ M and by 35 % at a concentration of 100  $\mu$ M. At lower concentrations, proliferation was still reduced by 23 % (50  $\mu$ M) and 18 % (10  $\mu$ M).

The effect on HCT 116 cells was less pronounced than in A549 or MDA-MB-231 cells. Nevertheless, cell proliferation decreased by 32 % at the highest ligand concentration of 200  $\mu$ M and by 18 % at a concentration of 100  $\mu$ M. Treatment with lower concentrations

had a much smaller effect: 50  $\mu\text{M}$  DA162 led to a 10 % decrease and 10  $\mu\text{M}$  DA162 to a 9 % decrease in cell proliferation compared to the control.

Taken together, DA162 reduces cell proliferation in several cancer cell lines from different origins with the strongest effect in the lung cancer cell line A549, where it decreased cell proliferation by up to 53 %.

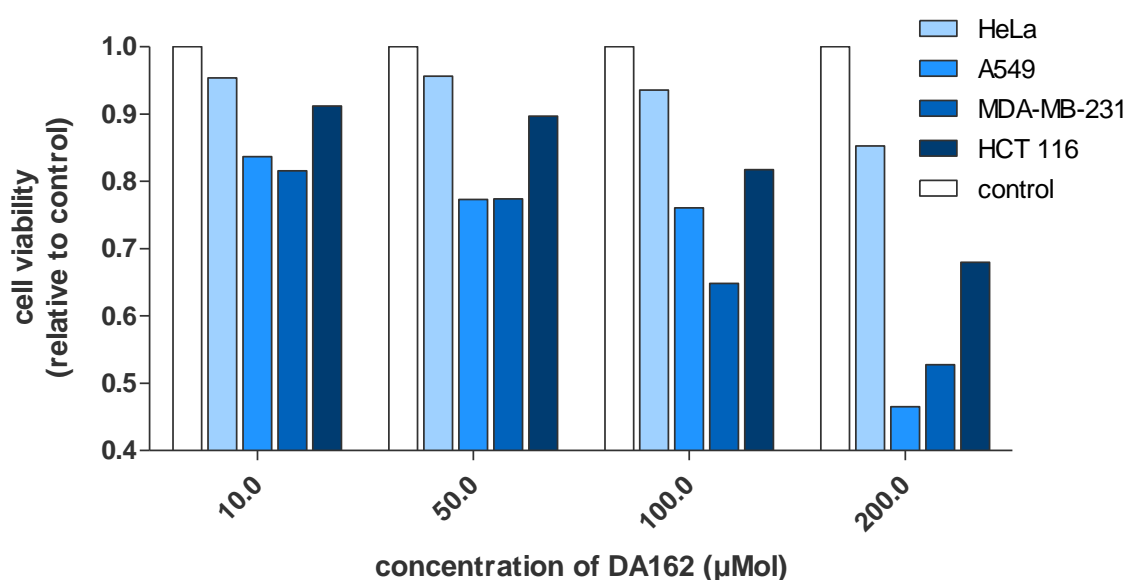


**Figure 3.19: DA162 treatment leads to a concentration-dependent inhibition of cell proliferation in different types of cancer cells.** HeLa, A549, MDA-MB-231 and HCT 116 cells were treated with different concentrations of DA162 or the respective amounts of  $\text{H}_2\text{O}$  and incubated for 72 h before cell proliferation was measured using the CellTiter 96<sup>®</sup> AQueous One Cell Proliferation Assay (Promega). The absorbance (490 nm) values of the samples were subtracted by a medium only control. Absorbance of DA162-treated cells is depicted relative to control.

### 3.2.7 APOPTOSIS INCREASES AFTER DA162 TREATMENT

The interaction between Survivin and Crm1 is essential for Survivin to be exported into the cytoplasm, where it fulfills its role as an inhibitor of apoptosis. By reducing the interaction between the two proteins with DA162, it would be expected that the proportion of cells undergoing apoptosis increases. To verify whether this is the case, several kinds of cancer cell lines were treated with different concentrations of DA162 for 72 h before they were analyzed with the ApoLive-Glo™ Multiplex Assay (Promega), which measures caspase 3/7 activation as an indicator for apoptosis. The cell lines used for this experiment were derived from different origins. HeLa cells are derived from cervical cancer, A549 cells from lung cancer, MDA-MB-231 from breast cancer and HCT 116 cells from colon cancer.

As expected, DA162 treatment increased caspase 3/7 activation in all four cancer cell lines (Fig. 3.15). In HeLa cells, caspase 3/7 activation increased by 13 % already at the lowest concentration tested (10  $\mu$ M). At higher concentrations, caspase 3/7 activation increased even more: by 30 % at 50  $\mu$ M, by 42 % at 100  $\mu$ M and by 37 % at 200  $\mu$ M.

The strongest effect on was observed in A549 cells. At a concentration of 200  $\mu$ M DA162, caspase 3/7 activation was increased by 73 % and at a concentration of 100  $\mu$ M by 52 %. DA162 still had an effect in lower concentrations: It increased caspase 3/7 activation by 30 % at 50  $\mu$ M and by 10 % at 10  $\mu$ M.

In MDA-MB-231 cells, DA162 treatment only had a minor effect in cells treated with low concentrations of the ligand. Caspase 3/7 activation was increased by 10 % at a concentration of 50  $\mu$ M, while no effect could be observed at a concentration of 10  $\mu$ M. Nevertheless, higher concentrations of DA162 increased caspase 3/7 activation by 20 % (100  $\mu$ M) or even 41 % (200  $\mu$ M).

The weakest effect was observed in HCT 116 cells. Only the highest concentration tested caused an increase of caspase 3/7 activation by 32 % compared to the control, while lower concentrations of DA162 increased caspase 3/7 activation by less than 5 %.

To sum up, caspase 3/7 activation, which is an indicator for apoptosis, was increased by DA162 treatment in all cancer cell lines tested. The highest effect could be observed in A549 cells, where caspase 3/7 activation was increased by up to 73 %.

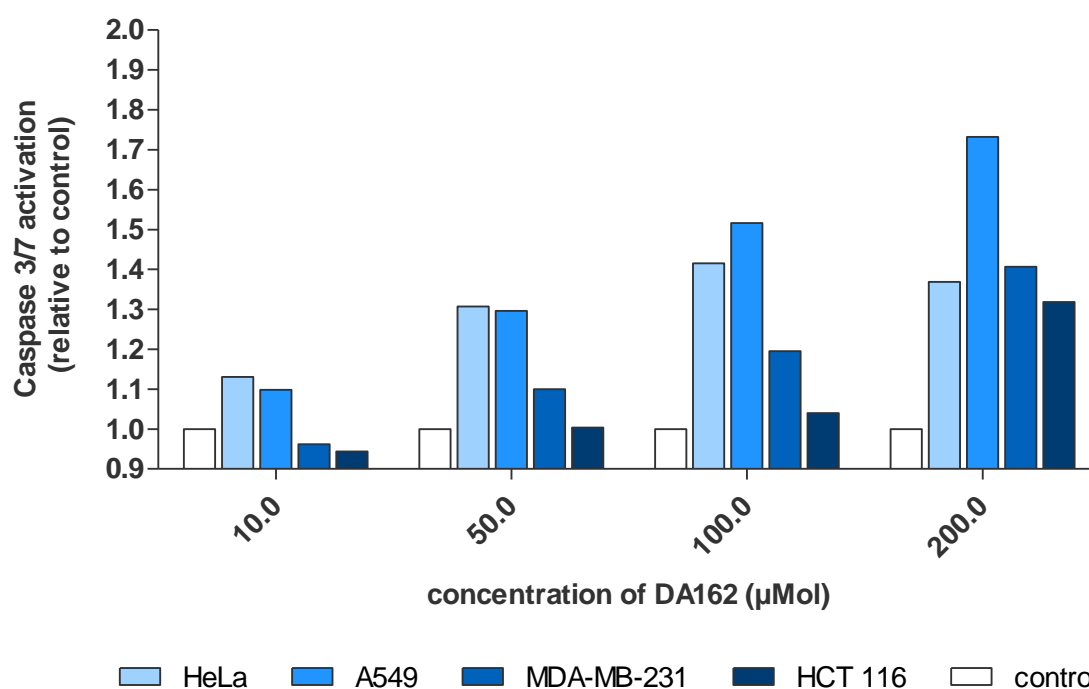


**Figure 3.20: DA162 treatment increases caspase 3/7 activation.** HeLa, A549, MDA-MB-231 and HCT 116 cells were treated with different concentrations of DA162 or the respective amounts of H<sub>2</sub>O and incubated for 72 h before caspase 3/7 activation was measured using the ApoLive-Glo™ Multiplex Assay (Promega). The luminescence of DA162 is depicted relative to control.

Taken together, this part of the project demonstrated that DA162 is able to bind to Survivin with a low micromolar  $K_D$  and that the ligand successfully reduces the interaction between Survivin and its export receptor Crm1, which affects both, Survivin's anti-apoptotic as well as its mitotic functions. DA162 decreases Survivin's Crm1-mediated nuclear export into the cytoplasm and thereby seems to interfere with Survivin's mitotic and anti-apoptotic functions.

In this thesis, several cellular and microscopic assays to analyze the influence of potential protein-protein inhibitors on Survivin's cellular functions were established. With the help of those assays, two potential inhibitors were tested regarding their effect on Survivin's role in cell proliferation and apoptosis. MM138 could be validated as promising Survivin-Histone H3 inhibitor, which seems to interfere with Survivin's mitotic functions, while DA162 was able to reduce the interaction between Survivin and Crm1, thereby interfering with Survivin's role in both apoptosis and cell proliferation.

## 4 DISCUSSION

The protein Survivin is considered a key player of carcinogenesis due to its anti-apoptotic function and its role in cell proliferation. It is highly upregulated in most cancers and associated with therapy resistance and a poor clinical outcome (11–15). As it is mainly expressed during embryonic development but mostly absent in terminally differentiated adult tissues, it might be one of the most cancer-specific proteins identified so far (105). As Survivin possesses no enzymatic activity, it is challenging to address the protein as a drug target. Current therapeutic strategies include antisense oligonucleotides, siRNAs, small molecule inhibitors, gene therapy and immunotherapy but none of those approaches has yet reached the clinic (86).

This thesis is part of the collaborative research project “Supramolecular Chemistry on Proteins” (CRC1093), which focuses on the development of supramolecular ligands to manipulate protein-protein interactions (PPIs). Instead of trying to downregulate the expression of Survivin, this project explored a new approach by identifying PPI inhibitors that interfere with Survivin’s cellular functions. In collaboration with the Schmuck group (Supramolecular Chemistry, University of Duisburg-Essen), the goal was to develop highly selective supramolecular ligands to target PPIs between Survivin and its functionally relevant binding partners. To identify such ligands, rational design ideas derived from known structural data of the target protein were combined with combinatorial approaches. The ligands are based on the guanidiniocarbonyl pyrrole cation (GCP), which is a highly specific anion binder. Hence, they target mainly anionic hot spots on the protein surface like glutamic and aspartic acids.

Survivin possesses two anionic hot spots that are surface exposed and functionally relevant: the Histone H3 binding site and the nuclear export signal (NES). The Schmuck group developed several supramolecular GCP ligands that were designed to specifically target one of Survivin’s anionic hot spots. In this thesis, two of the potential PPI inhibitors were characterized regarding their effect on Survivin’s cellular functions to gain a better understanding of Survivin’s biological role and contribute to the development of new approaches to target Survivin in the context of cancer therapy.

## 4.1 INHIBITION OF SURVIVIN-HISTONE H3 INTERACTION WITH GCP LIGAND MM138

The supramolecular GCP ligand MM138 was designed to specifically target Survivin's Histone H3 binding site <sup>51</sup>EPDLAQCFCKELEGWEPDDDDPIEEHKKH<sup>80</sup>. The interaction between Survivin and Histone H3 is crucial for Survivin to fulfil its role within the CPC during mitosis. Survivin's BIR domain directly binds to Histone H3 during pro- and metaphase and thereby tethers the CPC to the chromosome arms. Inhibiting the protein-protein interaction between Survivin and Histone H3 would therefore interfere with Survivin's role in cell proliferation. MM138 consists of two GCP groups and was designed to interact with surface accessible glutamic and aspartic acids within Survivin's BIR domain to interfere with Histone H3 binding.

### 4.1.1 MM138 BINDS TO SURVIVIN'S HISTONE H3 BINDING SITE

Preliminary docking studies suggested that MM138 preferably binds to Survivin's Histone H3 binding site. The amino groups of the cationic ligand presumably interact with the anionic glutamic acids 65 and 76 as well as aspartic acids 71 and 72 (section 3.1.1). This is in agreement with previous studies, which could show that GCP ligands are able to bind to target proteins through highly specific interactions with the anionic amino acids glutamic acid and aspartic acid (113, 114, 135, 136). They bind carboxylates by ion pairing in combination with hydrogen bonding (113). The hydrophobic character of GCP ligands facilitates cellular uptake, making them suitable to target Survivin inside the cell (115).

The predicted binding site of MM138 to the Histone H3 binding site of Survivin was verified by NMR titration. Previous dynamic simulations of the Survivin monomer and dimer revealed that the C-terminal  $\alpha$ -helix is very flexible and might destabilize the protein. So far, the only published NMR structure of Survivin is of a truncated version of the protein (aa 1–120) (122). Thus, truncated Survivin 1-120, which still contains both of Survivin's surface accessible anionic hot spots, the NES and the Histone H3 binding site, was used for NMR titration experiments. It could be shown that MM138 caused chemical shift perturbations at glutamic acids (E) 63, 65 and 68, aspartic acids (D) 70, 71 and 72 and glutamic acids (E) 75 and 76. Those amino acids correspond to the known Histone H3 binding site of Survivin, which comprises amino acids 51 to 80. Since chemical shift perturbations can also occur, when ligands interact with the protein for only a short period of time without actually binding to it, signal intensities were evaluated in addition. A more than average decrease in relative

intensity for glutamic acid (E) 68, aspartic acid (D) 70, 71 and 72 and glutamic acid (E) 75 confirmed an actual binding to Survivin's Histone H3 binding site (section 3.1.2). NMR data is therefore in agreement with previous docking results. The fact that MM138 seems to have only one distinct binding site on the protein surface of Survivin suggests that the GCP ligand is highly specific for this anionic hot spot.

#### 4.1.2 MM138 INHIBITS THE SURVIVIN-HISTONE H3 INTERACTION

Even though NMR experiments demonstrated that MM138 addresses Survivin's Histone H3 binding site, this does not necessarily mean that the ligand is able to inhibit the interaction between the two proteins. Moreover, the question arose whether the ligand is cell-permeable and able to interact with Survivin in a cellular environment. Previous results have shown that the hydrophobic character of the GCP group facilitates cellular uptake (115). Whether MM138 is taken up by cells and able to inhibit the interaction between Survivin and Histone H3 was tested via co-immunoprecipitation and Proximity Ligation Assay (PLA). Co-immunoprecipitation revealed that MM138 successfully inhibited the Survivin-Histone H3 interaction in a concentration-dependent manner. A concentration of 10  $\mu\text{M}$  MM138 already led to a 50 % decrease in Survivin-Histone H3 interaction (section 3.1.3). Unfortunately, MM138 is not water-soluble and has to be dissolved in DMSO. Therefore, it was not possible to test the ligand in concentrations higher than 50  $\mu\text{M}$ , as larger amounts of DMSO had severe toxic effects on the cells. Co-immunoprecipitation experiments required an overexpression of Survivin-HA. As this does not fully correspond to the natural conditions inside the cell and might have an influence on the outcome of the experiment, the results had to be validated with endogenous expression levels. In addition to that, Western Blot analysis is only semi-quantitative and not suitable to determine the effective concentration of the inhibitor.

To overcome these limitations, a PLA was established, which allows detection of protein-protein interactions on an endogenous level. The interaction between Histone H3 and Survivin takes place during the early phases of mitosis, where it is crucial to tether the CPC to the centromeres. Survivin's BIR domain directly binds to Histone H3 phosphorylated on threonine 3. In anaphase, Survivin and Histone H3 disengage and the CPC relocates to the spindle midzone (21, 61, 137). To verify the accuracy of the PLA, the Survivin-Histone H3 interaction was first examined in all mitotic phases. The fact that PLA signals could only be detected in prophase and metaphase, when the two proteins are known to interact with each other, confirmed that the assay is suitable to analyze the interaction

between the two proteins during mitosis. To quantify the interaction after MM138 treatment, cells were synchronized with the CDK1 inhibitor RO-3306, which enables the enrichment of cells in the early phases of mitosis. The PLA revealed that MM138 treatment significantly reduced the interaction between Survivin and Histone H3 (section 3.1.3). However, the number of foci per cell did not differ as much as expected, and interactions between Survivin and Histone H3 could still be detected after MM138 treatment. One reason could be that a PLA signal does not necessarily mean that the two proteins of interest really interact with each other. A signal can still be created when both proteins are in close proximity to each other (<40 nm) and not in direct contact. This means that Survivin and Histone H3 might still generate a PLA signal if they lie in close proximity but are not able to interact with each other anymore. Another problem could be that a concentration of 50  $\mu$ M MM138 might not have been sufficient to completely inhibit the interaction between the two proteins or that possibly not the entire amount of MM138 was taken up by the cell. To track the cellular uptake and localization of MM138, a possibility could be to link the ligand to a fluorophore. This would allow the visualization of the uptake and distribution of MM138 inside the cell.

#### **4.1.3 SURVIVIN DIMERIZATION IS INCREASED BY MM138 TREATMENT**

Initially, Survivin was thought to be dimeric inside cells, whereas the monomeric form seemed to have no biological function (24). In contrast to that, more recent studies show that both dimeric and monomeric Survivin have distinct functions within the cell. Monomeric Survivin interacts with the export receptor Crm1 during its nuclear export, with Smac/DIABLO and XIAP to fulfil its anti-apoptotic functions as well as with the members of the CPC during mitosis (18, 21, 84). It has been demonstrated that the homodimerization of Survivin antagonizes its nuclear export due to the overlap of the nuclear export signal (aa 89–98) and the dimer interface (aa 6–10 and 89–102). Dimeric Survivin has been shown to stabilize microtubules and to inhibit STAT3 (83). In addition, Survivin dimerization is important to prevent destabilization and degradation of the protein through the proteasome or autophagy. It could be demonstrated that inhibition of Survivin dimerization triggers its degradation (85). As dimerization and interaction with other binding partners seem to be competitive processes, the question was if the inhibition of the Survivin-Histone H3 interaction would have an influence on Survivin dimer formation inside the cell. To examine Survivin dimerization inside the cell, an Acceptor Photobleaching FRET Assay was established, which used Cerulean-Survivin as donor and Citrine-Survivin as acceptor. It could be observed that MM138 treatment significantly increased Survivin dimerization

(section 3.1.4). A reason for this could be that Survivin dimerization might be a kind of “storage form” inside the cell as the protein seems to be proteolytically degraded when in its monomeric form (138). Survivin appears to either interact with one of its binding partners or form homodimers to prevent degradation. In solution, when no potential binding partners are present, Survivin appears to always be dimeric (25). Disturbing the interaction between Survivin and Histone H3 might therefore promote Survivin dimerization as less of the protein is bound to Histone H. To examine whether MM138 really increases Survivin dimerization, the results should be verified with alternative assays.

Acceptor Photobleaching FRET is a relatively straightforward technique to measure Survivin dimerization in fixed cells but it is also very error prone. One problem that all existing FRET pairs share is the difference in brightness of donor and acceptor. In this case, the donor fluorophore Cerulean is dimmer than the acceptor fluorophore Citrine. Because of this, Cerulean is more affected by systematic noise, which is a problem when comparing cells with different expression levels of the donor construct as the signal-to-noise-ratio is less favorable in cells with a lower donor expression (139, 140). One solution might be to use a different FRET pair although most FRET pairs that have a comparable brightness are in turn more prone to bleed-through and cross-talk (139, 141). An issue when measuring FRET is always that the emission spectrum of the donor and the excitation spectrum of the acceptor need to overlap. Unfortunately, in most cases, this also means that the excitation spectra of donor and acceptor partially overlap and that the acceptor can be excited directly with light that was meant to excite the donor. In turn, fluorescence from the donor can similarly leak into the detection channel of the acceptor fluorophore (139). Another problem that is not to neglect when measuring FRET is that the fluorescent proteins might have an influence on the dimerization behavior of the protein(s) of interest. In the case of Survivin, the fluorescent proteins Cerulean and Citrine (27 kDa each) have a higher molecular weight than Survivin itself (16.5 kDa), which might hamper dimerization. In this work, Cerulean and Citrine were directly linked to Survivin. Using a small linker between the fluorophore and Survivin might help to facilitate dimerization and further increase the FRET efficiency. Another alternative to avoid most difficulties of Acceptor Photobleaching FRET would be to establish a FLIM-FRET assay. Fluorescent proteins exhibit an exponential decay in their fluorescence on a nanosecond timescale, and the rate of this decay is sensitive to quenching. Similar to the Acceptor Photobleaching FRET assay, the donor fluorescence is quenched when donor and acceptor are in close proximity. The FRET efficiency can then be determined by measuring the decrease in fluorescence decay time. Advantages are that FLIM-FRET measurements are insensitive to direct acceptor excitation and less prone to crosstalk (139, 142).

#### 4.1.4 MM138 INTERFERES WITH SURVIVIN'S ROLE IN CELL PROLIFERATION

As a member of the chromosomal passenger complex (CPC), Survivin acts as a key regulator of mitosis (59). The CPC plays a role in chromosome condensation, kinetochore-microtubule attachment, activation of the spindle assembly checkpoint and formation of the contractile ring during cytokinesis (60). Apart from Survivin, it consists of the kinase Aurora B and the two proteins INCENP and Borealin with which Survivin's C-terminal  $\alpha$ -helix forms a three helix bundle (20). In pro- and metaphase, Survivin plays a central role in kinetochore-microtubule attachment and is responsible for tethering the CPC to the chromosome arms through its interaction with Histone H3. This interaction is essential to enable the Aurora B kinase to phosphorylate Histone H3 on serine 10 and serine 28. Both phosphorylations are required for chromosome condensation during mitosis (143, 144). As MM138 seemed to be able to inhibit the interaction between Survivin and Histone H3 inside the cell, the question was whether the inhibitor would consequently also interfere with Survivin's role in cell proliferation. Experiments revealed that MM138 treatment drastically increased the number of mitotic defects in HeLa cells. Furthermore, MM138-treated cells showed a larger variety of mitotic defects. In addition to acentric fragments and lagging chromosomes, also chromatin bridges or multipolar spindles could be observed (section 3.1.5). Chromosome segregation defects like acentric fragments, lagging chromosomes or chromatin bridges can have many different reasons and are the most common mitotic defects observed in cancer cell lines like HeLa cells (131). This would explain why some untreated cells also exhibited the respective phenotypes. It is assumed that DNA damage or a defective DNA damage repair are the main causes of segregation defects (131, 145). Recent findings show that Survivin and the other members of the CPC seem to play a role in DNA damage response (146–149). Therefore, it could be speculated whether MM138 might also impair Survivin's functions during DNA damage repair. However, segregation defects can also be caused by factors such as defective chromosome condensation or kinetochore-microtubule attachment errors (150). This is in line with the known functions of the CPC during mitosis as the complex plays a central role in kinetochore-microtubule attachment and is responsible for the phosphorylation of Histone H3 on serine 10 and serine 28, which is required for chromosome condensation (60). Multipolar spindles are often associated with a malfunction of centrosomes or supernumerary centrosomes and can be linked to the emergence of anaphase lagging chromosomes (151–156). It has been shown that Survivin also localizes at the centromeres in interphase as well as during mitosis. Although the exact functional mechanism is not known yet, Survivin seems to have an important role in centrosome duplication and function (157). Therefore, the influence of MM138 on Survivin's centrosomal functions should be

further investigated. In previous studies where Survivin was depleted with siRNA, segregation defects, supernumerary centrosomes, aberrant mitotic spindles and reduced activity of Aurora B at the centromeres/kinetochores in cells could also be observed (3, 158, 159). This is in perfect agreement with the findings in MM138-treated cells and confirms that MM138 is indeed able to interfere with Survivin's mitotic functions. Whether these defects only result from an inhibition of the Survivin-Histone H3 interaction, or if other protein-protein interactions involving Survivin's BIR domain might also be impaired by MM138 treatment, needs to be further elucidated.

At best, a ligand targeting Survivin's mitotic functions should not only cause mitotic defects but also be able to decrease the proliferation rate of cancer cells. In other studies, the defects in cell division after a Survivin depletion were followed by an arrest of DNA synthesis due to checkpoint activation and eventually cell death (150). Similar effects could be observed in this work. A proliferation assay in several cancer cell lines from different origins revealed that MM138 was indeed able to inhibit cell proliferation in all cancer cell lines tested, albeit to different extents (section 3.1.6). In three of the four cell lines, proliferation could be decreased by more than 30 %. This is comparable to the decrease in proliferation observed in Survivin depleted cancer cells and therefore confirms that the supramolecular ligand MM138 is able to successfully inhibit cancer cell proliferation (160–162). A reason why the cell lines responded differently to MM138 treatment could be different expression levels of Survivin. Although it has been shown that Survivin is overexpressed in all cell lines tested, the expression levels vary (160, 163). A study of Yang *et al.* showed that DNA synthesis was arrested in Survivin depleted cells subsequent to abnormal mitosis and therefore speculated that a checkpoint had been activated to prevent DNA endoreduplication (150). Yang *et al.* observed that Survivin depletion increased the expression of p53 and its downstream target p21, which is a cell-cycle inhibitor, and concluded that the proliferative arrest caused by Survivin depletion had characteristics of the activation of a p53-dependent checkpoint response (150). Those results indicate that the p53 status plays a role in the response to Survivin malfunction. However, this is inconsistent with the fact that MDA-MB-231 cells responded to MM138 treatment although they were the only cell line with mutated p53. One could also assume that an impairment of the mitotic checkpoint might have an influence on the response to MM138 treatment. A dysfunctional mitotic checkpoint is a common phenotype in human cancer cells that promotes cell survival and increases the resistance to anti-cancer drugs (164). Aneuploidy is one indicator for mitotic checkpoint defects since the mitotic checkpoint is a cellular surveillance mechanism to maintain accurate segregation of sister (164). Three of the four cell lines tested in this thesis have an abnormal number of chromosomes. Only HCT 116

cells are near diploid (polyploidy occurring in only 6.8% of cells) (165). The fact that HCT 116 indeed responded best to MM138 treatment (decrease in cell proliferation of nearly 40 % at the highest inhibitor concentration) supports the assumption that mitotic checkpoint defects might have an influence on the efficacy of MM138 treatment.

Taken together it could be shown that the supramolecular GCP ligand MM138 binds to Survivin's Histone H3 binding site and is able to inhibit the interaction between the two proteins inside the cell. The ligand was able to inhibit Survivin's mitotic functions and to decrease cell proliferation in several different cancer cell lines. MM138 therefore seems to be a promising candidate ligand to target the interaction between Survivin and Histone H3 and thereby interfere with Survivin's promoting role in cancer cell proliferation.

## 4.2 INHIBITION OF SURVIVIN-CRM1 INTERACTION WITH GCP LIGAND DA162

Another possibility to target Survivin's cellular functions is to inhibit the interaction between Survivin's NES <sup>89</sup>VKKQFEELTL<sup>98</sup> and the export receptor Crm1. This interaction is not only essential for Survivin's Crm1-mediated nuclear export into the cytoplasm, where Survivin acts as an inhibitor of apoptosis, but also to tether the CPC to the centromeres during mitosis. Inhibiting the protein-protein interaction between Survivin and Crm1 would therefore interfere with both Survivin's role in cell proliferation as well as with its anti-apoptotic functions (21). Thus, the four-armed GCP ligand was designed to interact with surface accessible glutamic acids within Survivin's NES to prevent Crm1 binding.

### 4.2.1 DA162 ADDRESSES SURVIVIN'S NES

Preliminary docking studies demonstrated that the supramolecular GCP ligand DA162 preferably interacts with Survivin's NES. The four-armed ligand seems to be able to bind to both, the Survivin monomer and dimer. When binding to the Survivin monomer the amino groups of the cationic ligand presumably interact with glutamic acids 94 and 95, while docking to dimeric Survivin suggests that two of the ligand arms interact with glutamic acids 94 and 95 of one monomer, while the other two arms interact with glutamic acids 95 and 100 of the other monomer (section 3.2.1). Inside the cell, Survivin seems to be present either as a homodimer or in a complex with one of its binding partners. The protein is proteolytically degraded when in its monomeric form which suggests that Survivin dimerization might be a "storage state" inside the cell (138). Due to this and because Survivin's NES (aa 89–98) and its dimerization site (aa 6–10 and 89–102) partially overlap, Survivin dimerization and its interaction between the nuclear export receptor Crm1 are thought to be competitive processes. NMR studies revealed that interactions between lysines 6, 98 and 101/102 are most relevant for Survivin dimerization, while lysines 94, 95 and 100 do not seem to be involved in dimer formation and are surface accessible (Figure 4.1) (122). This explains why DA162 might also be able to bind to the Survivin dimer, even if amino acids 94, 95 and 100 theoretically lie within Survivin's dimerization site (aa 89–102).

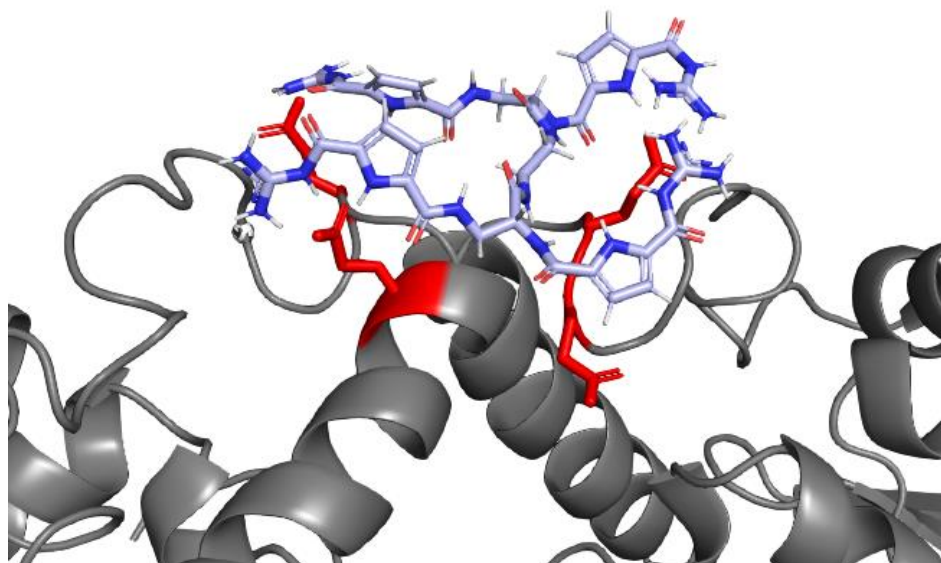


**Figure 4.1: DA162 is designed to interact with surface accessible glutamic acids 94, 95 and 100 of the Survivin homodimer.** Docking of the supramolecular GCP ligand DA162 to the Survivin dimer. Glutamic acids 94 and 95 of one monomer and glutamic acids 95 and 100 of the other monomer, with which the ligand presumably interacts, are depicted in red. (PDB: 1XOX) (25)

ITC experiments confirmed the binding of DA162 to Survivin with a  $K_D$  within the micromolar range. A sequential binding model with four sites provided the best fitting for the binding curve (section 3.2.2). However, this does not necessarily mean that a four sites binding model corresponds to the actual binding stoichiometry. It could rather be classified as a “n to 4” stoichiometry as on the one hand DA162 consists of 4 binding motifs, that might be able to interact with up to four proteins, and on the other hand Survivin displays several surface accessible anionic amino acids, which are potential ligand binding sites. This is in line with the results from docking experiments, which revealed that DA162 might be able to interact with more than one protein simultaneously. The fact that the binding curve reaches saturation at a molar ratio below 1:1 suggests that the ligand binds to Survivin on more than one site. A titration of Survivin to DA162 at first resulted in decreasing values of released energy before the values again increased as expected when binding events occur. This effect could suggest that the ligand forms aggregates or micelles that are broken up upon addition of the protein as this consumes energy while at the same time energy is released through ligand-protein interaction. Further UV titration or CD spectroscopy experiments could maybe clarify the stoichiometry of DA162-Survivin binding and NMR titration could reveal additional binding sites on the surface of the protein.

---

#### 4.2.2 SURVIVIN'S CRM1-MEDIATED NUCLEAR EXPORT IS INHIBITED BY DA162 TREATMENT

ITC measurements confirmed binding of DA162 to Survivin *in vitro*. This posed the question whether the supramolecular ligand would also accomplish to inhibit the interaction between Survivin and Crm1 and thereby Survivin's Crm1-mediated nuclear export inside the cell. A cellular PLA confirmed that DA162 was indeed able to significantly decrease the interaction between the two proteins inside the cell at a concentration of 50  $\mu$ M (section 3.2.3). The fact that PLA signals could still be detected in samples treated with DA162 indicates that higher ligand concentrations might be necessary to completely inhibit the protein-protein interaction or that probably not the entire amount of ligand was taken up by the cells. As already suggested for ligand MM138, connecting the ligand to a small fluorophore might allow visualizing its cellular uptake. Another reason could be that a PLA signal does not necessarily indicate that the two proteins of interest really interact with each other. A signal can still be created when both proteins are in close proximity (<40 nm). This means that Survivin and Crm1 might still generate a PLA signal if they are close by although they are not able to interact with each other anymore.

To confirm that the inhibition of the Survivin-Crm1 interaction also decreases Crm1-mediated nuclear export of Survivin, an SRV100 biosensor assay was performed. The assay demonstrated that DA162 treatment was indeed able to hamper Survivin's export into the cytoplasm, albeit only partially, as a small proportion of Survivin was still exported into the cytoplasm (section 3.2.3). Inhibiting the nuclear export completely might require a higher ligand concentration. In addition, the biosensor contains only a truncated version of Survivin (aa 1–100). As the ligand was predicted to bind to amino acids 94, 95 and 100, the assays appears to be suitable to analyze the influence of DA162 treatment on Survivin's nuclear export. Nevertheless, it should be taken into consideration that the truncation of the protein might have an influence on its folding, which in turn could have an effect on ligand binding.

As DA162 was not only able to inhibit the interaction between Survivin and Crm1 but also Survivin's Crm1-mediated nuclear export, the ligand appears to be a promising candidate ligand to interfere with both of Survivin's cancer-relevant functions: the inhibition of apoptosis and the promotion of cell proliferation.

### 4.2.3 DA162 HAS NO SIGNIFICANT EFFECT ON SURVIVIN DIMERIZATION

Survivin's nuclear export and its homodimerization are thought to be competitive processes as the NES (aa 89–98) and the dimer interface (aa 6–10 and 89–102) partially overlap. It has been shown that Survivin dimerization is important to prevent destabilization and degradation of the protein via the proteasome or autophagy. An inhibition of Survivin dimerization triggers its degradation (85). Inside the cell, Survivin seems to be either dimeric or in a complex with another binding partner. Homodimerization might therefore be seen as some kind of “storage state” inside the cell (138). To analyze the effect of DA162 treatment on Survivin dimerization, an Acceptor Photobleaching FRET Assay was performed. The assay revealed that DA162 had apparently no significant effect on Survivin's dimerization behavior, although the mean FRET efficiency was slightly increased in DA162-treated cells (section 3.2.5). An increase in FRET efficiency would be in agreement with the assumption that homodimerization and Crm1-binding are competitive processes, as a decreased Crm1-interaction would in turn cause increased homodimerization. As the supramolecular ligand only interacts with glutamic acids that are surface accessible in the homodimer (section 3.2.1) and most likely not essential for dimerization, it seems implausible for the ligand to interfere with dimerization. As discussed in section 4.1.3, Acceptor Photobleaching FRET is a very error prone technique. In addition, it is time consuming to analyze enough cells to obtain robust results. Thus, the results from the Acceptor Photobleaching FRET Assay should be verified with other methods like co-immunoprecipitation, where small protein tags can be utilized in stead of large fluorophores, or FLIM-FRET, which is less error prone.

### 4.2.4 DA162 INTERFERES WITH SURVIVIN'S MITOTIC AND ANTI-APOPTOTIC FUNCTIONS

DA162 has been shown to inhibit the interaction between Survivin and Crm1 and thereby Survivin's nuclear export. The interaction with Crm1 is not only relevant for Survivin's anti-apoptotic functions, for which the protein needs to be exported into the cytoplasm, but also for Survivin's mitotic functions since Crm1 is crucially involved in tethering the CPC to the centromeres (21). Therefore, an inhibition of the protein-protein interaction between Survivin and Crm1 was expected to interfere with both of Survivin's cancer-relevant functions: the inhibition of apoptosis and the promotion of cell proliferation. It could be demonstrated that DA162 indeed had an inhibiting effect on cell proliferation in several cancer cell lines from different origins. In addition, DA162 was also able to increase caspase 3/7 activation in all cell lines tested. As already observed in MM138-treated cells,

the effects varied between the different cancer cell lines. In this case, the lung cancer cell line A549 responded best to DA162 treatment. Cell proliferation could be reduced by more than 50 % and caspase 3/7-activation was increased by up to 73 % (section 3.1.6). Several theories why the cell lines responded differently to an inhibition of Survivin's mitotic functions have already been postulated in section 4.1.4. Concerning the inhibition of Survivin's anti-apoptotic functions, again several factors must be taken into account. Most cancer cells have a disrupted balance between pro- and anti-apoptotic proteins that modulate cell death. Not only IAPs like Survivin might be affected but probably also proteins of the Bcl-2 family, which is comprised of pro- as well as anti-apoptotic proteins (166). In addition, a lot of cancer cells exhibit a reduced expression of caspases, which was shown to affect the response to anti-cancer drugs (166).

Taken together it could be shown that the supramolecular GCP ligand DA162 binds to Survivin with a low micromolar  $K_D$  and is able to inhibit the interaction between Survivin and Crm1 inside the cell. The ligand decreased Survivin's Crm1-mediated nuclear export and was able to decrease cell proliferation and increase caspase-mediated apoptosis in cancer cell lines from various origins. DA162 therefore seems to be a promising candidate ligand to target the protein-protein interaction between Survivin and Crm1 and thereby interfere with Survivin's role in cancer cell proliferation and apoptosis inhibition.

### 4.3 CONCLUSION AND OUTLOOK

This work aimed to inhibit Survivin's cellular functions by targeting anionic hot spots on the protein surface with supramolecular GCP ligands. Survivin possesses two anionic hot spots that are surface exposed and functionally relevant: The Histone H3 binding site <sup>51</sup>EPDLAQCFCKELEGWEPDDDDPIEEHKKH<sup>80</sup> and the Crm1 interaction site <sup>89</sup>VKKQFEELTL<sup>98</sup> (NES). Targeting the Survivin-Histone H3 interaction aims to interfere with Survivin's role in cell proliferation, while an inhibition of the Survivin-Crm1 interaction targets Survivin's mitotic as well as anti-apoptotic functions. In cooperation with the Schmuck group, several supramolecular GCP ligands were developed to specifically target Survivin's anionic hot spots. The effect of two of those ligands on Survivin's cellular functions was analyzed in this thesis: MM138, which consists of two GCP groups and is supposed to bind to Survivin's Histone H3 binding site and DA162, which is a four-armed ligand designed to interfere with Survivin-Crm1 binding. It could be verified that MM138 binds to Survivin's Histone H3 binding site and is able to inhibit the interaction between the two proteins inside the cell. The ligand was able to interfere with Survivin's mitotic functions and decreased the proliferation of cancer cells. DA162 was demonstrated to bind to Survivin with a low micromolar  $K_D$  and hamper the interaction between Survivin and Crm1. This led to an inhibition of Survivin's nuclear export and a decreased proliferation of cancer cells. Taken together, targeting Survivin's anionic hot spots with supramolecular GCP ligands seems to be a promising approach for the development of new cancer therapies. Future challenges are to further improve solubility, selectivity and affinity of the ligands. The Histone H3 binding site contains in total 10 anionic amino acids. Hence, ligands with more GCP groups or more positive charges might increase affinity and selectivity. Examining the influence of different linkers and screening combinatorial libraries should thereby allow it to improve existing inhibitors. Currently, new aggregation-induced emission (AIE) fluorophores are designed that can be combined with the existing supramolecular GCP ligands for a simple, light-based readout upon successful protein binding and a visualization of the protein-ligand interactions inside the cell (167). In addition, multivalency is explored as an approach to further improve ligand specificity and affinity. For this, precision macromolecules are going to serve as scaffolds to combine supramolecular binding motifs with sequence-specific peptides and sensor molecules (168, 169). Overall, this thesis provided several cellular and microscopic assays to analyze the influence of potential protein-protein inhibitors on Survivin's cellular functions. This enabled the identification and characterization of two promising ligands, which accomplished to interfere with Survivin's cancer-promoting cellular functions and provided a new approach to address Survivin as a target in cancer therapy.

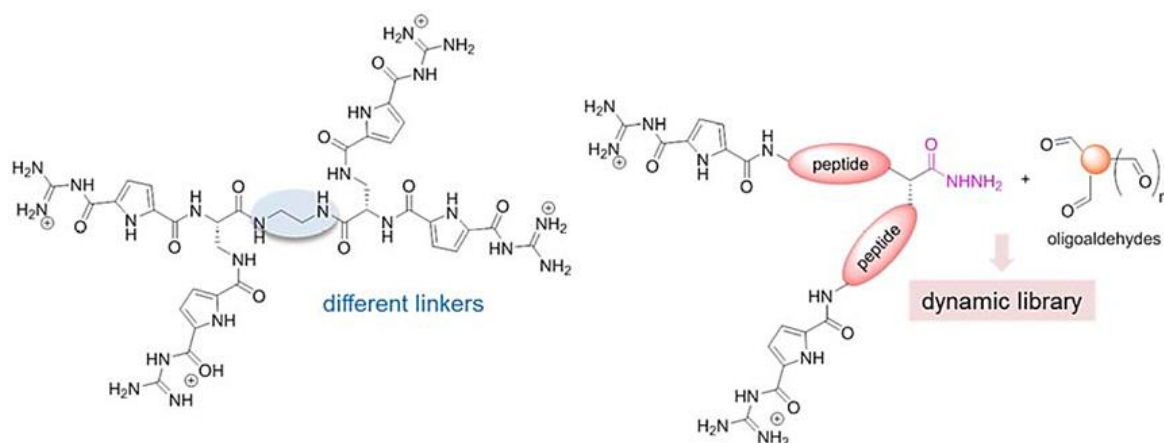


**Figure 4.2: Further improvement of current GCP ligands.** Ligands that have shown promising effects on Survivin's cellular functions are going to be further improved concerning their solubility, specificity and affinity. Strategies include the usage of different linkers and the screening of additional combinatorial libraries.

## 5 REFERENCES

1. World Health Organization (2018) *Cancer*. <http://www.who.int/en/news-room/fact-sheets/detail/cancer>.
2. Hanahan D, Weinberg RA (2011) Hallmarks of cancer. The next generation. *Cell* 144:646–674.
3. Li F *et al.* (1999) Pleiotropic cell-division defects and apoptosis induced by interference with survivin function. *Nature cell biology* 1:461–466.
4. Li F *et al.* (1998) Control of apoptosis and mitotic spindle checkpoint by survivin. *Nature* 396:580–584.
5. Li Z *et al.* (2016) Effects of survivin on angiogenesis in vivo and in vitro. *American journal of translational research* 8:270–283.
6. Vaira V *et al.* (2007) Regulation of survivin expression by IGF-1/mTOR signaling. *Oncogene* 26:2678–2684.
7. Xu Y, Fang F, Ludewig G, Jones G, Jones D (2004) A mutation found in the promoter region of the human survivin gene is correlated to overexpression of survivin in cancer cells. *DNA and cell biology* 23:527–537.
8. Tracey L *et al.* (2005) Expression of the NF-kappaB targets BCL2 and BIRC5/Survivin characterizes small B-cell and aggressive B-cell lymphomas, respectively. *The Journal of pathology* 206:123–134.
9. Hoffman WH, Biade S, Zilfou JT, Chen J, Murphy M (2002) Transcriptional repression of the anti-apoptotic survivin gene by wild type p53. *J. Biol. Chem.* 277:3247–3257.
10. Jiang Y, Saavedra HI, Holloway MP, Leone G, Altura RA (2004) Aberrant regulation of survivin by the RB/E2F family of proteins. *J. Biol. Chem.* 279:40511–40520.
11. Adida C, Berrebi D, Peuchmaur M, Reyes-Mugica M, Altieri DC (1998) Anti-apoptosis gene, survivin, and prognosis of neuroblastoma. *Lancet (London, England)* 351:882–883.
12. Capalbo G *et al.* (2007) The role of survivin for radiation therapy. Prognostic and predictive factor and therapeutic target. *Strahlentherapie und Onkologie : Organ der Deutschen Rontgengesellschaft ... [et al]* 183:593–599.
13. Engels K *et al.* (2007) Dynamic intracellular survivin in oral squamous cell carcinoma. Underlying molecular mechanism and potential as an early prognostic marker. *The Journal of pathology* 211:532–540.
14. Xu C *et al.* (2014) High survivin mRNA expression is a predictor of poor prognosis in breast cancer. A comparative study at the mRNA and protein level. *Breast cancer (Tokyo, Japan)* 21:482–490.
15. Chen P *et al.* (2014) Over-expression of survivin and VEGF in small-cell lung cancer may predict the poorer prognosis. *Medical oncology (Northwood, London, England)* 31:775.

16. Sah NK, Seniya C (2015) Survivin splice variants and their diagnostic significance. *Tumour biology : the journal of the International Society for Oncodevelopmental Biology and Medicine* 36:6623–6631.
17. Deveraux QL, Reed JC (1999) IAP family proteins---suppressors of apoptosis. *Genes & development* 13:239–252.
18. Jeyaprakash AA, Basquin C, Jayachandran U, Conti E (2011) Structural basis for the recognition of phosphorylated histone h3 by the survivin subunit of the chromosomal passenger complex. *Structure (London, England : 1993)* 19:1625–1634.
19. Kelly AE *et al.* (2010) Survivin reads phosphorylated histone H3 threonine 3 to activate the mitotic kinase Aurora B. *Science (New York, N. Y.)* 330:235–239.
20. Jeyaprakash AA *et al.* (2007) Structure of a Survivin-Borealin-INCENP core complex reveals how chromosomal passengers travel together. *Cell* 131:271–285.
21. Knauer SK, Bier C, Habtemichael N, Stauber RH (2006) The Survivin-Crm1 interaction is essential for chromosomal passenger complex localization and function. *EMBO reports* 7:1259–1265.
22. Knauer SK *et al.* (2007) Nuclear export is essential for the tumor-promoting activity of survivin. *FASEB journal : official publication of the Federation of American Societies for Experimental Biology* 21:207–216.
23. Knauer SK, Mann W, Stauber RH (2007) Survivin's dual role. An export's view. *Cell cycle (Georgetown, Tex.)* 6:518–521.
24. Engelsma D, Rodriguez JA, Fish A, Giaccone G, Fornerod M (2007) Homodimerization antagonizes nuclear export of survivin. *Traffic* 8:1495–1502.
25. Chantalat L *et al.* (2000) Crystal Structure of Human Survivin Reveals a Bow Tie–Shaped Dimer with Two Unusual  $\alpha$ -Helical Extensions. *Molecular cell* 6:183–189.
26. Gorlich D, Mattaj JW (1996) Nucleocytoplasmic Transport. *Science* 271:1513–1519.
27. Fahrenkrog B, Aebi U (2003) The nuclear pore complex: nucleocytoplasmic transport and beyond. *Nature reviews. Molecular cell biology* 4:757–766.
28. Nigg EA (1997) Nucleocytoplasmic transport: signals, mechanisms and regulation. *Nature* 386:779–787.
29. Beck M, Hurt E (2017) The nuclear pore complex: understanding its function through structural insight. *Nature reviews. Molecular cell biology* 18:73–89.
30. Wente SR, Rout MP (2010) The Nuclear Pore Complex and Nuclear Transport. *Cold Spring Harbor perspectives in biology* 2.
31. Sakiyama Y, Panatala R, Lim RYH (2017) Structural dynamics of the nuclear pore complex. *Seminars in cell & developmental biology* 68:27–33.
32. Dultz E, Ellenberg J (2010) Live imaging of single nuclear pores reveals unique assembly kinetics and mechanism in interphase. *The Journal of Cell Biology* 191:15–22.

33. Maul GG (1972) TIME SEQUENCE OF NUCLEAR PORE FORMATION IN PHYTOHEMAGGLUTININ-STIMULATED LYMPHOCYTES AND IN HELA CELLS DURING THE CELL CYCLE. *The Journal of Cell Biology* 55:433–447.
34. Kabachinski G, Schwartz TU (2015) The nuclear pore complex - structure and function at a glance. *Journal of cell science* 128:423–429.
35. Rabut G, Ellenberg J (2001) Nucleocytoplasmic transport: Diffusion channel or phase transition? *Current Biology* 11:R551-R554.
36. Chook YM, Blobel G (2001) Karyopherins and nuclear import. *Current opinion in structural biology* 11:703–715.
37. Moroianu J (1997) Molecular mechanisms of nuclear protein transport. *Critical reviews in eukaryotic gene expression* 7:61–72.
38. Ribbeck K, Görlich D (2001) Kinetic analysis of translocation through nuclear pore complexes. *The EMBO journal* 20:1320–1330.
39. Kalderon D, Richardson WD, Markham AF, Smith AE (1984) Sequence requirements for nuclear location of simian virus 40 large-T antigen. *Nature* 311:33–38.
40. Kalderon D, Roberts BL, Richardson WD, Smith AE (1984) A short amino acid sequence able to specify nuclear location. *Cell* 39:499–509.
41. Sorokin AV, Kim ER, Ovchinnikov LP (2007) Nucleocytoplasmic transport of proteins. *Biochemistry. Biokhimiia* 72:1439–1457.
42. Wen W, Meinkoth JL, Tsien RY, Taylor SS (1995) Identification of a signal for rapid export of proteins from the nucleus. *Cell* 82:463–473.
43. Kosugi S, Hasebe M, Tomita M, Yanagawa H (2008) Nuclear export signal consensus sequences defined using a localization-based yeast selection system. *Traffic (Copenhagen, Denmark)* 9:2053–2062.
44. Görlich D, Kutay U (1999) Transport between the cell nucleus and the cytoplasm. *Annual review of cell and developmental biology* 15:607–660.
45. Tran EJ, Bolger TA, Wentz SR (2007) SnapShot: nuclear transport. *Cell* 131:420.
46. Kim YH, Han M-E, Oh S-O (2017) The molecular mechanism for nuclear transport and its application. *Anatomy & cell biology* 50:77–85.
47. Fahrenkrog B, Aebi U (2003) The nuclear pore complex: nucleocytoplasmic transport and beyond. *Nature reviews. Molecular cell biology* 4:757–766.
48. Güttler T, Görlich D (2011) Ran-dependent nuclear export mediators: a structural perspective. *The EMBO journal* 30:3457–3474.
49. Alberts B *et al.* (2015) *Molecular biology of the cell* (Garland Science Taylor and Francis Group, New York, NY).
50. Hutten S, Kehlenbach RH (2007) CRM1-mediated nuclear export: to the pore and beyond. *Trends in cell biology* 17:193–201.
51. Nguyen KT, Holloway MP, Altura RA (2012) The CRM1 nuclear export protein in normal development and disease. *International Journal of Biochemistry and Molecular Biology* 3:137–151.

- 
52. Dickmanns A, Kehlenbach RH, Fahrenkrog B (2015) Nuclear Pore Complexes and Nucleocytoplasmic Transport: From Structure to Function to Disease. *International review of cell and molecular biology* 320:171–233.
53. Monecke T *et al.* (2015) Combining dehydration, construct optimization and improved data collection to solve the crystal structure of a CRM1-RanGTP-SPN1-Nup214 quaternary nuclear export complex. *Acta crystallographica. Section F, Structural biology communications* 71:1481–1487.
54. Port SA *et al.* (2015) Structural and Functional Characterization of CRM1-Nup214 Interactions Reveals Multiple FG-Binding Sites Involved in Nuclear Export. *Cell reports* 13:690–702.
55. Fox AM, Ciziene D, McLaughlin SH, Stewart M (2011) Electrostatic interactions involving the extreme C terminus of nuclear export factor CRM1 modulate its affinity for cargo. *The Journal of biological chemistry* 286:29325–29335.
56. Monecke T, Dickmanns A, Ficner R (2014) Allosteric control of the exportin CRM1 unraveled by crystal structure analysis. *The FEBS journal* 281:4179–4194.
57. Arnaoutov A *et al.* (2005) Crm1 is a mitotic effector of Ran-GTP in somatic cells. *Nature cell biology* 7:626–632.
58. Arnaoutov A, Dasso M (2005) Ran-GTP regulates kinetochore attachment in somatic cells. *Cell cycle (Georgetown, Tex.)* 4:1161–1165.
59. Wheatley SP, McNeish IA (2005) Survivin. A protein with dual roles in mitosis and apoptosis. *International review of cytology* 247:35–88.
60. Carmena M, Wheelock M, Funabiki H, Earnshaw WC (2012) The chromosomal passenger complex (CPC). From easy rider to the godfather of mitosis. *Nature reviews. Molecular cell biology* 13:789–803.
61. Ruchaud S, Carmena M, Earnshaw WC (2007) The chromosomal passenger complex. One for all and all for one. *Cell* 131:230–231.
62. Wheatley SP *et al.* (2007) Phosphorylation by aurora-B negatively regulates survivin function during mitosis. *Cell cycle (Georgetown, Tex.)* 6:1220–1230.
63. Wheatley SP, Henzing AJ, Dodson H, Khaled W, Earnshaw WC (2004) Aurora-B phosphorylation in vitro identifies a residue of survivin that is essential for its localization and binding to inner centromere protein (INCENP) in vivo. *J. Biol. Chem.* 279:5655–5660.
64. Vong QP, Cao K, Li HY, Iglesias PA, Zheng Y (2005) Chromosome alignment and segregation regulated by ubiquitination of survivin. *Science (New York, N.Y.)* 310:1499–1504.
65. Renehan AG, Booth C, Potten CS (2001) What is apoptosis, and why is it important? *BMJ (Clinical research ed.)* 322:1536–1538.
66. Chang HY, Yang X (2000) Proteases for cell suicide. Functions and regulation of caspases. *Microbiology and molecular biology reviews : MMBR* 64:821–846.
67. McIlwain DR, Berger T, Mak TW (2015) Caspase functions in cell death and disease. *Cold Spring Harbor perspectives in biology* 7.

- 
68. Fischer U, Jänicke RU, Schulze-Osthoff K (2003) Many cuts to ruin. A comprehensive update of caspase substrates. *Cell death and differentiation* 10:76–100.
69. Aggarwal BB (2003) Signalling pathways of the TNF superfamily. A double-edged sword. *Nature reviews. Immunology* 3:745–756.
70. Park HH *et al.* (2007) The death domain superfamily in intracellular signaling of apoptosis and inflammation. *Annual review of immunology* 25:561–586.
71. Westphal D, Dewson G, Czabotar PE, Kluck RM (2011) Molecular biology of Bax and Bak activation and action. *Biochimica et biophysica acta* 1813:521–531.
72. Wei MC *et al.* (2000) tBID, a membrane-targeted death ligand, oligomerizes BAK to release cytochrome c. *Genes & development* 14:2060–2071.
73. Adrain C, Creagh EM, Martin SJ (2001) Apoptosis-associated release of Smac/DIABLO from mitochondria requires active caspases and is blocked by Bcl-2. *The EMBO journal* 20:6627–6636.
74. Ow Y-LP, Green DR, Hao Z, Mak TW (2008) Cytochrome c. Functions beyond respiration. *Nature reviews. Molecular cell biology* 9:532–542.
75. Song Z, Yao X, Wu M (2003) Direct interaction between survivin and Smac/DIABLO is essential for the anti-apoptotic activity of survivin during taxol-induced apoptosis. *J. Biol. Chem.* 278:23130–23140.
76. David Dannheisig (2016) *Impact of survivin acetylation on its biological function.* Masterarbeit (Essen).
77. Riedl SJ, Shi Y (2004) Molecular mechanisms of caspase regulation during apoptosis. *Nature reviews. Molecular cell biology* 5:897–907.
78. Altieri DC (2010) Survivin and IAP proteins in cell-death mechanisms. *The Biochemical journal* 430:199–205.
79. Eckelman BP, Salvesen GS, Scott FL (2006) Human inhibitor of apoptosis proteins. Why XIAP is the black sheep of the family. *EMBO reports* 7:988–994.
80. Srinivasula SM, Ashwell JD (2008) IAPs. What's in a name? *Molecular cell* 30:123–135.
81. Dohi T, Beltrami E, Wall NR, Plescia J, Altieri DC (2004) Mitochondrial survivin inhibits apoptosis and promotes tumorigenesis. *The Journal of clinical investigation* 114:1117–1127.
82. Marusawa H *et al.* (2003) HBXIP functions as a cofactor of survivin in apoptosis suppression. *The EMBO journal* 22:2729–2740.
83. Wang H *et al.* (2010) Acetylation directs survivin nuclear localization to repress STAT3 oncogenic activity. *The Journal of biological chemistry* 285:36129–36137.
84. Pavlyukov MS *et al.* (2011) Survivin monomer plays an essential role in apoptosis regulation. *The Journal of biological chemistry* 286:23296–23307.
85. Qi J *et al.* (2016) Effective Targeting of the Survivin Dimerization Interface with Small-Molecule Inhibitors. *Cancer Res* 76:453–462.

86. Mobahat M, Narendran A, Riabowol K (2014) Survivin as a preferential target for cancer therapy. *International journal of molecular sciences* 15:2494–2516.
87. Talbot DC *et al.* (2008) First human dose study evaluating safety and pharmacokinetics of LY2181308, an antisense oligonucleotide designed to inhibit survivin. *JCO* 26:3518.
88. Wiechno P *et al.* (2014) A randomised phase 2 study combining LY2181308 sodium (survivin antisense oligonucleotide) with first-line docetaxel/prednisone in patients with castration-resistant prostate cancer. *European urology* 65:516–520.
89. Dong H *et al.* (2015) Combination of survivin siRNA with neoadjuvant chemotherapy enhances apoptosis and reverses drug resistance in breast cancer MCF-7 cells. *Journal of cancer research and therapeutics* 11:717–722.
90. Liu Z *et al.* (2017) Survivin downregulation using siRNA nanoliposomes inhibits cell proliferation and promotes the apoptosis of MHCC-97H hepatic cancer cells: An in vitro and in vivo study. *Oncology Letters* 13:2723–2730.
91. Chen X, Duan N, Zhang C, Zhang W (2016) Survivin and Tumorigenesis: Molecular Mechanisms and Therapeutic Strategies. *Journal of Cancer* 7:314–323.
92. Wall NR, O'Connor DS, Plescia J, Pommier Y, Altieri DC (2003) Suppression of Survivin Phosphorylation on Thr34 by Flavopiridol Enhances Tumor Cell Apoptosis. *Cancer Res* 63:230–235.
93. O'Connor DS *et al.* (2000) Regulation of apoptosis at cell division by p34cdc2 phosphorylation of survivin. *Proceedings of the National Academy of Sciences of the United States of America* 97:13103–13107.
94. Fenstermaker RA *et al.* (2016) Clinical study of a survivin long peptide vaccine (SurVaxM) in patients with recurrent malignant glioma. *Cancer immunology, immunotherapy : CII* 65:1339–1352.
95. Schmidt SM *et al.* (2003) Survivin is a shared tumor-associated antigen expressed in a broad variety of malignancies and recognized by specific cytotoxic T cells. *Blood* 102:571–576.
96. Chen C *et al.* (2018) Promoter-Operating Targeted Expression of Gene Therapy in Cancer: Current Stage and Prospect. *Molecular therapy. Nucleic acids* 11:508–514.
97. Chen J-S *et al.* (2004) Cancer-specific activation of the survivin promoter and its potential use in gene therapy. *Cancer gene therapy* 11:740–747.
98. Tolcher AW *et al.* (2012) A phase II study of YM155, a novel small-molecule suppressor of survivin, in castration-resistant taxane-pretreated prostate cancer. *Annals of oncology : official journal of the European Society for Medical Oncology* 23:968–973.
99. Kelly RJ *et al.* (2013) A phase I/II study of sepantronium bromide (YM155, survivin suppressor) with paclitaxel and carboplatin in patients with advanced non-small-cell lung cancer. *Annals of oncology : official journal of the European Society for Medical Oncology* 24:2601–2606.

100. Clemens MR *et al.* (2015) Phase II, multicenter, open-label, randomized study of YM155 plus docetaxel as first-line treatment in patients with HER2-negative metastatic breast cancer. *Breast cancer research and treatment* 149:171–179.
101. Garg H, Suri P, Gupta JC, Talwar GP, Dubey S (2016) Survivin: a unique target for tumor therapy. *Cancer cell international* 16:49.
102. Emily Burke (2018) *Gene Therapy Cures*. <https://weekly.biotechprimer.com/gene-therapy-cures/>.
103. Robinson R (2004) RNAi therapeutics: how likely, how soon? *PLoS biology* 2:E28.
104. Zara Kassam (2018) *Cancer vaccine strategy blocks death of tumour-specific cytotoxic T cells*. <https://www.europeanpharmaceuticalreview.com/news/75407/cancer-vaccine-strategy/>.
105. Shojaei F, Yazdani-Nafchi F, Banitalebi-Dehkordi M, Chehelgerdi M, Khorramian-Ghahfarokhi M (2018) Trace of survivin in cancer. *European journal of cancer prevention : the official journal of the European Cancer Prevention Organisation (ECP)*.
106. Hwang H, Vreven T, Janin J, Weng Z (2010) Protein-protein docking benchmark version 4.0. *Proteins* 78:3111–3114.
107. Fuller JC, Burgoyne NJ, Jackson RM (2009) Predicting druggable binding sites at the protein-protein interface. *Drug discovery today* 14:155–161.
108. Arkin MR, Tang Y, Wells JA (2014) Small-molecule inhibitors of protein-protein interactions: progressing toward the reality. *Chemistry & biology* 21:1102–1114.
109. Wells JA, McClendon CL (2007) Reaching for high-hanging fruit in drug discovery at protein-protein interfaces. *Nature* 450:1001–1009.
110. Basse MJ *et al.* (2013) 2P2ldb: a structural database dedicated to orthosteric modulation of protein-protein interactions. *Nucleic acids research* 41:D824-7.
111. Lehn JM (1993) Supramolecular chemistry. *Science* 260:1762–1763.
112. Lehn J-M (1995) *Supramolecular chemistry. Concepts and perspectives ; a personal account* (VCH, Weinheim, New York, Basel, Cambridge, Tokyo).
113. Schmuck C (2001) Stereoselective Complexation of Amino Acid Carboxylates in Aqueous Solutions: Automated, Parallel Synthesis of a Guanidiniocarbonyl-Pyrrole Receptor Library. *Journal of the Association for Laboratory Automation* 6:51–53.
114. Schmuck C, Heil M (2003) Using combinatorial methods to arrive at a quantitative structure-stability relationship for a new class of one-armed cationic peptide receptors targeting the C-terminus of the amyloid beta-peptide. *Organic & biomolecular chemistry* 1:633–636.
115. Li M, Schlesiger S, Knauer SK, Schmuck C (2015) A tailor-made specific anion-binding motif in the side chain transforms a tetrapeptide into an efficient vector for gene delivery. *Angewandte Chemie (International ed. in English)* 54:2941–2944.
116. Mullis KB, Faloona FA (1987) Specific synthesis of DNA in vitro via a polymerase-catalyzed chain reaction. *Methods in enzymology* 155:335–350.

117. Sanger F, Coulson AR (1975) A rapid method for determining sequences in DNA by primed synthesis with DNA polymerase. *Journal of molecular biology* 94:441–448.
118. Birnboim HC, Doly J (1979) A rapid alkaline extraction procedure for screening recombinant plasmid DNA. *Nucleic acids research* 7:1513–1523.
119. Laemmli UK (1970) Cleavage of structural proteins during the assembly of the head of bacteriophage T4. *Nature* 227:680–685.
120. Favier A, Brutscher B (2011) Recovering lost magnetization: polarization enhancement in biomolecular NMR. *Journal of biomolecular NMR* 49:9–15.
121. R L. J. Keller (2004) *Optimizing the process of NMR spectrum analysis and computer aided resonance assignment*. Dissertation (Zürich).
122. Sun C, Nettesheim D, Liu Z, Olejniczak ET (2005) Solution structure of human survivin and its binding interface with Smac/Diablo. *Biochemistry* 44:11–17.
123. Ayed A *et al.* (2001) Latent and active p53 are identical in conformation. *Nature structural biology* 8:756–760.
124. Merck *How Proximity Ligation Assay (PLA) Works*.  
<https://www.sigmaaldrich.com/technical-documents/protocols/biology/how-pla-works.html>.
125. García-Santisteban I *et al.* (2016) A cellular reporter to evaluate CRM1 nuclear export activity. Functional analysis of the cancer-related mutant E571K. *Cellular and molecular life sciences : CMLS* 73:4685–4699.
126. Förster T (2012) Energy migration and fluorescence. 1946. *Journal of biomedical optics* 17:11002.
127. Promega *CellTiter 96® Aqueous One Solution Cell Proliferation Assay (MTS)*.  
[https://www.promega.de/products/cell-health-assays/cell-viability-and-cytotoxicity-assays/celltiter-96-aqueous-one-solution-cell-proliferation-assay-\\_mts\\_/?catNum=G3582](https://www.promega.de/products/cell-health-assays/cell-viability-and-cytotoxicity-assays/celltiter-96-aqueous-one-solution-cell-proliferation-assay-_mts_/?catNum=G3582).
128. Corporation P ApoLive-Glo™ Multiplex Assay Technical Manual, TM325.
129. Sandra Bäcker (2018) *DISSECTION AND MODULATION OF (PATHO)BIOLOGICAL SURVIVIN FUNCTIONS BY SUPRAMOLECULAR LIGANDS*. Dissertation (Essen).
130. Niedzialkowska E *et al.* (2012) Molecular basis for phosphospecific recognition of histone H3 tails by Survivin paralogues at inner centromeres. *Molecular biology of the cell* 23:1457–1466.
131. Baudoin NC, Cimini D (2018) A guide to classifying mitotic stages and mitotic defects in fixed cells. *Chromosoma* 127:215–227.
132. Pampalona J *et al.* (2016) Chromosome Bridges Maintain Kinetochores-Microtubule Attachment throughout Mitosis and Rarely Break during Anaphase. *PLoS one* 11:e0147420.
133. Cimini D *et al.* (2001) Merotelic Kinetochores Orientation Is a Major Mechanism of Aneuploidy in Mitotic Mammalian Tissue Cells. *The Journal of Cell Biology* 153:517–528.

134. Cimini D, Moree B, Canman JC, Salmon ED (2003) Merotelic kinetochore orientation occurs frequently during early mitosis in mammalian tissue cells and error correction is achieved by two different mechanisms. *Journal of cell science* 116:4213–4225.
135. Zakeri B *et al.* (2018) Molecular recognition of carboxylates in the protein leucine zipper by a multivalent supramolecular ligand: residue-specific, sensitive and label-free probing by UV resonance Raman spectroscopy. *Physical chemistry chemical physics : PCCP* 20:1817–1820.
136. Carsten Microsoft Word - schmuck\_Supporting Information\_revised.
137. Ruchaud S, Carmena M, Earnshaw WC (2007) Chromosomal passengers. Conducting cell division. *Nature reviews. Molecular cell biology* 8:798–812.
138. Qi J *et al.* (2016) Effective Targeting of the Survivin Dimerization Interface with Small-Molecule Inhibitors. *Cancer research* 76:453–462.
139. Piston DW, Kremers G-J (2007) Fluorescent protein FRET: the good, the bad and the ugly. *Trends in biochemical sciences* 32:407–414.
140. Bunt G, Wouters FS (2004) Visualization of molecular activities inside living cells with fluorescent labels. *International review of cytology* 237:205–277.
141. Bajar BT, Wang ES, Zhang S, Lin MZ, Chu J (2016) A Guide to Fluorescent Protein FRET Pairs. *Sensors (Basel, Switzerland)* 16.
142. Rajoria S, Zhao L, Intes X, Barroso M (2014) FLIM-FRET for Cancer Applications. *Current molecular imaging* 3:144–161.
143. Sun J-M, Chen HY, Espino PS, Davie JR (2007) Phosphorylated serine 28 of histone H3 is associated with destabilized nucleosomes in transcribed chromatin. *Nucleic acids research* 35:6640–6647.
144. Goto H *et al.* (1999) Identification of a novel phosphorylation site on histone H3 coupled with mitotic chromosome condensation. *J. Biol. Chem.* 274:25543–25549.
145. Acilan C, Potter DM, Saunders WS (2007) DNA repair pathways involved in anaphase bridge formation. *Genes, chromosomes & cancer* 46:522–531.
146. Véquaud E, Desplanques G, Jézéquel P, Juin P, Barillé-Nion S (2016) Survivin contributes to DNA repair by homologous recombination in breast cancer cells. *Breast cancer research and treatment* 155:53–63.
147. Hu S *et al.* (2013) Nuclear survivin and its relationship to DNA damage repair genes in non-small cell lung cancer investigated using tissue array. *PloS one* 8:e74161.
148. Reichert S *et al.* (2011) Survivin inhibition and DNA double-strand break repair: a molecular mechanism to overcome radioresistance in glioblastoma. *Radiotherapy and oncology : journal of the European Society for Therapeutic Radiology and Oncology* 101:51–58.
149. Wiedemuth R *et al.* (2014) Survivin safeguards chromosome numbers and protects from aneuploidy independently from p53. *Molecular cancer* 13:107.

- 
150. Yang D, Welm A, Bishop JM (2004) Cell division and cell survival in the absence of survivin. *Proceedings of the National Academy of Sciences of the United States of America* 101:15100–15105.
  151. Maiato H, Logarinho E (2014) Mitotic spindle multipolarity without centrosome amplification. *Nature cell biology* 16:386–394.
  152. Godinho SA, Kwon M, Pellman D (2009) Centrosomes and cancer: how cancer cells divide with too many centrosomes. *Cancer metastasis reviews* 28:85–98.
  153. Brinkley BR (2001) Managing the centrosome numbers game: from chaos to stability in cancer cell division. *Trends in cell biology* 11:18–21.
  154. Silkworth WT, Nardi IK, Scholl LM, Cimini D (2009) Multipolar spindle pole coalescence is a major source of kinetochore mis-attachment and chromosome mis-segregation in cancer cells. *PloS one* 4:e6564.
  155. Silkworth WT, Cimini D (2012) Transient defects of mitotic spindle geometry and chromosome segregation errors. *Cell division* 7:19.
  156. Ganem NJ, Godinho SA, Pellman D (2009) A mechanism linking extra centrosomes to chromosomal instability. *Nature* 460:278–282.
  157. Temme A *et al.* (2003) Localization, dynamics, and function of survivin revealed by expression of functional survivinDsRed fusion proteins in the living cell. *Molecular biology of the cell* 14:78–92.
  158. Saito T *et al.* (2008) Centrosome amplification induced by survivin suppression enhances both chromosome instability and radiosensitivity in glioma cells. *British Journal of Cancer* 98:345–355.
  159. Muschol-Steinmetz C *et al.* (2013) Function of survivin in trophoblastic cells of the placenta. *PloS one* 8:e73337.
  160. Li Y *et al.* (2015) Silencing of Survivin Expression Leads to Reduced Proliferation and Cell Cycle Arrest in Cancer Cells. *Journal of Cancer* 6:1187–1194.
  161. Miao G-Y (2007) Downregulation of survivin by RNAi inhibits growth of human gastric carcinoma cells. *WJG* 13:1170.
  162. CHEN X-Q *et al.* (2012) Effects and mechanism of downregulation of survivin expression by RNA interference on proliferation and apoptosis of lung cancer cells. *Molecular Medicine Reports* 5:917–922.
  163. Yang L, Cao Z, Yan H, Wood WC (2003) Coexistence of high levels of apoptotic signaling and inhibitor of apoptosis proteins in human tumor cells: implication for cancer specific therapy. *Cancer research* 63:6815–6824.
  164. Wang X, Cheung HW, Chun ACS, Jin D-Y, Wong Y-C (2008) Mitotic checkpoint defects in human cancers and their implications to chemotherapy. *Frontiers in bioscience : a journal and virtual library* 13:2103–2114.
  165. Roschke AV, Stover K, Tonon G, Schäffer AA, Kirsch IR (2002) Stable Karyotypes in Epithelial Cancer Cell Lines Despite High Rates of Ongoing Structural and Numerical Chromosomal Instability. *Neoplasia (New York, N. Y.)* 4:19–31.

166. Wong RSY (2011) Apoptosis in cancer: from pathogenesis to treatment. *Journal of experimental & clinical cancer research* : CR 30:87.
167. Riebe S *et al.* (2017) Aromatic Thioethers as Novel Luminophores with Aggregation-Induced Fluorescence and Phosphorescence. *Chemistry (Weinheim an der Bergstrasse, Germany)* 23:13660–13668.
168. Gerling-Driessen UIM *et al.* (2015) Exploiting Oligo(amido amine) Backbones for the Multivalent Presentation of Coiled-Coil Peptides. *Biomacromolecules* 16:2394–2402.
169. Broecker F *et al.* (2016) Multivalent display of minimal *Clostridium difficile* glycan epitopes mimics antigenic properties of larger glycans. *Nature communications* 7:11224.

## 6 APPENDIX

### 6.1 LIST OF ABBREVIATIONS

μ	Micro
A	Ampere
aa	Amino acid
Approx.	Approximately
APS	Ammonium persulfate
ATP	Adenosine triphosphate
BIR	Baculovirus IAP repeat
BIRC5	Baculoviral IAP Repeat Containing 5
BSA	Bovine serum albumin
C	Centi
C-IAP	Cellular inhibitor of apoptosis protein
Carb	Carbenicillin
CARD	Caspase recruitment domain
Caspase	CysteinyI-aspartate specific protease
CBP	CREB-binding protein
CD	Circular dichroism
CDK	Cyclin-dependent kinase
Co-IP	Co-immunoprecipitation
CPC	Chromosomal passenger complex
CRC	Collaborative Research Centre
CRIME	Crm1, importin-β etc.
Crm1	Chromosome region maintenance 1
Da	Dalton
DIABLO	Direct IAP-binding protein with low pI
DISC	Death-inducing signaling complex
DMEM	Dulbecco's Modified Eagle Medium
DNA	Deoxyribonucleic acid
dNTP	Deoxynucleotide triphosphate
DPBS	Dulbecco's Phosphate-Buffered Saline

---

dsDNA	Double stranded desoxyribonucleic acid
DTT	Dithiothreitol
EDTA	Ethylenediaminetetraacetic acid
ER	Endoplasmic reticulum
Etc.	Et cetera
FADD	FAS-associated death domain
FCS	Fetal calf serum
Fig.	Figure
FRET	Förster resonance energy transfer
G	Gap
GAP	GTPase-activating protein
GEF	Guanine nucleotide exchange factor
GFP	Green fluorescent protein
h	Hour
H3T3p	Histone H3 phosphorylated on threonine 3
HA	Hemagglutinin
HBXIP	Hepatitis B X-interacting protein
HDAC1	Histone deacetylase 1
HEAT	Huntingtin, elongation factor 3, protein phosphatase 2A, and the yeast kinase target of rapamycin kinase 1
HRP	Horseradish peroxidase
IGF-1	Insulin-like growth factor 1
INCENP	Inner centromere protein
ITC	isothermal titration calorimetry
IP	Immunoprecipitation
K	Kilo
l	Liter
LB	Luria-Bertani
M	Mitosis
M	mol/liter
m	meter
m	milli
MEM	Minimal essential medium
mRNA	Messenger RNA

---

n	Nano
NAIP	Neuronal apoptosis inhibitory protein
NCBI	National Center for Biotechnology Information
NES	Nuclear export signal
NF- $\kappa$ B	Nuclear factor kappa-light-chain-enhancer of activated B-cells
NLS	Nuclear localization signal
NMR	nuclear magnetic resonance
NP40	Nonidet P40
NPC	Nuclear pore complex
NUP	Nucleoporin
PAGE	Polyacrylamide gel electrophoresis
PBS	Phosphate-buffered saline
PCR	Polymerase chain reaction
PEI	Polyethylenimine
pH	Potentia Hydrogenii
PLA	Proximity Ligation Assay
PMSF	Phenylmethanesulfonylfluoride
PPI	Protein-protein interaction
PTM	Post-translational modification
RCC1	Regulator of chromosome condensation 1
RING	Really interesting new gene
RIPA	Radioimmunoprecipitation assay buffer
RNA	Ribonucleic acid
RT	Room temperature
S	Synthesis
s.d.	Standard deviation
SDS	Sodium dodecylsulfate
Smac	Second mitochondria-derived activator of caspase
STAT3	Signal transducer and activator of transcription 3
Surv	Survivin
TAE	Tris-acetate-EDTA
TBS	Tris-buffered saline
TBST	Tris-buffered saline/Tween
TE	Tris-EDTA buffer

---

TEMED	N,N,N',N'-Tetramethylethylenediamine
TRAIL	Tumor Necrosis Factor Related Apoptosis Inducing Ligand
Tris	Tris(hydroxymethyl)aminomethane
Tris-HCl	Tris hydrochloride
tRNA	Transfer RNA
TSA	Trichostatin A
UV	ultraviolet
V	Volt
Vs.	Versus
wt	Wildtype
XAF1	XIAP-associated factor 1
XIAP	X-linked inhibitor of apoptosis protein
Zn	Zinc
°C	Degree Celsius

## 6.2 LIST OF FIGURES

Figure 1.1: The hallmarks of cancer.....	8
Figure 1.2: Structure and domain organization of Survivin.....	10
Figure 1.3: The Nuclear Pore Complex (NPC). ....	12
Figure 1.4: Nuclear import and export of proteins. ....	14
Figure 1.5: Domain organization of Crm1.....	15
Figure 1.6: The phases of the cell cycle.....	17
Figure 1.7: Regulation of cell cycle progress via the formation of cyclin-CDK complexes.....	18
Figure 1.8: Function and localization of the CPC during mitosis.....	19
Figure 1.9: The intrinsic and extrinsic apoptosis pathways.....	21
Figure 1.10: The members of the inhibitor of apoptosis protein (IAP) family.....	22
Figure 1.11: Survivin's dimerization interface.....	23
Figure 1.12: Targeting Survivin in cancer therapy.....	25
Figure 1.13: Guanidiniocarbonyl pyrrole group for binding anionic hot spots on proteins.....	27
Figure 1.14: Targeting Survivin's anionic hot spots.....	28
Figure 2.1: Setup for ITC experiments.....	51
Figure 2.2: The PLA enables the analysis of endogenous protein-protein interactions.....	57
Figure 2.3: PLA analysis conducted with Cell Profiler.....	58
Figure 2.4: The SRV100 biosensor assay enables the analysis of Crm1's export activity in a cellular system.....	60
Figure 2.5: FRET between Cerulean-Survivin and Citrine-Survivin.....	61
Figure 2.6: Structures of the MTS substrate and the product formazan.....	62
Figure 2.7: Detection of cell viability and caspase-3/7 activation using the ApoLive-Glo™ Multiplex Assay from Promega.....	63
Figure 3.1: Docking predicts binding of MM138 to Histone H3 binding site.....	65
Figure 3.2: 2D model predicts interactions with glutamic and aspartic acids within Survivin's Histone H3 binding site.....	66
Figure 3.3: Survivin's C-terminal $\alpha$ -helix destabilizes the protein.....	67
Figure 3.4: NMR titration reveals binding of MM138 to Survivin's Histone H3 binding site.....	68
Figure 3.5: Chemical peak shifts and a decrease in relative intensities confirms binding of MM138 to glutamic acid and aspartic acid residues within Survivin's Histone H3 binding site.....	69
Figure 3.6: Immunoprecipitation experiments reveal a concentration-dependent inhibition of the Survivin-Histone H3 interaction by MM138.....	71
Figure 3.7: MM138 inhibits Survivin-Histone H3 interaction in HeLa cells.....	73

---

Figure 3.8: Survivin dimerization can be analyzed with Acceptor Photobleaching FRET..	75
Figure 3.9: MM138 increases Survivin dimerization in HeLa cells. ....	76
Figure 3.10: MM138 causes mitotic defects in HeLa cells. ....	79
Figure 3.11: MM138 treatment leads to a concentration-dependent inhibition of cell proliferation in different types of cancer cells. ....	81
Figure 3.12: Docking predicts binding of DA162 to Survivin's NES. ....	83
Figure 3.13: 2D model of monomer predicts interactions with glutamic and aspartic acids within Survivin's NES. ....	84
Figure 3.14: 2D model of dimer predicts interactions with glutamic and aspartic acids within the NESs of both monomers. ....	85
Figure 3.15: DA162 binds to Survivin 1-120 with a nanomolar $K_D$ . ....	87
Figure 3.16: DA162 inhibits the Survivin-Crm1 interaction in HeLa cells. ....	88
Figure 3.17: DA162 inhibits the Crm1-mediated nuclear export of Survivin. ....	91
Figure 3.18: DA162 treatment does not have a significant influence on Survivin dimerization in HeLa cells. ....	92
Figure 3.19: DA162 treatment leads to a concentration-dependent inhibition of cell proliferation in different types of cancer cells. ....	94
Figure 3.20: DA162 treatment increases Caspase 3/7 activation. ....	96
Figure 4.1: DA162 interacts with surface accessible glutamic acids 94, 95 and 100 of the Survivin homodimer. ....	106
Figure 4.2: Further improvement of current GCP ligands. ....	111

---

## 6.3 LIST OF TABLES

Table 2.1: Instruments and devices .....	29
Table 2.2: Consumables .....	31
Table 2.3: Chemicals and reagents.....	32
Table 2.4: Buffers solutions and media .....	34
Table 2.5: Bacterial strains.....	37
Table 2.6: Eukaryotic cell lines.....	38
Table 2.7: Eukaryotic expression plasmids. ....	38
Table 2.8: Sequencing primers. ....	40
Table 2.9: Primary antibodies. ....	40
Table 2.10: Secondary antibodies.....	41
Table 2.11: DNA and protein standards. ....	42
Table 2.12: Kits.....	42
Table 2.13: Software.....	43
Table 2.14: PCR reaction mixture .....	44
Table 2.15: PCR program .....	45
Table 2.16: Composition of SDS-polyacrylamid gels with a thickness of 1.5 mm .....	49

---

## 6.4 AMINO ACIDS

A	Ala	Alanine
C	Cys	Cysteine
D	Asp	Aspartate
E	Glu	Glutamate
F	Phe	Phenylalanine
G	Gly	Glycine
H	His	Histidine
I	Ile	Isoleucine
K	Lys	Lysine
L	Leu	Leucine
M	Met	Methionine
N	Asp	Asparagine
P	Pro	Proline
Q	Gln	Glutamine
R	Arg	Arginine
S	Ser	Serine
T	Thr	Threonine
V	Val	Valine
W	Trp	Tryptophan
Y	Tyr	Tyrosine

## DANKSAGUNG

An erster Stelle möchte ich mich bei dir dafür bedanken, Shirley, dass ich meine Doktorarbeit in deiner Arbeitsgruppe anfertigen durfte. Ich hatte während der letzten Jahre eine tolle Zeit und könnte mir keine bessere Arbeitsgruppe vorstellen! Ich weiß es sehr zu schätzen, dass du mir immer genug Freiraum gegeben hast, um eigene wissenschaftliche Ideen zu entwickeln und umzusetzen, mir bei Fragen oder Problemen aber trotzdem immer zur Seite gestanden hast. Dankbar bin ich dir auch dafür, dass du mir die Möglichkeit gegeben hast, in so vielen thematisch unterschiedlichen Projekten mitzuarbeiten. Dadurch konnte ich nicht nur viele spannende Mikroskopie-Methoden kennenlernen, sondern habe auch mit anderen Wissenschaftlern aus den unterschiedlichsten Forschungsfeldern zusammenarbeiten können.

Vielen Dank auch an dich, Peri! Ich freue mich sehr, dass du dich dazu bereit erklärt hast, das Zweitgutachten für meine Arbeit zu übernehmen. Danke auch für den wissenschaftlichen Input zu meinem Projekt als meine Mentorin im Rahmen des Graduiertenkollegs!

Dann natürlich ein großes Dankeschön an alle „Shirley’s Girlies and Boys“! Ich freue mich, dass wir ein so tolles Team sind und uns nicht nur bei allen wissenschaftlichen Problemen gegenseitig unterstützen, sondern auch außerhalb der Arbeitszeit so viel zusammen unternehmen, seien es Wanderungen, Kinobesuche, Lauftrainings, Ausflüge zum Badesee oder einfach nur gemeinsame Abende in unserem „Networking-Raum“.

Ein besonderer Dank an dich, Elli, dass du meine Arbeit korrekturgelesen hast! Ich kenne niemanden, der so viele Arten von Bindestrichen unterscheiden kann wie du! Auch dafür, dass du bei uns im Labor immer den Überblick behältst und nicht nur (als einzige) weißt, wo alles seinen Platz hat, sondern auch, wie man es richtig benutzt ;-) Danke auch, dass du mich immer wieder neue Flechtfrisuren an dir ausprobieren lässt und bei (fast) jeder sportlichen Aktivität, die ich unbedingt ausprobieren möchte, mit am Start bist.

Danke, Annika, für den morgendlichen Austausch von Meerschweinchen- und Katzenfotos bei einer Tasse Tee in unserem Büro. Astrid, dafür, dass du immer wieder die leckere vegane Donauwelle backst, obwohl du sie selber gar nicht magst. Alex, dass du nach dem Schlammlauf-Vorfall immer noch Dinge mit uns unternimmst ;-) Danke an Britta: Der Wanderritt auf Islandponys steht noch aus, das habe ich nicht vergessen! Und vielen Dank auch an Christina für die gemeinsame Wanderung mit Lama Hannibal. Danke, Katha, für die vielen gemeinsamen Mittags- und Eispausen und Lisa dafür, dass du unser Tee-Regal

um die brasilianische Limette bereichert hast und mit mir die Leidenschaft für Nougatbits teilst. Dann danke ich natürlich dir, Sandra, für die vielen gemeinsamen Jahre im SFB. Mit dir ist es auf den ganzen Seminaren, Workshops, Symposien, Konferenzen und Vorträgen nie langweilig geworden! Außerdem ist keiner so gut im chemischen Rechnen und Meerschweinchenstimmen-Nachmachen wie du! Danke, Steffi, für die tolle Zeit in unserem gemeinsamen Büro, für dessen Einrichtung du dich sogar an den Duftkerzen im Ikea vorbei getraut hast (!), und für die gemeinsamen Mittagspausen auf der 360°-Sonnenliege. Selbstverständlich auch ein großer Dank an euch, Claudia und Kay, ohne eure SAP-Expertise wäre uns nicht nur das Labormaterial ausgegangen, sondern auch die eine oder andere Dienstreise-Abrechnung um die Ohren geflogen ;-)

Ich möchte mich auch bei allen Studenten bedanken, die während der letzten Jahre in unserer Gruppe waren: Daniela, David, Esther, Felix, Jana, Jessi, kleine Steffi, Lara, Laura, Marcel, Marina, Paul, Philip, Sarah, Sebastian uvm.. Ohne euch hätten wir mit Sicherheit nur halb so viel Spaß gehabt!

Ein großer Dank natürlich auch an „die Chemiker“! Besonders an Dennis, Marcel, Matthias und Martin und den Rest der „Schmucks“. Ohne euch hätte es dieses Projekt schließlich gar nicht gegeben. Ich schätze, wir konnten zeigen, dass es möglich ist, trotz kultureller Unterschiede zwischen Chemikern und Biologen zusammenzuarbeiten, und dabei auch noch Neues voneinander zu lernen. Vielen Dank, Jens, für die Hilfe beim Interpretieren der ITC-Ergebnisse und natürlich auch dem Rest der „Voskuhls“, besonders Steffen, für die vielen Zusammenarbeiten und gemeinsamen Paper.

Danke, Christine, für die tollen NMR-Ergebnisse, trotz der vielen Probleme bei der Aufreinigung von <sup>15</sup>N-markiertem Survivin! Vielen Dank auch an euch, Nina und Johannes, dass ihr bei allen Mikroskop-Problemen immer zur Stelle wart und selbst für die kompliziertesten CellProfiler-Anwendungen immer eine Lösung parat hattet. Dann auch ein großes Dankeschön an unsere lieben Nachbarn, die „Meyers“, für den regen Austausch von Labormaterialien, Chemikalien sowie Küchengeräten ;-)

Ich möchte mich natürlich auch bei alle weiteren Kooperationspartner bedanken mit denen ich während meiner Promotion für die verschiedensten Projekte und Methoden zusammenarbeiten durfte, deren namentliche Nennung allerdings leider den Rahmen dieser Arbeit sprengen würde.

Vielen Dank an Tina, Linda, Mylene, Jenny, Annika, Esra und Gesche, aka „die Medbios“, für die gemeinsame Zeit während des Studiums! Für die vielen schönen Momente wie das Feiern bestandener Prüfungen, die gemeinsame Zeit in Oxford oder unsere gemeinsamen

Stammtische mit leckerem Essen, aber auch für das Teilen der nicht so schönen Momente wie den Biochemie-Antestaten und dem täglichen Verzehr von „Universaltomatensauce“ in der Mensa.

Dann ein großes Dankeschön natürlich auch an meine Familie! Danke, Mutter, dass du mich in der Schulzeit schon immer für Chemieklausuren abgefragt hast, obwohl du das Fach selber immer gehasst hast. Danke auch für das Korrekturlesen aller meiner bisher geschriebenen Arbeiten! Niemand beherrscht die Kommasetzung so wie du! Danke, Papa, dass du dich damit abgefunden hast, dass ich mich leider nicht für Jura interessiere und Wissenschaftlerin geworden bin ;-). Danke auch an dich, Oma! Für die sonntäglichen Rummy Cup-Spiele und die allerleckersten Apfelpfannkuchen ohne die ich es niemals durch das Studium und die Promotion geschafft hätte. Danke, Mamie, dass du für meine Bachelor- und Masterverleihungen immer extra nach Deutschland angereist bist, um dabei zu sein!

Zuletzt möchte ich mich bei dir bedanken, René, dass du mich während des Studiums immer für sämtliche Klausuren abgefragt hast. Jetzt kannst du nicht nur hunderte histologische Schnitte menschlicher Organe auseinanderhalten, sondern auch bifaziale Flachblätter an Pflanzen erkennen! Nicht zuletzt hast du dadurch, dass du mich immer wieder zum Schreiben motiviert hast, wenn du mich bei Netflix anstatt bei pubmed „erwischt“ hast, wesentlich zur Fertigstellung dieser Arbeit beigetragen!

## PUBLICATIONS

### 2018

Siemer, Svenja; Hahlbrock, Angelina; Vallet, Cecilia; McClements, David Julian; Balszuweit, Jan; Voskuhl, Jens et al. (2018a): **Nanosized food additives impact beneficial and pathogenic bacteria in the human gut: a simulated gastrointestinal study**. In: *NPJ science of food* 2 (1), S. 22. DOI: 10.1038/s41538-018-0030-8.

Westmeier, Dana; Hahlbrock, Angelina; Reinhardt, Christoph; Fröhlich-Nowoisky, Janine; Wessler, Silja; Vallet, Cecilia et al. (2018a): **Nanomaterial-microbe cross-talk: physicochemical principles and (patho)biological consequences**. In: *Chemical Society reviews* 47 (14), S. 5312–5337. DOI: 10.1039/c6cs00691d.

Siemer, Svenja; Westmeier, Dana; Vallet, Cecilia; Becker, Sven; Voskuhl, Jens; Ding, Guo-Bin et al. (2018b): **Resistance to Nano-Based Antifungals Is Mediated by Biomolecule Coronas**. In: *ACS applied materials & interfaces*. DOI: 10.1021/acsami.8b12175.

Westmeier, Dana; Posselt, Gernot; Hahlbrock, Angelina; Bartfeld, Sina; Vallet, Cecilia; Abfalder, Carmen et al. (2018b): **Nanoparticle binding attenuates the pathobiology of gastric cancer-associated Helicobacter pylori**. In: *Nanoscale* 10 (3), S. 1453–1463. DOI: 10.1039/c7nr06573f.

Westmeier, Dana; Solouk-Saran, Djamschid; Vallet, Cecilia; Siemer, Svenja; Docter, Dominic; Götz, Hermann et al. (2018c): **Nanoparticle decoration impacts airborne fungal pathobiology**. In: *Proceedings of the National Academy of Sciences of the United States of America* 115 (27), S. 7087–7092. DOI: 10.1073/pnas.1804542115.

Siemer, Svenja; Westmeier, Dana; Vallet, Cecilia; Steinmann, Jörg; Buer, Jan; Stauber, Roland H.; Knauer, Shirley K. (2018c): **Breaking resistance to nanoantibiotics by overriding corona-dependent inhibition using a pH-switch**. In: *Materials Today*. DOI: 10.1016/j.mattod.2018.10.041.

Mueller, Jonathan W.; Idkowiak, Jan; Gesteira, Tarsis F.; Vallet, Cecilia; Hardman, Rebecca; van den Boom, Johannes et al. (2018): **Human DHEA sulfation requires direct interaction between PAPS synthase 2 and DHEA sulfotransferase SULT2A1**. In: *The Journal of biological chemistry* 293 (25), S. 9724–9735. DOI: 10.1074/jbc.RA118.002248.

Stelzer, Jacqueline; Vallet, Cecilia; Sowa, Andrea; Gonzalez-Abradelo, Dario; Riebe, Steffen; Daniliuc, Constantin G. et al. (2018): **On the Influence of Substitution Patterns in Thioether-Based Luminophores with Aggregation-Induced Emission Properties**. In: *ChemistrySelect* 3 (4), S. 985–991. DOI: 10.1002/slct.201702900.

Schrenk, Christian; Fetz, Verena; Vallet, Cecilia; Heiselmayer, Christina; Schröder, Elisabeth; Hensel, Astrid et al. (2018): **TFIIA transcriptional activity is controlled by a 'cleave-and-run' Exportin-1/Taspase 1-switch**. In: *Journal of molecular cell biology* 10 (1), S. 33–47. DOI: 10.1093/jmcb/mjx025.

## 2017

Riebe, Steffen; Vallet, Cecilia; van der Vight, Felix; Gonzalez-Abradelo, Dario; Wölper, Christoph; Strassert, Cristian A. et al. (2017): **Aromatic Thioethers as Novel Luminophores with Aggregation-Induced Fluorescence and Phosphorescence**. In: *Chemistry (Weinheim an der Bergstrasse, Germany)* 23 (55), S. 13660–13668. DOI: 10.1002/chem.201701867.

## 2015

Littwitz-Salomon, Elisabeth; Akhmetzyanova, Ilseyar; Vallet, Cecilia; Francois, Sandra; Dittmer, Ulf; Gibbert, Kathrin (2015): **Activated regulatory T cells suppress effector NK cell responses by an IL-2-mediated mechanism during an acute retroviral infection**. In: *Retrovirology* 12, S. 66. DOI: 10.1186/s12977-015-0191-3.

Steffensen, Annette Buur; Refsgaard, Lena; Andersen, Martin Nybo; Vallet, Cecilia; Mujezinovic, Amer; Haunsø, Stig et al. (2015): **IKs Gain- and Loss-of-Function in Early-Onset Lone Atrial Fibrillation**. In: *Journal of cardiovascular electrophysiology* 26 (7), S. 715–723. DOI: 10.1111/jce.12666.

## In preparation

Vallet, Cecilia; Aschmann, Dennis; Beuck, Christine; Killa, Matthias; Mertel, Marcel; Bayer, Peter; Schmuck, Carsten; Knauer, Shirley (2019): **Inhibition of Survivin-associated cancer cell proliferation with supramolecular ligands (working title)**.

Aschmann, Dennis; Vallet, Cecilia; Killa, Matthias; Knauer, Shirley; Schmuck, Carsten (2019): **Targeting Survivin's cancer-promoting functions with supramolecular ligands (working title)**.

Bäcker, Sandra; Meiners, Annika; Heid, Christian; Beuck, Christine; Hadrovic, Inesa; Pörschke, Marius; Ruiz-Blanco, Yasser B.; Grad, Jean-Noël; Vallet, Cecilia; Oelschläger, Lisa; Hoffmann, Daniel; Sanchez-Garcia, Elsa; Bayer, Peter; Schrader, Thomas; Knauer, Shirley (2019): **Specific inhibition of the Survivin-CRM1 interaction by peptide-modified molecular tweezers (working title)**.

## Books

Vallet, Cecilia (2015): **Analyse des tumorrelevanten Proteins Survivin. Molekulare Charakterisierung der Dimerisierung**. Zugl.: Duisburg, Essen, Univ., Masterarbeit. Wiesbaden: Springer Spektrum (BestMasters).

## TALKS

Joint CRC 858 (University of Münster) and CRC 1093 (University of Duisburg-Essen) Graduate Student Symposium 2018 "Synergistic and Supramolecular Aspects of Chemistry and Biology", Billerbeck: **"Molecular characterization and modulation of Survivin's cellular functions with supramolecular ligands"**

Joint CRC 765 (Free University of Berlin) and CRC 1093 (University of Duisburg-Essen) Graduate Student Symposium 2016 "Protein-Ligand Interactions", Hannover: **"Molecular impact of Survivin acetylation on its biological function"**

CRC 1093 Graduate Student Symposium 2014 "Supramolecular Chemistry on Proteins", Kleve: **"Analysis of Survivin mutants via CD Spectroscopy, Gelfiltration Chromatography and FRET-Assay"**

## POSTER PRESENTATIONS

International Fall Meeting of the German Society for Biochemistry and Molecular Biology (GBM) 2017 "Molecular Basis of Life", Bochum: **"Molecular characterization and modulation of Survivin's cellular functions with supramolecular ligands"**

CRC 1093 International Symposium 2017 "Supramolecular Chemistry on Proteins", Essen: **"Molecular characterization and modulation of Survivin's cellular functions with supramolecular ligands"**

Joint CRC 765 (Free University of Berlin) and CRC 1093 (University of Duisburg-Essen) Graduate Student Symposium 2016 "Protein-Ligand Interactions", Hannover: **"Molecular impact of Survivin acetylation on its biological function"**

CRC 1093 International Symposium 2015 "Supramolecular Chemistry on Proteins", Essen: **"Molecular impact of Survivin acetylation on its biological function"**

CRC 1093 Graduate Student Symposium 2014 "Supramolecular Chemistry on Proteins", Kleve: **"Analysis of Survivin mutants via CD Spectroscopy, Gelfiltration Chromatography and FRET-Assay"**

## AWARDS

CRC 1093 and CRC 858 **Presentation Award 2018**

**"Best Masters"-Award 2014** from Springer-Verlag

# CURRICULUM VITAE

## PERSONAL DETAILS

---

Name	Cecilia Vallet
Address	Isenbrockstraße 39 44867 Bochum
Date of Birth	29 <sup>th</sup> of April 1990
Place of Birth	Bochum, Germany

## EDUCATION

---

since 10/2014	Ph.D. student and research assistant, Department of Molecular Biology II, Centre for Medical Biotechnology, University of Duisburg-Essen
04/2014 – 09/2014	Master thesis at the Department of Molecular Biology II, Centre for Medical Biotechnology, University of Duisburg-Essen (grade: 1.0)
10/2012 - 09/2014	Studies in Medical Biology at the University of Duisburg-Essen Degree awarded: Master of Science (MSc) in Medical Biology (grade: 1.3)
04/2012 – 08/2012	Bachelor thesis at the Department of experimental Virology, Institute of Virology, University Hospital Essen (grade: 1.0)
10/2009 – 09/2012	Studies in Medical Biology at the University of Duisburg-Essen Degree awarded: Bachelor of Science (BSc) in Medical Biology (grade: 1.9)
08/2000 – 06/2009	General higher education entrance qualification at the Hellweg-Gymnasium in Bochum (grade: 1.4)

## INTERNSHIPS

---

01/2014 - 02/2014	Internship at the Department of Toxicology, Institute of Forensic Medicine, University Hospital Essen
09/2013 - 12/2013	Internship at the Department of Viral Immunology, Nuffield Department of Medicine, University of Oxford
08/2011 - 09/2011	Internship at the Department of Cardiovascular Physiology, Institute of Biomedical Sciences, University of Copenhagen

Essen, 1<sup>st</sup> of April 2019

---

Cecilia Vallet

## EIDESSTATTLICHE ERKLÄRUNGEN

### Erklärung:

Hiermit erkläre ich, gem. § 7 Abs. (2) d) + f) der Promotionsordnung der Fakultät für Biologie zur Erlangung des Dr. rer. nat., dass ich die vorliegende Dissertation selbstständig verfasst und mich keiner anderen als der angegebenen Hilfsmittel bedient, bei der Abfassung der Dissertation nur die angegebenen Hilfsmittel benutzt und alle wörtlich oder inhaltlich übernommenen Stellen als solche gekennzeichnet habe.

Essen, den \_\_\_\_\_

\_\_\_\_\_  
Cecilia Vallet

### Erklärung:

Hiermit erkläre ich, gem. § 7 Abs. (2) e) + g) der Promotionsordnung der Fakultät für Biologie zur Erlangung des Dr. rer. nat., dass ich keine anderen Promotionen bzw. Promotionsversuche in der Vergangenheit durchgeführt habe und dass diese Arbeit von keiner anderen Fakultät/Fachbereich abgelehnt worden ist.

Essen, den \_\_\_\_\_

\_\_\_\_\_  
Cecilia Vallet

### Erklärung:

Hiermit erkläre ich, gem. § 6 Abs. (2) g) der Promotionsordnung der Fakultät für Biologie zur Erlangung der Dr. rer. nat., dass ich das Arbeitsgebiet, dem das Thema "Modulation of Survivin's cancer-promoting functions with supramolecular ligands" zuzuordnen ist, in Forschung und Lehre vertrete und den Antrag von Cecilia Vallet befürworte und die Betreuung auch im Falle eines Weggangs, wenn nicht wichtige Gründe dem entgegenstehen, weiterführen werde.

Essen, den \_\_\_\_\_

\_\_\_\_\_  
Prof. Dr. Shirley Knauer